Roles for NUCKS1 in cell cycle progression and the DNA damage response

A thesis presented for the degree of
Doctor of Philosophy

Samuel Benjamin Hume

Supervisors:
Prof. Grigory Dianov
Prof. Kristijan Ramadan

University College
MRC Oxford Institute for Radiation Oncology
Department of Oncology
University of Oxford

Michaelmas Term 2020

DEPARTMENT OF ONCOLOGY
Medical Sciences Division

Contents

List of figures 6

List of tables 7

List of acronyms 8

Acknowledgements 10

Declaration 10

Abstract 11

Introduction 12

Mitogens 12

DNA damage 14

Cyclins, CDKs, and CDK inhibitors 14

CDK4's activation and inhibition 15

CDK2's activation and inhibition 18

Mitogen-DNA damage competition 19

S phase commitment 19

Initial experiments 20

New experiments 21

SCF-SKP2 24

SCF-SKP2 structure 24

Roles for SCF-SKP2 in the cell cycle and the DNA damage response 25

Cell cycle checkpoints 26

Intra-S checkpoint 26

S/G2 checkpoint 27
G2/M checkpoint 27
p53 28
Control of p53 by MDM2 29
Transcriptional repression by p53 30
The G1/S transition in cancer 32
p53 in cancer 32
ATM in cancer 33
p21 in cancer 33
MDM2 in cancer 34
Cyclin D1 in cancer 34
Short G1 phases in cancer 35
G1/S components in therapy 35
NUCKS1 36
Functions of NUCKS1 36
NUCKS1 expression 38
NUCKS1 in cancer 38
Aims of the study 38
Materials and Methods 40
Cell culture 40
Transfections 40
CRISPR-Cas9 genome editing 41

Western blotting 42
Whole cell extracts 42
Cytoplasmic/Nuclear/chromatin fractionations 42
SDS-PAGE 43
RT-qPCR 44
ChIP 44
Flow cytometry 47
Bioinformatics 47
Comet assay 47
EMSA 48
Proliferation assays 48
Statistics 48
Results 49
Results chapter 1: NUCKS1 regulates G1/S progression 49
Results chapter 2: NUCKS1-dependent *SKP2* transcription controls S phase entry 51
Results Chapter 3: DNA damage inhibits the NUCKS1-SKP2 axis through p53 63
Results Chapter 4: NUCKS1 and SKP2 prevent genomic instability in the absence of p53 66
Results Chapter 5: *NUCKS1* and *SKP2* are overexpressed in cancer 69
Discussion 73
Integration of mitogenic and DNA damage signalling 73
Regulation of *SKP2* by NUCKS1 75

Regulation of NUCKS1 by the cell cycle 76

Regulation of NUCKS1 by mitogens 77

Regulation of NUCKS1 by DNA damage 77

Regulation of cancer by NUCKS1 79

Genomic instability triggered by loss of the NUCKS1-SKP2 axis in p53-deficient cells 79

Conclusion and future perspectives 80

Appendix 82

Collaborative project 1: E2F1 proteolysis via SCF-cyclin F underlies synthetic lethality between cyclin F loss and Chk1 inhibition 82

Collaborative project 2: TEX264 coordinates p97- and SPRTN-mediated resolution of topoisomerase 1-DNA adducts 85

Collaborative project 3: Interplay between base excision repair protein XRCC1 and ALDH2 predicts overall survival in lung and liver cancer patients 86

Publications 90

References 91

List of figures

Figure number	Figure title	Page number
Introduction		
1	Mitogens and DNA damage regulate S phase entry	13
2	Stoichiometric control of CDKs by cyclins and CDK inhibitors	16
3	Classical and updated models for S phase commitment	22
Chapter 1: NUCKS1 regulates G1/S progression		
4	Validation of depletion, knockout, and overexpression	50
5	NUCKS1 is required for cell cycle progression	50
6	NUCKS1 is required for proliferation	52
7	NUCKS1 depletion does not cause DNA damage	52
Chapter 2: NUCKS1-dependent SKP2 transcription controls S phase entry		
8	Identification of putative NUCKS1 targets	53
9	Correlation analysis of NUCKS1 and *SKP2* mRNA levels	55
10	Binding of NUCKS1 at the *SKP2* promoter	56
11	Purification of NUCKS1	56
12	Characterisation of NUCKS1's binding at the *SKP2* promoter by EMSA: phosphorylated vs. dephosphorylated NUCKS1	58
13	Characterisation of NUCKS1's binding at the *SKP2* promoter by EMSA: competition with WT and mutant probes	58
14	Characterisation of NUCKS1's binding at the *SKP2* promoter by EMSA: WT vs. NUCKS1-KO nuclear extract	59
15	NUCKS1 is required for *SKP2* expression	59
16	NUCKS1 depletion inhibits the SKP2 pathway	61
17	NUCKS1 is required for S phase entry, and phenocopies SKP2	61
18	SKP2 overexpression reduces the accumulation of p21 and p27 in NUCKS1-depleted cells	62
19	NUCKS1 controls cell cycle progression via the SKP2-p21/p27 axis	62
20	NUCKS1 controls proliferation via the SKP2 axis	64
21	NUCKS1 is stimulated during G1/S progression and by mitogens	64
Chapter 3: DNA damage inhibits the NUCKS1-SKP2 axis through p53		
22	DNA damage inhibits the NUCKS1-SKP2 axis through p53	65
23	p53 mediates transcriptional repression of *NUCKS1* and *SKP2* following DNA damage	67
24	Wildtype p53 suppresses levels of *NUCKS1* and *SKP2*	68
Chapter 4: NUCKS1 and SKP2 prevent genomic instability in the absence of p53		

25	Characterisation of NUCKS1 depletion in p53-deficient cells	70
26	NUCKS1 and SKP2 protect genome stability in p53-deficient cells	70
Chapter 5: NUCKS1 and SKP2 are overexpressed in cancer		
27	Analysis of *NUCKS1* and *SKP2* mRNA levels in cancer	72
28	Analysis of *NUCKS1* and *SKP2* copy numbers in cancer	72
29	Analysis of *NUCKS1* and *SKP2* mRNA levels in WT vs. *TP53*-mutant tumours	74
30	Model	74
Appendix		
31	Chk1 inhibition induces massive DSB formation in *CCNF*-KO cells	84
32	Loss of TEX264 delays repair of CPT-induced lesions via the TDP1 pathway	87
33	Analysis of the inverse relationship between *XRCC1* and *ALDH2*	89

List of tables

Table number	Table title	Page number
-	List of figures	6
-	List of tables	7
-	List of acronyms	8
1	Cell lines	40
2	siRNAs	41
3	Plasmids	41
4	Antibodies	43
5	Primers	46

List of acronyms

Acronym	In full
5-FU	5-fluorouracil
ACC	Adrenocortical carcinoma
ALDH2	Alcohol dehydrogenase 2
AML	Acute myeloid leukaemia
APC/C	Anaphase-promoting complex/cyclosome
ATAC-Seq	Assay for transposase-accessible chromatin using sequencing
ATM	Ataxia Telangiectasia Mutated
ATR	Ataxia Telangiectasia and Rad3-related
BER	Base excision repair
BLCA	Bladder urothelial carcinoma
BRCA	Breast invasive carcinoma
CDK	Cyclin-dependent kinase
CESC	Cervical squamous cell carcinoma
Chk1	Checkpoint kinase 1
ChIP	Chromatin immunoprecipitation
CHOL	Cholangiocarcinoma
CIP/KIP	CDK interacting protein/Kinase inhibitory protein
COAD	Colon adenocarcinoma
CP1, 2, 3	Commitment point 1, 2, 3
CPT	Camptothecin
DDR	DNA damage response
DLBC	Diffuse large B-cell lymphoma
DPC	DNA-protein crosslink
DREAM	Dimerization partner, RB-like, E2F and multi-vulval class B
DSB	Double-strand break
EGF	Epidermal growth factor
EGFR	Epidermal growth factor receptor
EMSA	Electrophoretic mobility shift assay
ESCA	Esophageal carcinoma
FACS	Fluorescence-activated cell sorting
FBS	Fetal bovine serum
GBM	Glioblastoma multiforme
HMG	High-mobility group
HNSC	Head and neck squamous cell carcinoma
HR	Homologous recombination
IGF	Insulin growth factor
IGFR	Insulin growth factor receptor
INK4	Inhibitor of CDK4
IR	Ionising radiation
KICH	Kidney chromophobe
KIRC	Kidney renal clear cell carcinoma
KIRP	Kidney renal papillary cell carcinoma
LGG	Lower grade glioma
LIHC	Liver hepatocellular carcinoma
LUAD	Lung adenocarcinoma
LUSC	Lung squamous cell carcinoma

MAPK	Mitogen-activated protein kinase
MESO	Mesothelioma
METABRIC	Molecular taxonomy of breast cancer international consortium
NUCKS1	Nuclear casein kinase and cyclin-dependent kinase substrate 1
OV	Ovarian serous cystadenocarcinoma
PAAD	Pancreatic adenocarcinoma
PCNA	Proliferating cell nuclear antigen
PCPG	Pheochromocytoma and paraganglioma
PCV	Packed cell volume
PI	Propidium iodide
PIP	PCNA-interacting protein
PRAD	Prostate adenocarcinoma
PROTAC	Proteolysis-targeting chimera
qPCR	Quantitative polymerase chain reaction
Rb	Retinoblastoma protein
READ	Rectum adenocarcinoma
RNAPII	RNA polymerase II
SARC	Sarcoma
SCF	Skp, cullin, F-box
SDS-PAGE	Sodium dodecyl sulphate-polyacrylamide gel electrophoresis
SKCM	Skin cutaneous melanoma
SKP2	S phase kinase-associated protein 2
SSB	Single-strand break
STAD	Stomach adenocarcinoma
TCGA	The cancer genome atlas
TDP1	Tyrosyl-DNA phosphodiesterase 1
TGCT	Testicular germ cell tumours
THCA	Thyroid carcinoma
THYM	Thymoma
Top1	Topoisomerase 1
Top1-CC	Topoisomerase 1-covalent complex
UCEC	Uterine corpus endometrial carcinoma
UCS	Uterine carcinosarcoma
UVM	Uveal melanoma
VHL	von Hippel-Lindau
WT	Wildtype
XRCC1	X-ray repair cross-complementing protein 1

Acknowledgements

Thank you to Prof. Dianov and Prof. Ramadan for giving me the opportunity to pursue my DPhil in Oxford, for providing such a stimulating project, for their enthusiasm and ideas, for giving advice that has matured me as a person and a scientist, for coordinating the numerous paper submissions and re-submissions, and for supporting me as I move on with my career. Thank you to Dr. Arnaud Legrand for initiating the project with me, for ambition-driving discussions, and for the continued support. Thank you also to the other members of the Dianov lab (Dr. Claudia Grou, Dr. Mattia Poletto, Dr. Sally Fletcher, Dr. Xin Chen, Siobhan Cunniffe MSc, Di Yang MSc) and Ramadan lab (Dr. Abhay Singh, Dr. Ignacio Torrecilia, Dr. Annamaria Ruggiano, Dr. John Fielden, Dr. Wei Song, Susan Kilgas MSc, Dr. Cristiano Peron MD, Pauline Lascaux MSc, Shudong Li MSc, Ftoon Aljarbou MSc, Gwendoline Hoslett Bsc) for their laughs and experimental support along the way. Finally, I am incredibly grateful to the funders of this project, the Medical Research Council, as well as my personal scholarship, the Oxford-Radcliffe Oncology Studentship.

Declaration

I declare that this thesis is wholly my own work, with the following exception:

The protein purification presented in Figure 11, and the gel shown in this figure, were performed by Dr. Claudia Grou.

Abstract

Regulated progression through the cell cycle is essential for healthy physiology, including for embryonic development and for repairing tissue. The transition from G1 to S phase is subject to particularly intricate regulation, since its overactivity can result in DNA damage and carcinogenesis. Although the G1/S transition has been studied extensively, gaps remain in our knowledge, and crucial questions remain unanswered. Mitogens, such as growth factors, stimulate S phase entry to promote proliferation, while DNA damage, such as ionising radiation, reduces S phase entry. Strikingly, new results show that is a competition between mitogens and DNA damage that determines whether cells enter S phase, suggesting that cells deploy dedicated proteins to integrate the antagonistic mitogen and DNA damage information. Here, we identify NUCKS1 as one such integrator. NUCKS1 is a transcription factor implicated in cell cycle progression, DNA replication, and tumourigenesis. However, detailed mechanistic studies explaining how NUCKS1 controls these functions have not been performed. We show that NUCKS1 is required for S phase entry through transcriptional stimulation of *SKP2*, the F-box component of the SKP1-Cullin-F box (SCF) ubiquitin ligase complex, which is responsible for degradation of the CDK inhibitors, p21 and p27. During G1 progression, and following mitogenic stimulation, NUCKS1 is upregulated and recruited to chromatin, where it is required for *SKP2*'s transcriptional upregulation. Upon DNA damage, NUCKS1 and SKP2 are both downregulated, through p53-dependent transcriptional repression. Consistently, NUCKS1 levels are increased in p53-deficient cells, and this is rescued through expression of wildtype – but not mutant – p53. Finally, we show that cancer cells upregulate both *NUCKS1* and *SKP2*, driven through increased copy number and loss of p53 activity. Altogether, this study identifies NUCKS1 as an important regulator of S phase entry, which integrates mitogenic and DNA damage signalling to control the S phase entry decision.

Introduction

Progression through the cell cycle is essential for cell proliferation, which is necessary to maintain healthy physiological processes such as embryonic development, digestion, and immune responses. The G1/S transition, the phase of the cell cycle during which cells prepare for DNA replication, is the major focus of this thesis. The S phase entry decision is particularly strictly regulated, since overzealous S phase entry can cause replication stress and DNA damage, which can lead to mutations, genomic instability and, ultimately, cancer (Macheret and Halazonetis, 2018; Hills and Diffley, 2014). Most positive regulation for the G1/S transition is sourced from mitogens, which increase the probability of S phase entry (Witsch et al., 2010). On the other hand, DNA damage provides the major inhibitory source for S phase entry (Kastan and Bartek, 2004). Mitogens and DNA damage regulate S phase entry by controlling the levels of cyclins and cyclin-dependent kinase (CDK) inhibitors, which modulate the activity of CDKs (Yang et al., 2017; Hume et al., 2020). In turn, CDKs phosphorylate a multitude of substrates to enforce cell cycle progression and DNA replication (Malumbres, 2014) (Figure 1).

Mitogens

Mitogens, such as insulin, fibroblast, and epidermal growth factors (IGF, FGF, and EGF), stimulate the G1/S transition. These growth factors bind cell surface receptors (IGF receptor (IGFR), FGFR, and EGFR for IGF, FGF, and EGF, respectively), triggering intracellular signalling cascades, such as the mitogen-activated protein kinase (MAPK) and AKT pathways (Witsch et al., 2010; Manning and Toker, 2017). In these pathways, growth factor binding leads to activation of the Ras-Raf-Mek-ERK1/2 and mTOR cascades, respectively, and stimulates pro-proliferative transcription factors such as Jun, Fos, β-Catenin, and c-Myc (Meloche and Pouysségur, 2007; Liu and Sabatini, 2020). c-Myc provides the strongest positive effect on S phase entry, which acts as a transcriptional amplifier (Lin et al., 2012) but also specifically activates the expression of

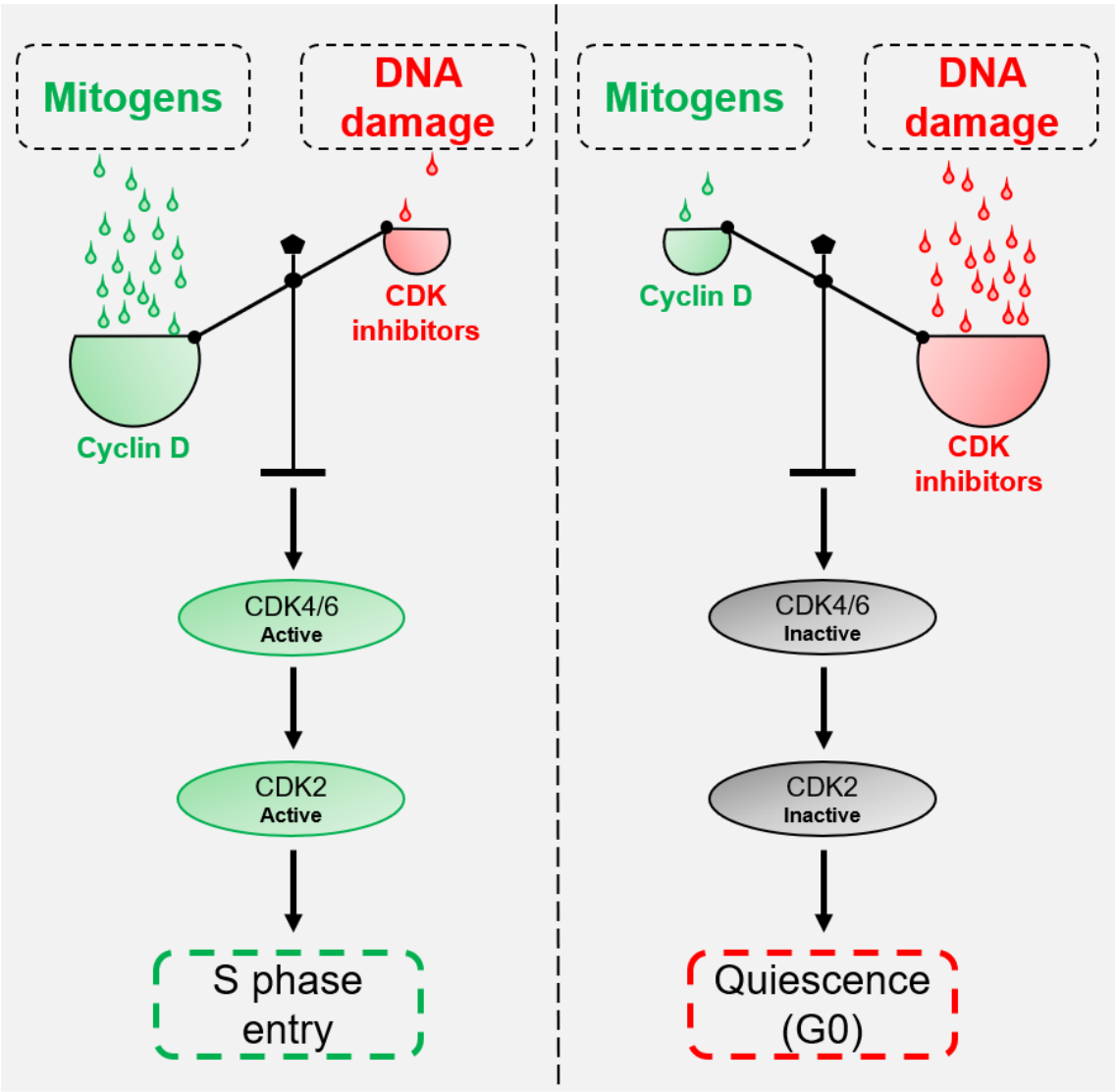


Figure 1: Mitogens and DNA damage regulate S phase entry. Competition between mitogens and DNA damage regulates the G1/S transition through control of cyclin D and the CDK inhibitors, which regulate CDKs in turn. This figure, designed and prepared myself, is from Hume et al., *Nucleic Acids Research* 2020, published by Oxford University Press.

certain genes, such as *CCND2* (which encodes cyclin D2) (Dang et al., 2006; Dang, 2012; Pelengaris et al., 2002). Since cyclin D2 is a core cyclin driving S phase entry, mitogens promote entry to S phase.

DNA damage

On the other hand, DNA damage, from endogenous and exogenous sources, inhibits the G1/S transition. Endogenous DNA damage can arise from cellular respiration, as well as from DNA replication, while exogenous DNA damage can be induced, for example, by sunlight or chemotherapy (Tubbs and Nussenzweig, 2017; Lord and Ashworth, 2012; Hoeijmakers, 2009; Khoronenkova and Dianov, 2015). DNA damage leads to activation of the major DNA damage response (DDR) kinases, Ataxia-Telangiectasia mutated (ATM) and Ataxia Telangiectasia and Rad3-related (ATR), which coordinate cell cycle arrest and DNA repair in response to DNA damage (Blackford and Jackson, 2017). The major cell cycle inhibitory target of ATM and ATR is p53, a transcription factor that elicits widespread transcriptional changes in response to DNA damage (Vousden and Prives, 2009). Most prominently, p53 promotes the transcription of the CDK inhibitor, *CDKN1A* (encoding p21) (Abbas and Dutta, 2009). In this way, DNA damage inhibits entry to S phase.

Cyclins, CDKs, and CDK inhibitors

Cyclins D1-3 and E1-2 are the major cyclins responsible for regulation of the G1/S transition. These cyclins pair with CDK4/6 and CDK2, respectively, to phosphorylate their targets and promote S phase entry (Wood and Endicott, 2018; Malumbres, 2014; Malumbres and Barbacid, 2009). Protein levels of cyclin D – and the activity of CDK4 and 6 as a result - are predominantly controlled through the abundance of mitogens, which stimulate cyclin D's transcription and translation (Min et al., 2020), while cyclin Es are under more direct control by the cell cycle itself, through the activity of the major cell cycle transcription factor, E2F1 (Bertoli et al., 2013; Geng et al., 1996). Accordingly, cyclin D levels gradually increase following mitogen stimulation, and peak in G2 phase

of a healthy cell cycle (Min et al., 2020), while cyclin E is specifically present at the G1/S transition (Bertoli et al., 2013; Malumbres and Barbacid, 2009; Geng et al., 1996). This ensures high CDK2 activity at the G1/S transition, which is subsequently maintained throughout S phase by cyclin A2 (Bertoli et al., 2013; Malumbres and Barbacid, 2009; Malumbres, 2014).

Antagonistic control of these CDKs is provided by two families of CDK inhibitors. The CDK interacting protein/kinase inhibitory protein (CIP/KIP) members, p21, p27, and p57, bind both cyclin and CDK components of cyclin D-CDK4/6 and cyclin E-CDK2 complexes, while the inhibitors of CDK4 (INK4) members specifically bind and sequester CDK4/6 (Wood and Endicott, 2018; Malumbres, 2014; Malumbres and Barbacid, 2009; Hume et al., 2020) (Figure 2).

CDK4's activation and inhibition

Newly-translated CDK4 molecules, unlike other CDKs, require the Cdc37-Hsp90 chaperone complex for folding, and monomeric CDK4 is rare in cells as a result (Hallett et al., 2017). However, INK4 proteins release CDK4 from Cdc37-Hsp90, interacting directly with CDK4 and preventing formation of CDK4's active holoenzyme (Blain, 2008; Brotherton et al., 1998; Jeffrey et al., 2000; Russo et al., 1998) (Figure 2A: 1-4). Interestingly, the small molecule anti-cancer CDK4 inhibitor, Palbociclib, prevents CDK4 activity in a similar manner, by preventing CDK4 holoenzyme formation (Guiley et al., 2019) (Figure 2A: 5).

In curious findings, cyclin D and CDK4 are unable to interact in cells deficient in the CIP/KIP CDK inhibitors, p21, p27, and p57, leading to the conclusion that CIP/KIP inhibitors actually facilitate the binding of cyclin D to CDK4 (Cheng et al., 1999; Tateishi et al., 2012) (Figure 2A: 6). Structurally, CIP/KIP members interact with both cyclin and CDK components to draw the proteins together and enforce their interaction (Guiley et al., 2019). Nevertheless, cyclin D-CDK4 complexes containing p21 or p57 are inhibited,

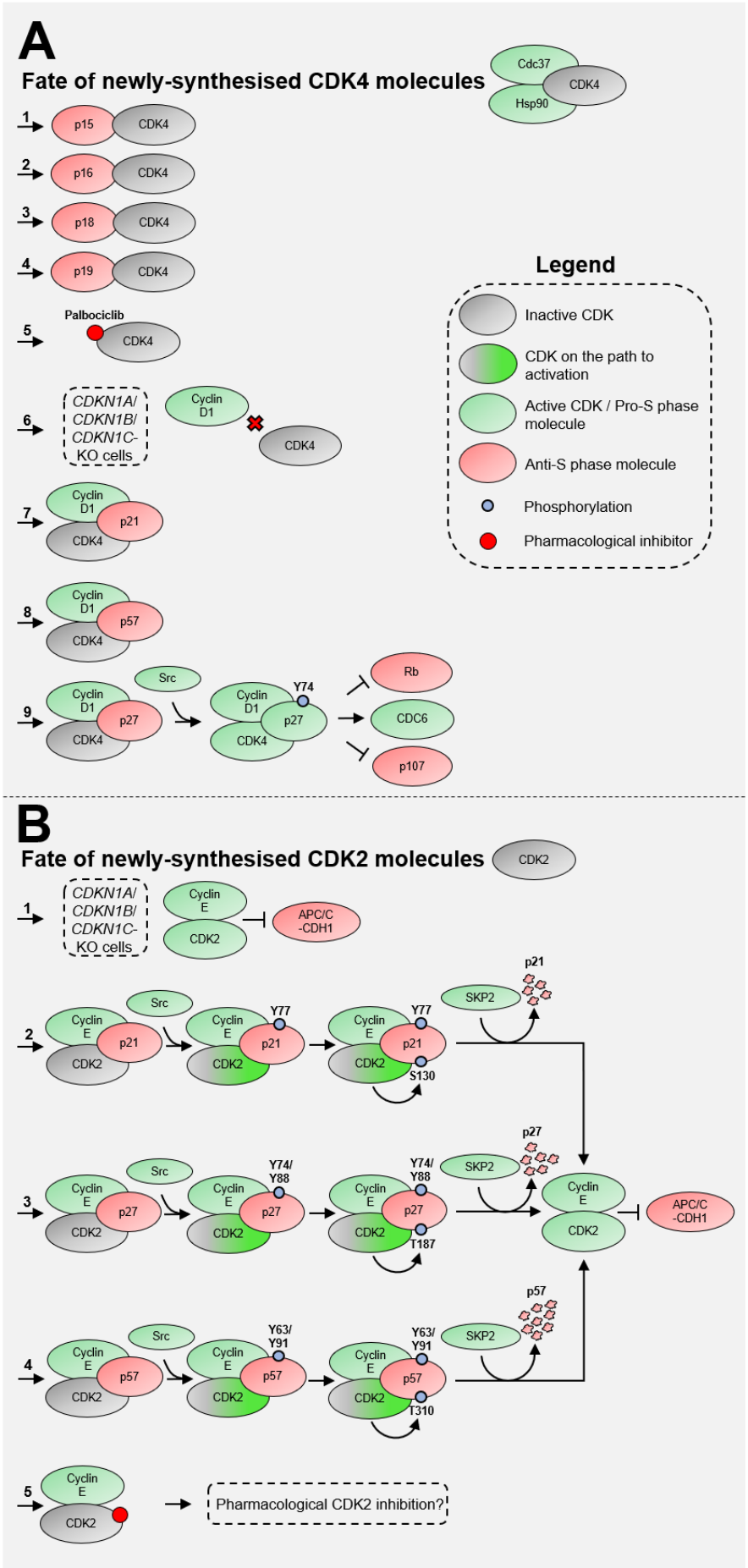


Figure 2: Stoichiometric control of CDKs by cyclins and CDK inhibitors. A) Fate of newly-synthesised CDK4 molecules. **B)** Fate of newly-synthesised CDK2 molecules. This figure, designed and prepared myself, is from Hume et al., *Nucleic Acids Research* 2020, published by Oxford University Press.

and unable to phosphorylate targets (Guiley et al., 2019; Cheng et al., 1999; Tateishi et al., 2012) (Figure 2A: 7-8).

If cyclin D-CDK4 complexes cannot form alone, and if CIP/KIP proteins, which inhibit these complexes, are required for interaction, then how is cyclin D-CDK4 activated? This molecular paradox is solved by p27. Like p21 and p57, p27 facilitates the interaction of cyclin D with CDK4, and inhibits CDK4. However, p27 contains a tyrosine residue, Y74 – an equivalent for which is not present in p21 and p57 – that serves as a substrate for Src-family kinases (Guiley et al., 2019; Patel et al., 2015; Larrea et al., 2008; Chu et al., 2007; Blain, 2008). Phosphorylation of p27 at Y74 not only relieves p27's inhibition towards cyclin D-CDK4, but, impressively, induces structural rearrangements that *increase* CDK4's activity (Guiley et al., 2019) (Figure 2A: 9). Indeed – and surprisingly – p27 is a core component of the CDK4 holoenzyme in cells, forming cyclin D-CDK4-p27 (Y74-p) complexes (and raising questions about oncogenic activities of p27, a protein typically considered a prototype tumour suppressor) (Guiley et al., 2019; Patel et al., 2015). Cyclin D-CDK4-p27 (Y74-P) complexes phosphorylate a number of factors – most importantly the retinoblastoma protein (Rb), which inhibits E2F1 (Dick and Rubin, 2013) (Figure 2A: 9).

This means that p21 provides much stronger and more reliable CDK4 inhibition than p27, which acts as a duplicitous CDK4 'inhibitor' (Cheng et al., 1999; Guiley et al., 2019). These differences in inhibition capacity are exacerbated because, unlike p27, p21 encodes a PCNA-interacting protein (PIP)-box motif in its C-terminal tail that enables an interaction with the replication fork processivity factor, PCNA (Waga et al., 1994). Remarkably, p21's binding to PCNA is stronger than PCNA's interaction with any other protein, enabling potent p21-dependent inhibition of PCNA (Moldovan et al., 2007; Arias and Walter, 2006; Gulbis et al., 1996). Nevertheless, both p21 and p27 strongly inhibit CDK2.

CDK2's activation and inhibition

CDK2 monomers are able to spontaneously assemble into cyclin E-CDK2 complexes, requiring no input from chaperones or CDK inhibitors (Malumbres, 2014; Wood and Endicott, 2018) (Figure 2B: 1). Nevertheless, cyclin E-CDK2's activation mechanism is also intricately regulated.

In early G1 phase, levels of the CIP/KIP inhibitors, which inhibit CDK2, are very high, saturating cyclin E-CDK2 complexes (Malumbres, 2014; Wood and Endicott, 2018). These CIP/KIP inhibitors must be degraded, by the proteasome, to allow activation of CDK2. However, CDK2 is the protein that instigates the degradation, phosphorylating CIP/KIP proteins to form the phosphodegron for subsequent polyubiquitylation (Huang et al., 2015). This highlights a second molecular paradox underpinning the regulation of CDKs: how can an inhibited CDK2 promote its own activation?

Providing the answer (in a manner similar to CDK4) is Src family-dependent phosphorylation of CDK inhibitors. Src-mediated phosphorylation of p21, p27, or p57, at Y77, Y74/Y88, or Y73/Y91, respectively, weakens CIP/KIP members' inhibition of cyclin E-CDK2, increasing CDK2 activity and enabling CKD2-mediated phosphorylation of p21/p27/p57 (Huang et al., 2015). This generates the binding site and phosphodegron for the ubiquitin ligase, SCF-SKP2 (Tsytlonok et al., 2019; Chu et al., 2007; Grimmler et al., 2007; Huang et al., 2015) (Figure 2B: 2-4). Consequent SCF-SKP2-dependent polyubiquitylation, and the resulting proteasomal degradation of p21/p27/p57, liberates free cyclin E-CDK2 molecules, which phosphorylate factors including - most importantly - the cell cycle inhibitor and ubiquitin ligase, APC/C-CDH1 (Cappell et al., 2016). This prevents APC/C-CDH1-directed degradation of S phase proteins, including cyclin A2, thereby promoting S phase entry (Zhou et al., 2016). Finally, pharmacological inhibition of cyclin E-CDK2 complexes is possible, but complicated by off target effects and toxicity in the clinic, highlighting the further research that must go into development of specific CDK2 pharmacological inhibitors (Tadesse et al., 2019) (Figure 2B: 5).

Mitogen-DNA damage competition

Although mitogens and DNA damage independently exert well-established antagonistic control over the S phase entry decision, landmark studies showed that it is the *competition* between mitogens and DNA damage that ultimately regulates the S phase entry decision. In a particularly fascinating study, Yang *et al* employed single cell analysis to confirm that increasing the concentration of mitogens increases the probability for S phase entry (Yang et al., 2017). Similarly, increasing the concentration of DNA-damaging agents reduces the probability for S phase entry. Both of these results are expected; however, in striking findings, Yang *et al* also showed that dosing cells with very high levels of mitogens in the presence of high levels of DNA damage causes cells to enter S phase inappropriately, inducing DNA damage-resistant S phase entry. This leads to the conclusion that mitogens and DNA damage are in direct competition with one another for control of the S phase entry decision: where mitogens outcompete DNA damage, cells enter S phase, while where DNA damage outcompetes mitogens, cells quiesce (Yang et al., 2017). To achieve this regulation, the balance of mitogens to DNA damage controls, in turn, the balance of cyclins to CDK inhibitors. When mitogens outweigh DNA damage, cyclins outweigh CDK inhibitors, and CDKs are active, while where DNA damage outweighs mitogens, CDK inhibitors outweigh cyclins, and CDKs are inactive (Yang et al., 2017; Chen et al., 2013a; Heldt et al., 2018) (Figure 1).

However, this model leaves one question unanswered: how is the mitogen: DNA damage competition translated into the competition between cyclins and CDK inhibitors? We previously proposed that dedicated proteins act to *integrate* the antagonistic mitogen and DNA damage signals, and suggested six conditions that integrators would fulfil (Hume et al., 2020). We explore this concept throughout this thesis.

S phase commitment

Cells deploy a commitment point for S phase entry – after which the S phase entry decision cannot be reversed – to prevent incomplete DNA replication (Zetterberg et al.,

1995; Yao et al., 2008). After the commitment point, cells cannot return to quiescence, even if they lose mitogenic stimulation or encounter DNA damage, and will irreversibly complete S phase [although not necessarily the entire cell cycle (Krenning et al., 2014)] (Zetterberg et al., 1995).

The E2F family of transcription factors are the major transcriptional regulators of S phase commitment, comprising the activator E2Fs, E2F1, E2F2, and E2F3, which partner with – and are inhibited by – Rb (Bertoli et al., 2013; Malumbres, 2014). Upon activation, E2Fs transcribe a host of genes required for S phase entry and DNA replication, including cyclins (e.g. *CCNE1*, *CCNA2*) (Schulze et al., 1995), replisome components (e.g. *PCNA*), and S phase-associated DNA repair proteins [e.g. homologous recombination (HR) genes, mismatch repair genes] (Ren et al., 2002; Bertoli et al., 2013; Kent and Leone, 2019).

Initial experiments

Initial experiments studying the G1/S transition generated a model showing that a single commitment point, the restriction point, controls entry to S phase. This commitment point was temporally placed at the end of G1 phase (Yao et al., 2008; Pardee, 1974; Narasimha et al., 2014). In the original model, loss of mitogens or induction of DNA damage - only occurring between cell birth and the commitment point - prevents entry to S phase (Pardee, 1974; Dulić et al., 1994; Slebos et al., 1994; Zetterberg et al., 1995; Narasimha et al., 2014; Yao et al., 2008) (Figure 3A).

Hyperphosphorylation of Rb was identified as the likely basis of the commitment point (Yao et al., 2008; Kent and Leone, 2019). The initial model concluded that, following mitogen stimulation, cyclin D-CDK4/6-mediated phosphorylation of Rb allowed partial E2F activity, leading to E2F-dependent expression of cyclin E and an associated increase in CDK2 activity. Active cyclin E-CDK2 consequently fully (hyper)-phosphorylates Rb, initiating a positive feedback loop underpinned by continued cyclin E (or A)-CDK2-mediated E2F activation, and E2F-driven cyclin E (and A) expression

(Harbour et al., 1999). It is this positive feedback loop that was proposed to support mitogen-independent and DNA damage-resistant S phase commitment and completion (Dulić et al., 1994; Slebos et al., 1994; Yao et al., 2008; Narasimha et al., 2014) (Figure 3A).

New experiments

However, in contrast to models generated by initial studies, intricate, single cell analyses have produced an updated model (Figure 3B). Intriguingly, these studies demonstrate that the S phase entry decision is initiated in mother cells (Spencer et al., 2013; Barr et al., 2017; Min et al., 2020; Moser et al., 2018; Yang et al., 2017). Specifically, mother cells sense mitogens over their entire cell cycle to control the daughter G1/S transition, and even brief deprivation of mitogens from mother cells reduces S phase entry of daughter cells (Min et al., 2020). Similarly, mother cells sense DNA damage to control their daughters' S phase entry decision, which, during physiological progression through the cell cycle, is mainly introduced through DNA replication stress. As a result, replication stress occurring in mother cells blocks the G1/S transition of daughters (Barr et al., 2017; Arora et al., 2017; Yang et al., 2017).

Driven by sensing of mitogens and DNA damage in mother cells, and consistent with delicate regulation of S phase entry, the more recent studies have revealed that cells employ three commitment points to control their S phase entry decision, designated commitment points 1, 2, and 3 (CP1, 2 and 3) (Spencer et al., 2013; Cappell et al., 2016; Hume et al., 2020).

CP1

CP1 is temporally located at the end of the mother cell cycle, and is controlled through antagonistic mitogen and DNA damage-dependent regulation of Rb hyperphosphorylation (Spencer et al., 2013; Cappell et al., 2016; Moser et al., 2018; Min et al., 2020). During a healthy mother cell cycle, mitogens are well-sourced and DNA damage is largely avoided, leading to Rb hyperphosphorylation in mother cells' mitosis.

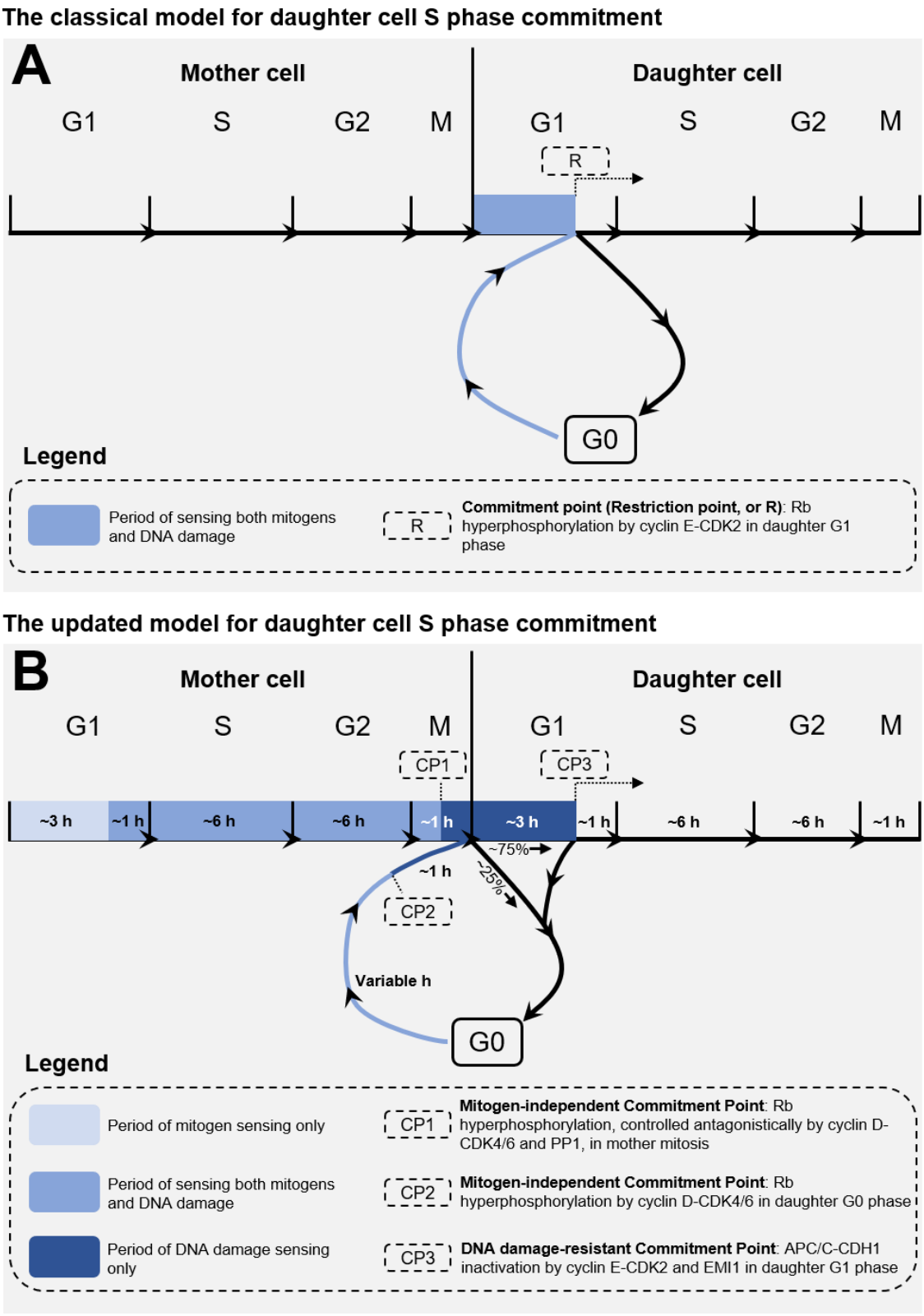


Figure 3: Classical and updated models for S phase commitment. A) Classical model for the S phase entry decision, with a single commitment point (the restriction point) in daughter G1 cells. **B)** The updated model for the S phase entry decision, with three disctinct commitment points, CP1, CP2, and CP3. This figure, designed and prepared myself, is from Hume et al., *Nucleic Acids Research* 2020, published by Oxford University Press.

Successful Rb hyperphosphorylation is the requirement for CP1 passage, and these cells no longer require mitogens to enter S phase in daughter cells. That is, cells that have passed CP1 are committed to enter S phase without mitogens, and deprivation of mitogens after passage through CP1 does not impact S phase entry (Spencer et al., 2013; Barr et al., 2017; Yang et al., 2017; Min et al., 2020; Moser et al., 2018) (Figure 3B).

CP2

In contrast, during an unhealthy mother cell cycle, mitogens are in poor supply, or cells experience replication stress-associated DNA damage, causing dephosphorylation of Rb in mitosis. These cells do not satisfy the condition for passage through CP1, and, as a result, are born in G0, and must try again for Rb hyperphosphorylation in G0. This presents a second commitment point: CP2 (Spencer et al., 2013; Moser et al., 2018; Yang et al., 2017) (Figure 3B).

CP3

Cells will enter S phase irrespective of mitogens after passing through CP1 or CP2, but DNA damage can still induce quiescence up to CP3, which is positioned about one hour before S phase (Cappell et al., 2016, 2018; Yang et al., 2020; Hume et al., 2020). CP3 has a distinct molecular basis from CP1/2, and is instead underpinned by APC/C-CDH1 (Zhou et al., 2016; Yamano, 2019; Pines, 2011; Cappell et al., 2016, 2018). After CP3, cells will enter and complete S phase even upon DNA damage, and may only rely on the intra-S checkpoint (which slows down, but does not stop, DNA replication) upon DNA damage (Cappell et al., 2016, 2018; Yang et al., 2020; Hume et al., 2020). CP3 is extremely sensitive, and requires only a single DSB to be activated (van den Berg et al., 2018) (Figure 3B).

To achieve passage through CP3, cells must satisfy two conditions. Firstly, cells must attain high activity of cyclin E-CDK2, which phosphorylates and partially inactivates APC/C-CDH1 (Cappell et al., 2016, 2018). Secondly, cells must retain Rb inactivation

and associated E2F activation (achieved at either CP1 or CP2), which enables E2F-dependent expression of EMI1, an APC/C-CDH1 inhibitor that completes APC/C-CDH1 inhibition (Cappell et al., 2016, 2018). If cells encounter DNA damage before inactivating APC/C-CDH1, Rb hyperphosphorylation is lost, E2F is inactivated, cyclin E-CDK2 is not activated, EMI1 is not expressed, and APC/C-CDH1 cannot be inactivated, inducing quiescence (Yang et al., 2020).

Therefore, three commitment points, CP1, CP2, and CP3, control entry to S phase. CP1 and CP2, in the mother mitosis and the daughter G0, respectively, are mitogen-independent commitment points, after which cells will enter S phase even in the absence of mitogens. CP3 is the DNA damage-resistant commitment point, at the end of the daughter G1 phase, after which cells will enter S phase even in the presence of DNA damage. The cell cycle inhibitors, Rb and APC/C-CDH1, are the ultimate effectors for CP1/2 and CP3, respectively (Figure 3B).

SCF-SKP2

Acting antagonistically with APC/C-CDH1 is the ubiquitin ligase SCF-SKP2, which we discuss throughout the thesis, and which provides the major proteolytic stimulation of S phase entry by coordinating the degradation of the CIP/KIP CDK inhibitors p21, p27, and p57 in late G1 phase (Frescas and Pagano, 2008).

SCF-SKP2 structure

SCF-SKP2 is a protein complex composed of molecules of SKP1, CUL1, and an F-box protein (Frescas and Pagano, 2008; Hao et al., 2005). SKP2 is an F-box protein, the adaptable constituent that provides substrate specificity to the SCF complex, and is generally the component that is regulated, for example, by the cell cycle or DNA damage (D'Angiolella et al., 2012, 2013; Frescas and Pagano, 2008). SCF-SKP2's role is to transfer ubiquitin molecules to substrates from the E2 ubiquitin-conjugating enzyme, and is linked to the E2 enzyme via RBX1 (Hao et al., 2005; Frescas and Pagano, 2008). To

polyubiquitylate substrates, SCF-SKP2 additionally requires Cks1, a SKP2 cofactor (Hao et al., 2005; Bornstein et al., 2003), and phosphodegron formation (mediated by CDK2 for p21, p27, and p57) (Vlach et al., 1997; Bornstein et al., 2003; Carrano et al., 1999; Kamura et al., 2003). SCF-SKP2's substrate polyubiquitylation permits recognition of targets by the proteasome, which degrades the target (Frescas and Pagano, 2008).

Roles for SCF-SKP2 in the cell cycle and the DNA damage response

SKP2's protein levels are maintained at low levels in early G1 phase through its ubiquitin-dependent degradation mediated by APC/C-CDH1 (Bashir et al., 2004; Wei et al., 2004), and SKP2's upregulation at the G1/S transition is reinforced because *SKP2* transcription is also induced during the G1/S transition (Imaki et al., 2003; Zhang and Wang, 2006; Yung et al., 2007). SCF-SKP2-dependent degradation of CDK inhibitors is a key switch for entry into S phase (Heldt et al., 2018), and these co-ordinated control mechanisms ensure that SKP2 is only present at high levels when it is safe to initiate DNA replication.

In addition to its regulation of CDK inhibitors, SKP2 also provides direct (but non-proteolytic) inhibition of p53. To achieve this, SKP2 binds to p300, an acetylase essential for p53 activity (Tang et al., 2008), preventing p300-dependent p53 acetylation (Kitagawa et al., 2008). Consequently, p53-dependent transcription of p21 (encoded by *CDKN1A*) is inhibited (Kitagawa et al., 2008). Strengthening its pro-proliferative activities, SKP2 also acts as a coactivator for c-Myc-dependent transcription (Kim et al., 2003), and, since c-Myc represses *CDKN1A* expression (Wu et al., 2003), this provides a third method of p21 repression by SCF-SKP2. In these ways, SCF-SKP2 directs unimodal control of p21's protein stability, and additional bimodal control of *CDKN1A* mRNA levels.

Many proteins that promote cell cycle progression have simultaneously evolved mechanisms to ensure the fidelity of the DNA replication that they stimulate. SKP2 is no exception and, through ubiquitination of a key DSB repair protein, promotes the localisation of ATM to DSBs, in this way promoting DSB repair (Wu et al., 2012). This is

an activity that takes place within seconds of DSB induction, but, at longer timepoints after treatment with the topoisomerase II inhibitor doxorubicin (which also induces DSBs), SKP2 is subject to degradation by the von Hippel-Lindau (VHL) ubiquitin ligase, shutting off pro-proliferative SKP2 signalling (Roe et al., 2011).

Consistent with these functions, SCF-SKP2 is a potent oncogene, and its potential pharmacological inhibition has attracted significant attention (Frescas and Pagano, 2008). Most prominently, encouraging data demonstrate that a small molecule inhibitor for SCF-SKP2, which inhibits the SKP1-SKP2 interaction to halt the proteasomal degradation of p21 and p27, reduces tumourigenesis in a mouse model (Chan et al., 2013).

Cell cycle checkpoints

In addition to the G1/S checkpoint, cells employ other cell cycle checkpoints, at other stages of the cell cycle, to maintain the integrity of the genome.

Intra-S checkpoint

The intra-S phase checkpoint slows down replication – but does not induce a full arrest – to allow time for DNA repair upon DNA damage in S phase (Chao et al., 2017). The major regulators of the intra-S checkpoint are the kinases, ATR and checkpoint kinase 1 (Chk1) (Iyer and Rhind, 2017). Agents that induce replication stress, such as hydroxyurea or topoisomerase poisons, cause the formation of ssDNA (Iyer and Rhind, 2017). This ssDNA becomes coated by RPA molecules (Fanning et al., 2006), which activate ATR either via RAD9a-TOPB1 (Kumagai et al., 2006; Cotta-Ramusino et al., 2011), or ETAA1 (Haahr et al., 2016; Bass et al., 2016). Subsequently, ATR phosphorylates Chk1 at S317 and S345, causing its activation (Liu et al., 2000).

Although these mechanisms depend on formation of ssDNA, Chk1 is also required for the progression of physiological, non-stressed DNA replication, where extensive stretches of ssDNA are not generated. In this context, the SPRTN metalloprotease

directly cleaves Chk1, evicting Chk1 from chromatin and generating active fragments of Chk1 that phosphorylate substrates such as SPRTN itself, which degrades DPCs ahead of the fork to sustain healthy DNA replication (Halder et al., 2019; Panagopoulos and Altmeyer, 2020).

Chk1 activated by the intra-S checkpoint phosphorylates Cdc25A, a phosphatase that removes inhibitory phosphorylations from CDK1/2 (Shen and Huang, 2012). This Chk1-mediated phosphorylation tags Cdc25a for degradation via β-TrCP (Busino et al., 2003), increasing the inhibitory phosphorylation on CDKs and preventing DNA replication (Sørensen et al., 2003; Xiao et al., 2003; Mailand et al., 2000; Busino et al., 2003).

S/G2 checkpoint

An S/G2 checkpoint ensures that cells do not proceed into G2 phase until DNA replication is complete (Saldivar et al., 2018). During DNA replication, ATR is maintained in an active state by ETAA1, and ATR phosphorylates Chk1, which in turn inactivates the mitotic CDK, CDK1. This prevents the activating phosphorylation of the G2/M transcription factor, FOXM1, by CDK1, and inhibits premature cyclin B expression during an unfinished S phase. As such, ATR inhibition causes premature G2 and mitotic entry, under-replicated DNA, and DNA damage (Saldivar et al., 2018).

G2/M checkpoint

The G2/M checkpoint prevents cells with damaged DNA from entering mitosis, which can exacerbate DNA damage, cause mitotic catastrophe, or transfer damage to the next generation (Gelot et al., 2015). The G2 checkpoint is temporally located closer to the boundary with mitosis than the G1 checkpoint is to the S phase boundary (Chao et al., 2017), and, for this reason, cells in G2 are the most sensitive to cell cycle arrest. In G2, the load of DNA damage proportionally increases the duration of arrest (Chao et al., 2017).

The G2/M checkpoint is largely controlled through p53 (Taylor and Stark, 2001), which directs the transcriptional repression of the G2/M cyclin B1 (encoded by *CCNB1*) in response to DNA damage, reducing cyclin B1-CDK1 activity and preventing inappropriate entry into mitosis (Innocente et al., 1999). p53-mediated expression of p21 (Niculescu et al., 1998), which reduces activity of cyclin B-CDK1 (Bunz et al., 1998; Bates et al., 1998), GADD45 (Wang et al., 1999), which inhibits cyclin B-CDK1 activity (Zhan et al., 1999), and 14-3-3σ (Hermeking et al., 1997), which prevents entry of cyclin B1/CDK1 to the nucleus (Chan et al., 1999), also contribute to G2/M arrest. In parallel, p53-independent control of the G2/M checkpoint is mediated by the ATR-Chk1 axis (Parker and Piwnica-Worms, 1992; O'Connell et al., 1997).

In summary, checkpoints exist at every stage of the cell cycle, to prevent the replication or division of cells with damaged DNA, and to allow time for DNA repair.

p53

p53, the 'Guardian of the genome', is predominantly responsible for coordinating the cell cycle checkpoints (Lane, 1992), and is a significant focus of this thesis. p53 is a transcription factor that is rapidly upregulated in response to many cellular stresses, including DNA damage, hypoxia, nucleotide depletion, and oncogene activation (Kastenhuber and Lowe, 2017; Vogelstein et al., 2000; Bieging et al., 2014; Vousden and Prives, 2009). p53 mediates tumour suppression by eliciting transcriptional changes to control the cell cycle (Kastenhuber and Lowe, 2017), apoptosis (Fridman and Lowe, 2003), metabolism (Vousden and Ryan, 2009), and DNA repair (Janic et al., 2018; Poletto et al., 2016). Under basal conditions, p53 is subject to continuous polyubiquitylation and degradation by the ubiquitin ligase MDM2 (Haupt et al., 1997; Kubbutat et al., 1997). As a result, p53 has one of the shortest half-lives of any protein: ~30 minutes (Ute M. Moll, 2002; Haupt et al., 1997; Kubbutat et al., 1997). Crucially, *MDM2* is a direct transactivation target of p53, forming a negative feedback loop that causes oscillation of p53 levels after DNA damage, with a period of ~5.5 h (Lahav et al.,

2004; Geva-Zatorsky et al., 2006; Loewer et al., 2010). While p53 pulsing in this canonical manner transactivates cell cycle arrest and DNA repair genes (like *CDKN1A* and *XPC*), sustained p53 activation – for example, caused by combined irradiation and nutlin-3 treatment – induces more irreversible apoptosis and senescence genes (like *BAX* and *PML*) (Purvis et al., 2012).

Control of p53 by MDM2

Demonstrating the importance of MDM2, MDM2-deficient mice exhibit embryonic lethality, and, highlighting MDM2's regulation of p53, this lethality is rescued in p53 co-deficient mice (Montes de Oca Luna et al., 1995). Lethality of MDM2-deficient mice is also partially rescued in Bax co-deficient mice, indicating excessive p53/Bax-dependent apoptosis as the mechanism for lethality (Chavez-Reyes et al., 2003).

In addition to controlling p53 stability through p53 polyubiquitination, MDM2 provides second-line p53 inhibition through p53 monoubiquitination, which causes p53's export from the nucleus (Li et al., 2003; Boyd et al., 2000; Geyer et al., 2000), and third-line inhibition by preventing p53-dependent transactivation. MDM2 mediates this inhibition through several mechanisms (Momand et al., 1992; Kussie et al., 1996), including by binding and concealing p53's transactivation domain (Oliner et al., 1993; Leng et al., 1995), and by inhibiting the basal transcription machinery at p53 target promoters (Thut et al., 1997).

The major mechanism contributing to increased p53 stability after DNA damage is ATM-mediated phosphorylation of MDM2. ATM is among the first proteins activated in response to SSBs (Khoronenkova and Dianov, 2015), DSBs (Lee and Paull, 2005), and oxidative stress (Guo et al., 2010), and phosphorylates a network of substrates in turn (Matsuoka et al., 2007). Mechanistically, ATM-mediated MDM2 phosphorylation prevents the oligomerisation of MDM2 via its RING domains, in this way inhibiting MDM2-dependent polyubiquitylation of p53, increasing p53 stability and promoting p53 upregulation (Cheng et al., 2009, 2011; Cheng and Chen, 2010).

In addition to ATM, other factors also converge on the MDM2-p53 interaction. Under basal conditions, MDM2 undergoes auto-ubiquitination, triggering its persistent degradation. However, this activity is counteracted by USP7, the major deubiquitinase (DUB) for MDM2 (Cummins et al., 2004; Li et al., 2004, 2002). As such, USP7 pharmacological inhibition destabilises MDM2, upregulates p53, and inhibits the growth of p53-WT tumours (Turnbull et al., 2017; Kategaya et al., 2017). Furthermore, USP7S, a serine-containing isoform of USP7, provides an additional layer to the intricacy of the MDM2-p53 axis (Khoronenkova et al., 2012). USP7S is phosphorylated in unperturbed conditions at S18 by CK2, blocking its ubiquitin-dependent degradation. However, after DNA damage, ATM phosphorylates and activates the phosphatase PPM1G, which dephosphorylates USP7S at S18, leading to ubiquitination and degradation of USP7S. In turn, this causes MDM2 auto-ubiquitination and destabilisation, and allows p53 upregulation upon DNA damage (Khoronenkova et al., 2012).

In addition, specific inhibition of MDM2 following SSBs is mediated by the tumour suppressor ARF, which typically responds to oncogene activation to inhibit MDM2 and stabilise p53 (Ozenne et al., 2010). However, ARF is also upregulated by SSBs, inhibiting MDM2 and upregulating p53 (Orlando et al., 2014). Finally, small molecule inhibition of the p53-MDM2 interaction, by Nutlin-3a (Vassilev et al., 2004) or RITA (Issaeva et al., 2004), also leads to p53 upregulation.

Transcriptional repression by p53

The expression of ~2200 genes is increased after p53 induction, while ~2700 genes' expression is reduced (Fischer et al., 2014). p53 activation results in the transcriptional downregulation of a range of genes that promote cell cycle progression, ensuring maintenance of cell cycle arrest in G0 and G2, and allowing complete repair of damaged DNA (Fischer, 2017; Fischer et al., 2014; Engeland, 2018). Many of these genes are repressed indirectly by p53, for example through the DREAM (DP, RB-like, E2F and MuvB) complex (Fischer et al., 2016; Engeland, 2018; Nikulenkov et al., 2012), which is

under the control of p21 (Sadasivam and DeCaprio, 2013; Engeland, 2018; Litovchick et al., 2007; Schmit et al., 2007; Mannefeld et al., 2009). The DREAM complex represses the transcription of ~250 cell cycle genes, including the G1/S and S phase genes, *CDK2* and *CCNA2* (Engeland, 2018). To produce the DREAM complex, p21 reduces CDK activity and causes accumulation of hypophosphorylated p130/p107 complexes, which, along with the repressive E2Fs, E2F4-5/DP, and the MuvB core complex, form transcriptionally repressive DREAM complexes (Litovchick et al., 2007; Schmit et al., 2007). Consequently, the DREAM complex binds CHR or E2F elements in target promoters to repress transcription (Engeland, 2018).

The repression of other genes, however, depends on direct binding of p53 to DNA. The *MYC* gene (encoding c-Myc) serves as a useful case study to highlight p53-mediated transcriptional repression. *MYC* was initially identified as a target for direct p53 repression; p53 binds the *MYC* promoter at non-canonical p53-binding sequences, causing histone deacetylation at *MYC*'s promoter. This repression is independent of p21, and important for p53-mediated quiescence (Ho et al., 2005). A later study discovered an additional mechanism, showing that repression of *MYC* by p53 is dependent on direct binding of p53 to a distal enhancer in the *MYC* gene, ~50 kb downstream of the transcription start site (Porter et al., 2017). p53 binding increases chromatin accessibility at this site, but accessibility to the *MYC* promoter region is reduced as a result, due to deposition of nucleosomes (Porter et al., 2017). This study also reproduced previous data (Ho et al., 2005), demonstrating that c-Myc overexpression could cause DNA damage-resistant S phase entry (Porter et al., 2017). A later discovery demonstrated that, although p53 *does* bind ~50 kb downstream of the *MYC* transcription start site, this region actually encodes a different gene, the long non-coding RNA, *Pvt1b*. *Pvt1b* is a direct p53 target gene, which accumulates at the *MYC* transcription start site upon p53 activation to repress *MYC* expression (Olivero et al., 2020). Finally, another study reported further binding sites of p53 in the *MYC* gene (Santoro et al., 2019). This study

showed that, in untreated conditions, p53 binds *MYC*'s 3' UTR, but after DNA damage p53 is further enriched at two sites near *MYC*'s transcriptional start site. As a consequence, p53 loss (in mammary stem cells) leads to *MYC* activation, which promotes increased proliferation in turn (Santoro et al., 2019).

Therefore, it is likely that p53 directs *MYC* transcriptional repression through both *MYC* locus binding-dependent and -independent mechanisms.

The G1/S transition in cancer

p53 in cancer

Cancer cells deregulate the G1/S transition in order to boost their proliferation and to induce and potentiate genomic instability (Hanahan and Weinberg, 2011; Hume et al., 2020). The most common mutation target in human cancer is *TP53* (Muller and Vousden, 2013), germline mutations in which cause Li-Fraumeni syndrome, a cancer predisposition syndrome (Malkin, 2011). Most loss-of-function mutations in p53 are point mutations localised to its DNA-binding domain, including the hotspot mutations R175, G245, R248, R249, R273 and R282. These mutations inhibit p53's DNA-binding, and cause p53 misfolding, inactivating the protein (Muller and Vousden, 2013). Since p53's active conformation is tetrameric, a single mutant p53 molecule oligomerising with wildtype molecules disrupts the function of the tetrameric complex, exerting a dominant-negative effect (Boettcher et al., 2019; Muller and Vousden, 2013). Although these mutants disturb p53's DNA-binding capacity, they leave its transactivation domain intact, allowing p53 to promote the transcription of novel genes through an oncogenic gain-of-function mechanism (Muller and Vousden, 2013). For example, mutant p53 can direct the aberrant transactivation of chromatin regulatory genes, causing widespread, oncogenic transcriptional changes (Zhu et al., 2015a). However, whether p53 gain-of-function or dominant-negative loss of function constitutes the major oncogenic activity of p53 mutation remains debated (Boettcher et al., 2019).

ATM in cancer

p53's activity and stability are under the control of ATM. Germline mutations in ATM cause Ataxia Telangiectasia, a disease characterised by susceptibility to lymphoma and leukaemia (Rothblum-Oviatt et al., 2016). Most ATM mutations in Ataxia telangiectasia result in protein truncation, causing no protein to be expressed (Rothblum-Oviatt et al., 2016). However, sporadic mutation to ATM can also occur. The most common sporadic ATM mutations found in cancer are R250*, R337H, and R3008H, but mutations span the entirety of the >3000 amino acid protein (Choi et al., 2016). Sporadic ATM mutations are most often found in blood cancers, with more than 45% of mantle cell lymphoma cases expressing mutant ATM. Deletion of the *ATM* gene, and hypermethylation of its promoter, are also common in cancer, inhibiting DNA repair and p53 signalling (Choi et al., 2016; The ICGC/TCGA Pan-Cancer Analysis of Whole Genomes Consortium, 2020).

p21 in cancer

CDKN1A expression is low in p53-deficient tumours, due to loss of its transcriptional activation (Abbas and Dutta, 2009), and p21's degradation is also enhanced in cancer, for example through hyperactive SCF-SKP2-mediated degradation (Gstaiger et al., 2001; Yokoi et al., 2004). In contrast, mutations in p21 are rarely – but not never – found. For example, an R94W mutation to p21 was detected in breast cancer patients, which prevents p21 from inhibiting CDKs (Balbin et al., 1996). Finally, the *CDKN1A* gene itself is rarely deleted more frequently than would be expected in cancer (Abbas and Dutta, 2009; The ICGC/TCGA Pan-Cancer Analysis of Whole Genomes Consortium, 2020).

Conversely, p21 can also play oncogenic roles. For example, chronic, p53-independent p21 expression can atypically occur in proliferating Ki67-positive cells. In these cells, p21 inhibits the PCNA-dependent ubiquitin ligase, CRL4-CDT2, preventing CRL4-CTD2-dependent degradation of replication licencing factors, causing re-replication, genomic instability, and oncogenesis (Galanos et al., 2016). Furthermore, in addition to sequestration away from its targets, aberrant localisation of p21 to the cytosol can also

have gain-of-function oncogenic properties, such as inhibition of pro-apoptotic proteins (Roninson, 2002).

MDM2 in cancer

MDM2 is the major negative regulator of p53, and is commonly amplified or overexpressed in cancer. The majority of the time this occurs in p53 wild-type tumours, where *MDM2* overexpression can have maximal impact (Wade et al., 2013). For example, ~16% of osteosarcomas harbour *MDM2* gene amplifications (Mejia-Guerrero et al., 2010; Wade et al., 2013; The ICGC/TCGA Pan-Cancer Analysis of Whole Genomes Consortium, 2020).

Cyclin D1 in cancer

Cyclin D1, whose degradation is required to induce quiescence after DNA damage (Santra et al., 2009) is frequently overexpressed in cancer, and this is an event which occurs early during cancer development, suggesting it is a driving event (Kim and Diehl, 2009; Diehl, 2002). Much of cyclin D1 overexpression can be attributed to amplification of the *CCND1* gene. For example, *CCND1*, encoded on 11q13, is amplified in ~15% of breast tumours (Roy and Thompson, 2006; The ICGC/TCGA Pan-Cancer Analysis of Whole Genomes Consortium, 2020).

Loss of cyclin D1's ubiquitin-mediated degradation is also often frequently found in cancer. For example, the E3 ligase for DNA damage-mediated cyclin D1 degradation, FBXO31 (Santra et al., 2009), is encoded on chromosome 16q24.3, a region frequently lost in breast tumours (Kumar et al., 2005). Furthermore, mutations in SCF-Fbx4, an E3 ligase which also degrades cyclin D1, prevent dimerization of Fbx4 and inactivate the ligase (Barbash et al., 2008) [although more recent data cast doubt on the roles of these factors in the regulation of cyclin D1's stability, instead identifying CRL4-AMBRA1 as the E3 ligase for cyclin D1 (Simoneschi et al., 2021)]. Finally, increased *CCND1* transactivation also contributes to its overexpression (Inoue and Fry, 2015).

In summary, these studies highlight the myriad (but far from exhaustive) mechanisms that cancer cells deploy to hyperactivate pro-cell cycle factors, and to inactivate anti-cell cycle factors.

Short G1 phases in cancer

Although hyperactivation of proteins that promote S phase entry increases proliferation, hastening S phase entry also has a second, more insidious function.

Increases in the copy numbers of *MYC* (8q24.1) and *CCNE1* (19q12-13) are among the most frequent events in human cancer (Beroukhim et al., 2010; The ICGC/TCGA Pan-Cancer Analysis of Whole Genomes Consortium, 2020). Overexpression of these genes shortens G1 phase, causing premature entry into S phase (Macheret and Halazonetis, 2018). Strikingly, this causes transcription-replication collisions, which lead, in turn, to replication fork collapse, DSB formation, and chromosome aberration (Macheret and Halazonetis, 2018; Halazonetis et al., 2008; Hills and Diffley, 2014). In a similar manner, disruption of cyclin F-dependent E2F1 degradation accelerates S phase entry, causing replication stress and DSB formation (Burdova et al., 2019; Clijsters et al., 2019). In this way, expediting S phase entry provides a two-pronged oncogenic mechanism. Firstly, faster S phase entry means faster proliferation. Secondly, faster S phase entry induces genomic instability, driving tumour evolution and therapy resistance.

G1/S components in therapy

Given hyperactivation of G1/S transition components in cancer, some components are targeted by cancer therapies. The most promising drugs target CDK4/6, such as Palbociclib, which prevents CDK4 holoenzyme formation by sequestering CDK4 away from the other holoenzyme constituents, cyclin D and p27 (Y74-p) (Alvarez-Fernandez and Malumbres, 2020; Guiley et al., 2019). Palbociclib is FDA-approved for use in a subset of breast cancers, used alongside oestrogen antagonists, and other pre-clinical studies have demonstrated that its use in combination with chemotherapies such as the

mitotic poison, docetaxel, also displays synergistic anti-cancer effect (Salvador-Barbero et al., 2020; Alvarez-Fernandez and Malumbres, 2020). Nevertheless, given the intricate and multi-layered nature of signalling at the G1/S transition, other targets should also be explored – both through the use of small molecule inhibitors, but also through use of proteolysis-targeting chimeras (PROTACs), which recruit ubiquitin ligases to target molecules to induce selective proteolytic degradation (Sun et al., 2019).

NUCKS1

This thesis is primarily focused on NUCKS1 (nuclear casein kinase and cyclin-dependent kinase substrate 1). Discovered in 1985, NUCKS1 is a nuclear-localised transcription factor (Ostvold et al., 1985). NUCKS1's major functional domain is a DNA-binding domain, spanning amino acid residues 183-192, that encompasses a GRP DNA-binding motif (Ostvold et al., 2001; Grundt et al., 2002, 2007). NUCKS1 is 27 kDa (although migrates at ~45 kDa by SDS-PAGE) (Ostvold et al., 2001, 1985), and is targeted by more post-translational modifications than any other protein (Wisniewski et al., 2008). Most prominently, CDK1 (at S181), ATM/ATR (at S14 and S54), and CK2 all phosphorylate the NUCKS1 protein (Grundt et al., 2002; Matsuoka et al., 2007; Wisniewski et al., 2008; Parplys et al., 2015). The functions of these phosphorylations are not characterised, with the exception of CDK1, whose phosphorylation of NUCKS1 at S181, during G2/M phase of the cell cycle, inhibits the binding of NUCKS1 to DNA (Grundt et al., 2002). NUCKS1 is a member of the high-mobility group (HMG) family of proteins, which regulate chromatin accessibility to control transcription (Ozturk et al., 2014), in this way regulating pathways including cell cycle progression (He et al., 2018), DNA repair (Lange et al., 2008), and oncogenesis (Wood et al., 2000).

Functions of NUCKS1

Insulin regulation

NUCKS1 has three major reported functions. Firstly, NUCKS1 regulates the expression of the insulin receptor gene, *INSR*, as well as other genes in the insulin pathway (Qiu et

al., 2014). Mechanistically, NUCKS1 binds at the promoters of these genes, opening chromatin and enabling recruitment of RNA polymerase II (RNAPII). As a consequence, deletion of *NUCKS1* in mice reduces insulin receptor levels, leading to insulin resistance and obesity (Qiu et al., 2014).

DNA repair regulation

Secondly, NUCKS1 regulates DNA repair - in a manner that does not depend on its transcriptional activity - via homologous recombination (HR). In HR, sister chromatids are used to template DNA synthesis during S and G2 phases of the cell cycle (Hustedt and Durocher, 2016). HR is initiated by end resection of a nascent DSB, giving rise to a stretch of single-stranded DNA, which becomes coated by the single-stranded DNA-binding protein, RPA. Subsequently, BRCA2 recruits Rad51 to perform strand invasion, before repair is completed by Holliday junction resolution (Tarsounas and Sung, 2020).

NUCKS1 is a paralogue of RAD51AP1 (Parplys et al., 2015), a protein that stimulates RAD51's recombinase activity in the HR pathway (Wiese et al., 2007). However, NUCKS1 does not interact with RAD51, and does not stimulate RAD51's recombinase activity (Parplys et al., 2015). Instead, NUCKS1 interacts with and stimulates the activity of RAD54, a partner of RAD51 that also participates in strand invasion during HR (Maranon et al., 2020). Consistent with its role in HR, high NUCKS1 levels correlate with low levels of the ATM target and DNA damage marker, γH2AX (De Angelis et al., 2018).

Cell proliferation regulation

Thirdly, NUCKS1 promotes cell proliferation. Although the full details are yet to be elucidated, NUCKS1 engages this function through stimulation of the mTOR pathway (Zhao et al., 2020a), and regulation of CDK1 levels (Zhao et al., 2020b). As a result, loss of NUCKS1 significantly perturbs cell cycle progression (Yuan et al., 2019; Huang et al., 2019; Zhao et al., 2020b; a).

NUCKS1 expression

In addition, several studies have focused on how the expression of NUCKS1 is regulated. Most prominently, both amino acids and hormones are able to trigger substantial upregulation of NUCKS1, leading to NUCKS1-dependent control of milk synthesis in mammary epithelial cells – an effect mediated through a putative regulation of the mTOR pathway by NUCKS1 (Yuan et al., 2019). Furthermore, an interesting report showed that the expression of *NUCKS1* is regulated by miRNAs, with significant relevance in cancer. MicroRNA-137 binds the 3'UTR of *NUCKS1*, negatively regulating its expression and, because miRNA-137 is frequently lost in lung cancer, contributing to *NUCKS1* upregulation in lung cancer (Shen et al., 2016). Moreover, putative binding sites for p53 are found in the *NUCKS1* promoter (Nikulenkov et al., 2012), suggesting regulation of NUCKS1 after DNA damage. Finally, the *NUCKS1* locus is frequently targeted for amplification in breast cancer (Naylor et al., 2005; Drosos et al., 2009), and wider analysis reveals copy number gains and amplifications of the *NUCKS1* gene in most cancer types (The ICGC/TCGA Pan-Cancer Analysis of Whole Genomes Consortium, 2020).

NUCKS1 in cancer

Given its widespread overexpression in cancer, numerous reports have investigated a putative use of NUCKS1 as a cancer biomarker (Qiu et al., 2015), including for recurrence-free survival in cervical cancer (Gu et al., 2014), and for prognosis and recurrence in endometrial cancer (Liu et al., 2015). Consistent with this, impressive data demonstrate that NUCKS1 promotes tumourigenesis in mouse models of hepatocellular carcinoma (Cheong et al., 2016) and lung cancer (Zhao et al., 2020b).

Aims of the study

Despite clear regulation of proliferation and oncogenesis by NUCKS1, precise mechanistic studies have not been performed, and many details remain uncharacterised. In particular, the following major questions remain unanswered:

1) Does NUCKS1 have a direct or indirect impact on the cell cycle?
2) Which phase(s) of the cell cycle does NUCKS1 affect?
3) Does NUCKS1 directly regulate the transcription of any cell cycle genes?
4) Is NUCKS1 regulated by the cell cycle?
5) Is NUCKS1 regulated by mitogens?
6) Is NUCKS1 regulated by DNA damage?
7) What are the full mechanisms driving NUCKS1 overexpression in cancer?

Here, we set out to address these questions.

Materials and Methods

Cell culture

Cell lines, shown in Table 1, were cultured in a humidified incubator at 37ºC and 5% CO_2. All cell lines were cultured in DMEM (Life Technologies) with 10% foetal bovine serum (FBS), other than TIG-1 and NBE1-hTERT, which were cultured with 15% FBS.

Cell lines		
Cell line	**Tissue of origin**	**Source**
TIG-1	Primary embryonic fibroblasts	Coriell Institute Cell Repository
RPE1-hTERT	Retinal pigment epithelial	Prof. Stephen Jackson (Cambridge)
RPE1-hTERT *TP53*-knockout	Retinal pigment epithelial	Prof. Stephen Jackson (Cambridge)
NBE1-hTERT	Normal bronchial epithelial	Prof. Anderson Ryan (Oxford) via Pamela Rabbitts (Leeds) (Stead et al., 2012)
U2OS	Osteosarcoma	ATCC
U2OS *NUCKS1*-knockout	Osteosarcoma	This study
A549 SKP2 doxycycline-inducible	Lung adenocarcinoma	Prof. Shyamala Maheswaran (Tajima et al., 2019)
HCT116	Colorectal cancer	ATCC
HCT116 *TP53*-knockout	Colorectal cancer	Prof. Vogelstein (Bunz et al., 1998)
RKO	Colorectal cancer	ATCC
HT29	Colorectal cancer	ATCC
DLD1	Colorectal cancer	ATCC
CACO2	Colorectal cancer	ATCC

Table 1: Cell lines.

Transfections

siRNA transfections were performed using Lipofectamine RNAiMAX, according to the manufacturer's instructions, using siRNAs as indicated in Table 2. siRNA was used at 30 nM, and cells were transfected for 3 days, with the exception of proliferation assays, where cells were analysed at the indicated days after transfection. Plasmid transfections

were performed using Lipofectamine 3000, according to the manufacturer's instructions, using plasmids as indicated in Table 3.

siRNAs	
Target	**Forward sequence (+ 3' TT)**
Control	Eurogentec, SR-CL000-005
NUCKS1 (1)	GAGGCGAUCUGGAAAGAAU
NUCKS1 (2)	GGCAUCUAAAGCAGCUUCU
NUCKS1 3' UTR	GCAGGAGGGACUAGAGAAAUU
SKP2	GCUUCACGUGGGGAUGGGA
p21	GAUGGAACUUCGACUUUGU
p27	AAGGUUGCAUACUGAGCCAAG
p53	AAGACUCCAGUGGUAAUCUAC

Table 2: siRNAs.

Plasmids	
Name	**Source**
SKP2	Prof. Vincenzo D'Angiolella (Oxford)
p53 WT	Prof. Eric O'Neill (Oxford)
p53 R175H	Prof. Eric O'Neill (Oxford)
p53 R248W	Prof. Eric O'Neill (Oxford)
p53 R273H	Prof. Eric O'Neill (Oxford)
NUCKS1	Abgent (Generon)

Table 3: Plasmids.

CRISPR-Cas9 genome editing

NUCKS1 CRISPR plasmids were purchased from SantaCruz (sc-413018 and sc-413018-HDR), transfected into U2OS cells using Lipofectamine 3000 for 48 h, selected in 5 µg/ml puromycin for three days, and were expanded as colonies from single cells. Successful *NUCKS1*-knockouts were screened using RT-qPCR and Western blotting.

Western blotting

Whole cell extracts

Pelleted cells were resuspended in 1 packed-cell volume (PCV) of buffer I (10 mM Tris-HCl pH 7.8 and 200 mM KCl, complete with aprotinin, chymostatin, leupeptin, pepstatin (1 µg/ml), 1 mM PMSF, 1 mM DTT, and 1 mM NEM), followed by 2 PCV of buffer II (10 mM Tris-HCl pH 7.8, 600 mM KCl, 2 mM EDTA, 40% glycerol, 0.2% Nonidet P-40, complete with aprotinin, chymostatin, leupeptin, pepstatin (1 µg/ml), 1 mM PMSF, 1 mM DTT, and 1 mM NEM), and incubated for 30 min at 4^{o}C. Samples were then centrifuged at 21,380 g for 30 min, supernatants (containing whole cell extracts) were recovered, and protein concentrations were measured using the Bradford assay.

Cytoplasmic/Nuclear/chromatin fractionations

Pelleted cells were resuspended in 2 PCV buffer A (10 mM Hepes, 10 mM KCl, 340 mM sucrose, 10% glycerol, pH 7.45, complete with aprotinin, chymostatin, leupeptin, pepstatin (1 µg/ml), 1 mM PMSF, 1 mM DTT, and 1 mM NEM), followed by treatment with 0.1% Triton X-100 for 5 min at 4^{o}C. Cells were then centrifuged at 300 g for 3 min; the supernatant contains the cytosol, while pellets are nuclei. Nuclear pellets were washed twice with buffer A and then resuspended in buffer B (3 mM EDTA, 0.2 mM EGTA, 5 mM Hepes, pH 7.9, complete with aprotinin, chymostatin, leupeptin, pepstatin (1 µg/ml), 1 mM PMSF, 1 mM DTT, and 1 mM NEM) and incubated for 10 min at 4^{o}C. Nuclei were then centrifuged at 1700 g for 3 min; the supernatant is the nuclear soluble fraction, while the pellet is chromatin. The chromatin pellet was then resuspended in benzonase buffer (25 mM Tris, 20 mM NaCl, 2 mM KCl, pH 7.9) and centrifuged for 5000 g for 5 min. The pellet was resuspended in digestion buffer (benzonase buffer supplemented with 4 mM $MgCl_2$, 200 U/ml Benzonase, 25 U/µl RNAse A) and incubated overnight at 4^{o}C. The resulting suspension is the chromatin fraction.

SDS-PAGE

Samples were separated by SDS-PAGE on polyacrylamide gels for 2 h at 125 V and transferred to Immobilon-FL PVDF membranes (Millipore) for 3 h at 25 V. Membranes were immediately fixed in 0.4% glutaraldehyde for 15 min (to improve the signal of NUCKS1), stained with Ponceau S solution, and blocked in Odyssey Blocking Buffer for 1 h at RT. Antibodies (as outlined in Table 4) were added overnight at 4ºC in Odyssey Blocking Buffer:PBS-T 1:1. After washing in PBS-T, secondary antibodies (as outlined in Table 4) were added for 1 h. Membranes were washed further with PBS-T, followed by PBS, and were scanned using the Odyssey image analysis system (Li-Cor Biosciences).

Antibodies			
Antibody	**Catalogue number**	**Source**	**Dilution**
NUCKS1		Kind gift from Prof. Anne Østvold (Ostvold et al., 1985)	1:2000
NUCKS1	12023-2-AP	ProteinTech	1:1000
SKP2	32-3300	Thermofisher	1:1000
p21	#2947	Cell signalling	1:2000
p27	#2552	Cell signalling	1:500
p53	sc-126	Santa Cruz	1:500
PCNA	sc-56	Santa Cruz	1:1000
MLH1	ab92312	Abcam	1:2000
Beta-Actin	ab6276	Abcam	1:10,000
Alpha-Tubulin	T6199	Sigma	1:5,000
Alpha-Tubulin	ab4074	Abcam	1:5,000
Vinculin	ab18058	Abcam	1:1,000
Histone H3	ab201456	Abcam	1:2000
Cyclin A2	ab181591	Abcam	1:2000
IRDye® 800CW Goat anti-Rabbit IgG (H + L)	925-32211	Li-Cor	1:10,000
IRDye® 680RD Goat anti-Mouse IgG (H + L)	925-68070	Li-Cor	1:10,000
IRDye® 680RD Goat anti-Rabbit IgG Secondary Antibody	925-68071	Li-Cor	1:10,000

IRDye® 800CW Goat anti-Mouse IgG Secondary Antibody	926-32210	Li-Cor	1:10,000

Table 4: Antibodies.

RT-qPCR

RNA extraction was performed using the RNeasy kit (Qiagen), according to the manufacturer's instructions. Reverse transcription was performed using the Superscript II Reverse Transcriptase kit (Thermofisher), according to the manufacturer's instructions. RT-qPCR was performed using Fast SYBR Green Master Mix (Thermofisher) and the 7500 Fast Real-Time PCR system (Applied Biosystems), using primers as indicated in Table 5.

ChIP

Cells were fixed in 1% formaldehyde for 15 min, followed by quenching in 125 mM glycine for 5 min. Cells were then harvested and centrifuged at 250 g for 5 min, and pellets were resuspended in SDS lysis buffer (1% SDS, 10 mM EDTA, 50 mM Tris pH 8.0, complete with protease inhibitors) for 10 min at 4 ^{o}C. Lysates were then sonicated using the Bioruptor Plus (Diagenode) to achieve DNA fragments of size 100-500 bp. Samples were centrifuged at 8000 g for 10 min. The supernatant was diluted 5-fold in ChIP dilution buffer (0.01% SDS, 1.1% Triton X-100, 1.2 mM EDTA, Tris pH 8.0 16.7 mM, NaCl 167 mM, with protease inhibitors) before pre-clearing with protein A and G beads for 1 h at 4^{o}C. Immunoprecipitation was performed at 4^{o}C overnight, using 5 µg normal rabbit IgGs or NUCKS1 antibody.

Protein A/G beads were blocked in ChIP dilution buffer with salmon sperm DNA (0.1 µg/µl) and BSA (0.1 µg/µl) for 30 min, and then 30 µl beads were added per IP, for 2 h at 4^{o}C. After this, samples were washed sequentially in low salt wash solution (0.1% SDS, 1% Triton X-100, EDTA 2 mM, Tris pH 8.0 20 mM, NaCl 150 mM), high salt wash solution (0.1% SDS, 1% Triton X-100, 2 mM EDTA, 20 mM Tris pH 8.0, NaCl 500 mM),

LiCl wash buffer (0.25 M LiCl, 1% Ipegal NP-40, 1% deoxycholate Na, 1 mM EDTA, 10 mM Tris pH 8.0), and finally TE buffer, pH 8.0. Elution was performed in elution buffer (0.1 M $NaHCO_3$, 1% SDS), before samples were incubated with proteinase K (0.04 mg/ml) and RNase A (0.02 mg/ml) at 55°C for 3 h followed by 65°C overnight.

DNA was purified using the QIAquick PCR purification kit (Qiagen) and quantification was performed by qPCR, using primers as indicated in Table 5.

Primers			
Primer	**Use in thesis**	**Forward sequence**	**Reverse sequence**
B2M	RT-qPCR	ATGTCTCGCTCCGTGGCCTTA	ATCTTGGGCTGTGACAAAGTC
GAPDH	RT-qPCR	AGCCACATCGCTCAGACAC	GCCCAATACGACCAAATCC
TBP	RT-qPCR	CGGTTTGCTGCGGTAATCAT	TTTCTTGCTGCCAGTCTGGAC
NUCKS1	RT-qPCR	GCCCGAATCTCTTCCATAATC	TTCTCGACTCGGTCCTGTTT
SKP2	RT-qPCR	GGAAGGGAGTCCCATGAAA	GCTGAAGAGCAAAGGGAGTG
CDKN1A	RT-qPCR	CATGGGTTCTGACGGACATC	TGCCGAAGTCAGTTCCTTGT
CDKN1B	RT-qPCR	TTCATCAAGCAGTGATGTATCTGA	AAGAAGCCTGGCCTCAGAAG
CCNB1	RT-qPCR	CGGGAAGTCACTGGAAACAT	AAACATGGCAGTGACACCAA
RB1	RT-qPCR	TCAGTTGGTCCTTCTCGGTC	TGTGAACATCGAATCATGGAA
CDK6	RT-qPCR	CACTCCAGGCTCTGGAACTT	TGGAGACCTTCGAGCACC
CCND1	RT-qPCR	AGTTGTTGGGGCTCCTCAG	AGACCTTCGTTGCCCTCTGT
MYC	RT-qPCR	CACCGAGTCGTAGTCGAGGT	TTTCGGGTAGTGGAAAACCA
PCNA	RT-qPCR	AAGAGAGTGGAGTGGCTTTTG	TGTCGATAAAGAGGAGGAAGC
MDM2	RT-qPCR	GCAGTGAATCTACAGGGACGC	ATCCTGATCCAACCAATCACC
E2F3	RT-qPCR	AAGTGCCTGACTCAATAGAGAGCC	AGTCTCTTCTGGACATAAGTAAACCTCA
CCND3	RT-qPCR	TTGAGCTTCCCTAGGACCAG	TGACCATCGAAAAACTGTGC
SKP2: -9806 - -9695	ChIP-qPCR	TCTGAGATAGGCTGAGAGGAAA	CTTCAGTAGACGGTAGTGAGAAAC
SKP2 F: -1448 - -1298	ChIP-qPCR	CAATCTTCAGGGAAAGGACGTAG	CTAGGCTAAGCCGTTCATCAAA
SKP2 F: -855 - -673	ChIP-qPCR	CAGCAGAGATAGGCTGAAAG	GCCTTGACAGGTCTCATAAA
SKP2 F: -417 - -266	ChIP-qPCR	GCTACTGTCACCACTCAGCA	GATCGGACGGTGAGCCTAAG
SKP2 F: -346 - -197	ChIP-qPCR	CTCTCTTTCCGCCTGCTCTC	GTGGATCCCAGAACCTGGAC
SKP2 F: -25 - +148	ChIP-qPCR	GTATCTCGAAGGCGGGTAAAG	TAAGCCTAGCAACGTTCCATC
SKP2 F: +420 - +575	ChIP-qPCR	GTGAATGGATGGATGCCTTAG	GCAGAAGGCCTCAAGAATTT
SKP2 F: +843 - +1001	ChIP-qPCR	TGGGATTCCAGCAAGACTTC	GTCACTCCCTTTGCTCTTCA
SKP2 F: +1455 - +1592	ChIP-qPCR	TATCAGTGGACTGCGAAGTGA	CGGGTTGGGTGATTAAACAGATAG
SKP2 F: +10467 - +10629	ChIP-qPCR	CTCTCCCTTGCCCTGTTTAAT	AGGTGTTGGGAAGGAGTAGTA

Table 5: Primers.

Flow cytometry

For the propidium iodide (PI) assay, cells were fixed and permeabilised in 70% ethanol, then treated with RNase A (0.5 µg/ml) and PI (10 µg/ml) for 30 min at 37°C.

For the EdU/PI assay, cells were processed using the Click-iT Plus EdU Flow Cytometry kit (Thermofisher), according to the manufacturer's instructions, using an Alexa Fluor Picolyl Azide 488 dye.

Acquisition following both protocols was performed using the FACS Calibur, followed by analysis using either FlowJo or ModFit.

Bioinformatics

Figure 8A was generated using the SEEK Princeton database (Zhu et al., 2015b), NUCKS1 ChIP-Seq data (Qiu et al., 2014), and Genecodis3 (Tabas-Madrid et al., 2012). Figures 9A-C were generated using GEPIA2 (Tang et al., 2019), Figures 27A and B using UCSC XENA (Goldman et al., 2019), and Figures 28A/B and 29 were generated using CBioPortal (Cerami et al., 2012; Gao et al., 2013).

Comet assay

Cells were trypsinised, mixed with 1% low-melting point agarose (in PBS), and added to microscope slides pre-coated with 1% normal-melting point agarose (in water).

For the alkaline assay, cells were lysed for 1 h in lysis buffer (2.5 M NaCl, 100 mM EDTA, 10 mM Tris base, 1% DMSO, 1% Triton-X100, pH 10.5), and then transferred to electrophoresis buffer (300 mM NaOH, 1 mM EDTA, 1% DMSO, pH 13) for 30 min. Electrophoresis was performed at 25 V (300 mA) for 25 min, followed by neutralisation in 500 mM Tris-HCl, pH 8.1.

For the neutral assay, cells were lysed for 2 h in lysis buffer (2.5 M NaCl, 100 mM EDTA, 10 mM Tris base, 1% sodium lauryl sarcosinate, 10% DMSO, 0.5% Triton X-100, pH 9.5), washed twice in TBE buffer, and electrophoresis was performed at 25 V for 25 min.

DNA was stained in SYBR Gold (1:10,000) (Thermofisher) and analysis was performed using a Nikon NiE microscope and Andor Komet 7.1 software.

EMSA

To dephosphorylate NUCKS1, purified NUCKS1 was incubated with lambda phosphatase (100 units/1 µg of pure NUCKS1), 1X Protein MetalloPhosphatases buffer, and 1 mM $MnCl_2$, for 90 min at 30°C, followed by addition of phosphatase inhibitors (50 X, Merck Millipore).

Binding reactions were set up using indicated quantities of phosphorylated or dephosphorylated NUCKS1, or nuclear extract, in binding buffer (20 mM Tris pH 7.5, 100 mM KCl, 0.2% NP-40, 20% glycerol, 2 mM DTT) using 50 ng salmon sperm DNA (for recombinant protein) or 1 µg salmon sperm DNA (for nuclear extracts) per reaction as non-specific competition. The sequence of the WT *SKP2* probe used was Gccgaccagtcccgctcccgcgggggttgtgggtatctcgaaggcgggtaaagctgca, and for the mutant *SKP2* probe was GccgaccagtcccgctcccgcgggggttgtgggtatctcgaaAAAAAAtaaagctgca. Probes were labelled with fluorescent IRDye 800. In competition assays, a 100-fold molar excess of unlabelled ('cold') probe was included in binding reactions. Reactions were incubated for 15 min at 37°C, loaded on 6% native polyacrylamide gels, and run at 150 V for 50 min. Gels were then scanned using the Odyssey image analysis system (Li-Cor Biosciences). Quantifications were performed using ImageStudio.

Proliferation assays

Cells were treated as indicated and counted at subsequent days, using Trypan Blue and the Countess cell counter (Thermofisher).

Statistics

Statistical tests used for each experiment are shown in figure legends. Statistical analyses were performed in GraphPad Prism 8. ns: $p>0.05$, *: $p\leq0.05$, **: $p\leq0.01$, ***: $p\leq0.001$, ****: $p\leq0.0001$.

Results

Results chapter 1: NUCKS1 regulates G1/S progression

Given putative – but poorly defined – roles for NUCKS1 in cell cycle progression, proliferation, and the DNA damage response, we set out to investigate mechanisms behind these phenotypes. We first validated successful siRNA-mediated depletion (Figure 4A), CRISPR-Cas9-mediated deletion (Figure 4B), and overexpression of NUCKS1 (Figure 4C) by Western blotting.

We then confirmed and expanding on DNA content-based analysis of NUCKS1 cell cycle profiles (Yuan et al., 2019; Huang et al., 2019; Zhao et al., 2020b) by performing EdU/PI bivariate staining and flow cytometry. We found that siRNA-mediated NUCKS1 depletion from the colorectal cancer line HCT116 reduces EdU incorporation and induces G0/G1 arrest, an effect that we found is rescued through overexpression of NUCKS1 (Figure 5A). Similarly, CRISPR/Cas9-mediated deletion of *NUCKS1* from the osteosarcoma line, U2OS, increases G0/G1 and reduces S phase proportions (Figure 5B). Consistent with this, depletion of NUCKS1 from TIG-1 (non-immortalised fibroblasts), NBE1-hTERT (bronchial epithelial cells), or RPE1-hTERT (retinal epithelial cells) produces G0/G1 arrest (Figure 5C). As a consequence, NUCKS1-depleted TIG1, NBE1-hTERT, and *NUCKS1*-knockout U2OS cells display severe proliferation defects (Figure 6A-C). Together, these data confirm previous reports (Yuan et al., 2019; Huang et al., 2019; Zhao et al., 2020b; a), and demonstrate that NUCKS1 is required for cell cycle progression and proliferation.

These phenotypes could potentially be explained by DNA damage signalling in NUCKS1-depleted cells, where DNA damage triggers an ATM-p53-p21 pathway that prevents S phase entry and DNA replication. However, we ruled out this explanation, showing that NUCKS1-depleted TIG-1 or U2OS cells do not accumulate DNA damage,

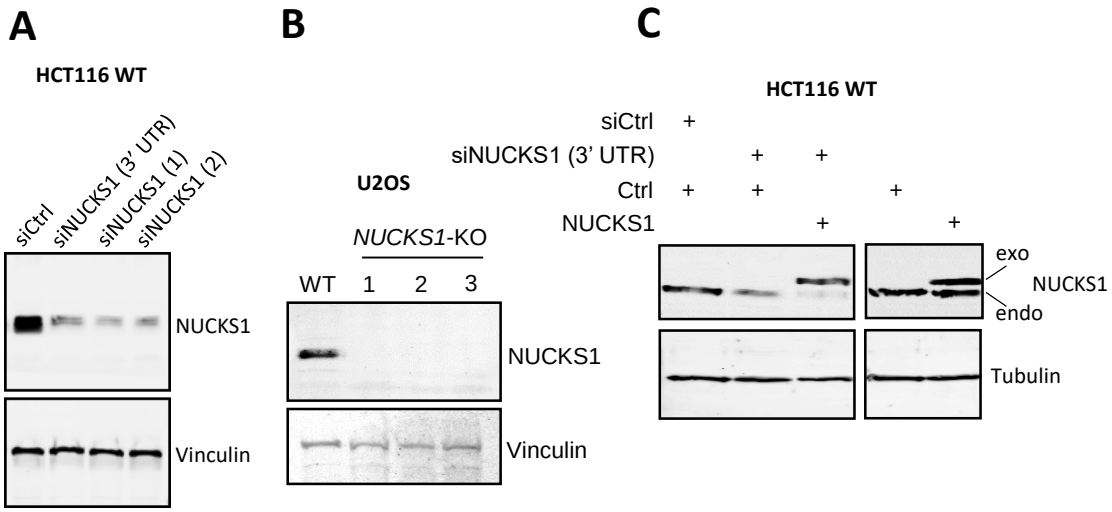


Figure 4: Validation of depletion, knockout, and overexpression. A) siRNA-mediated depletion of NUCKS1, with three distinct siRNA sequences, in HCT116 cells. B) CRISPR-mediated *NUCKS1*-knockout (three distinct clones) in U2OS cells. C) Depletion or overexpression of NUCKS1 in HCT116 cells. Exogenous NUCKS1 is Myc- and His-tagged, and is heavier than endogenous NUCKS1 as a result.

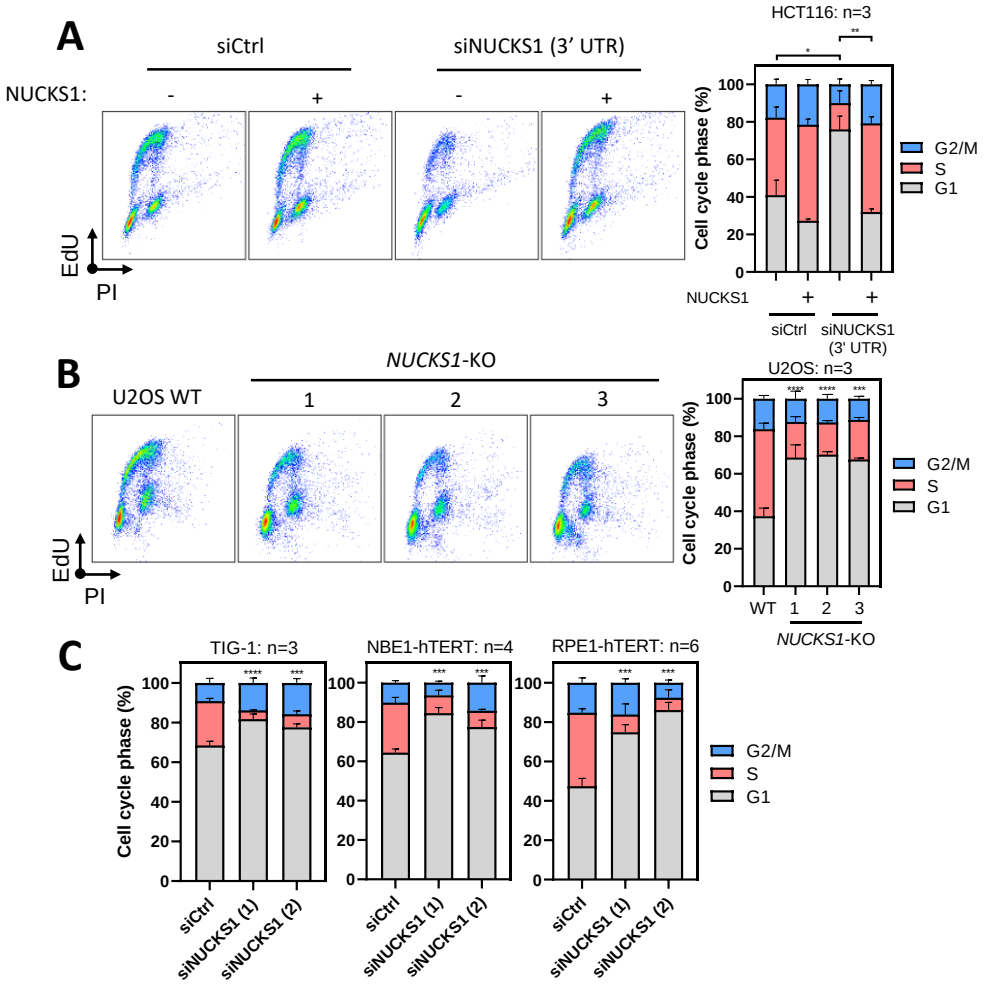


Figure 5: NUCKS1 is required for cell cycle progression. A) Overexpression of NUCKS1 rescues cell cycle progression in NUCKS1-depleted HCT116 cells. Ordinary one-way ANOVA with Sidak multiple comparisons test on S phase population. **B)** CRISPR-mediated *NUCKS1* deletion delays cell cycle progression in U2OS cells. Ordinary one-way ANOVA with Dunnett multiple comparisons test on S phase population. **C)** NUCKS1 depletion delays cell cycle progression in TIG-1, NBE1-hTERT, and RPE1-hTERT cells. Ordinary one-way ANOVAs with Dunnett multiple comparisons test on S phase population. Error bars are SEMs.

measured by the alkaline comet assay (which detects both SSBs and DSBs), unlike treatment with H_2O_2 (used as a positive control) (Figure 7).

Together, these results demonstrate that NUCKS1 plays an active and required role in cell cycle progression, and, since NUCKS1-deficient cells accumulate in G0/G1 phase, suggests that NUCKS1 could play a role at the G1/S transition.

Results chapter 2: NUCKS1-dependent *SKP2* transcription controls S phase entry

Given the reported role for NUCKS1 as a chromatin-remodelling transcription factor, we wondered whether NUCKS1 may regulate the transcription of cell cycle genes – and, in particular, any genes with roles at the G1/S transition.

To investigate this, we combined genome-wide NUCKS1 ChIP-Sequencing data (Qiu et al., 2014) with *NUCKS1* mRNA correlation data (Zhu et al., 2015b). Shared between lists of 586 promoters bound by NUCKS1 (from ChIP-Sequencing) and the top 1000 genes correlating positively with *NUCKS1* in cancer cell lines and patient datasets (from correlation analyses) were genes which we considered putative transcriptional targets of NUCKS1. The GO Biological Processes for the top hits were enriched in pathways including the mitotic cell cycle and the G1/S and G2/M transitions, and included genes regulating DNA replication, the G1/S transition, and the p53 pathway (Figure 8A). We measured the mRNA levels of many of these genes after NUCKS1 depletion by RT-qPCR, and discovered that *SKP2* displays the most reproducible and pronounced downregulation (Figure 8B). SKP2 plays an essential role at the G1/S transition, through its degradation of CIP/KIP CDK inhibitors (Frescas and Pagano, 2008).

Exploring this further, we found that *NUCKS1* exhibits strong and statistically significant positive correlation with *SKP2* across multiple tumour types (Figure 9A), despite no correlation with the control genes that play housekeeping functions, *B2M* and *GAPDH* (Figure 9B). Most prominently, NUCKS1 exhibits strong positive correlation with *SKP2*

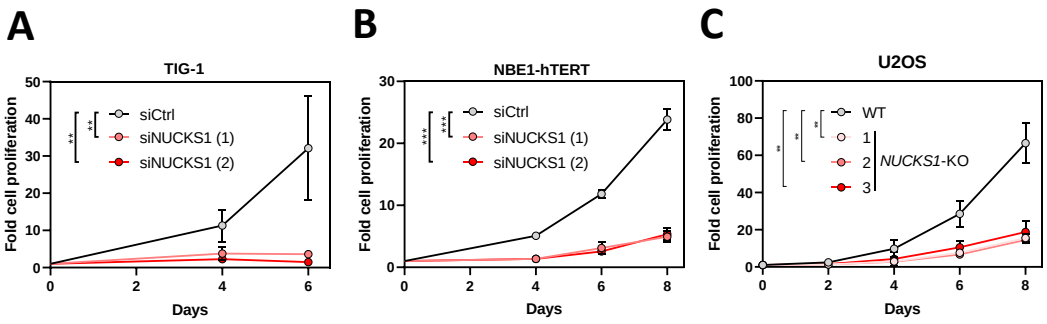


Figure 6: NUCKS1 is required for proliferation. NUCKS1 depletion delays proliferation in **A)** TIG-1 cells and **B)** NBE1-hTERT cells. One-way ANOVAs with Dunnett multiple comparisons test at day 6 or 8, respectively. **C)** CRISPR-mediated *NUCKS1* deletion delays proliferation in U2OS cells. Ordinary one-way ANOVA with Dunnett multiple comparisons test at day 8. Cell proliferation is plotted as a fold change relative to the number of cells seeded at day 0. Error bars are SDs.

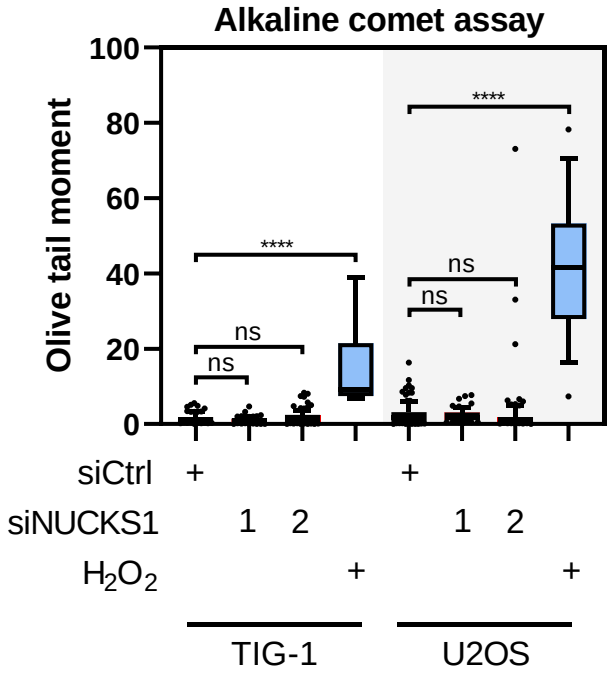


Figure 7: NUCKS1 depletion does not cause DNA damage. NUCKS1 depletion does not induce DNA damage in TIG-1 or U2OS cells, measured by alkaline comet assay. Treatment with 50 µM H2O2 for 10 m was used as a positive control. Kruskal-Wallis with Dunn's multiple comparisons test. Box plots show values at median, 25/75%, and 10/90%.

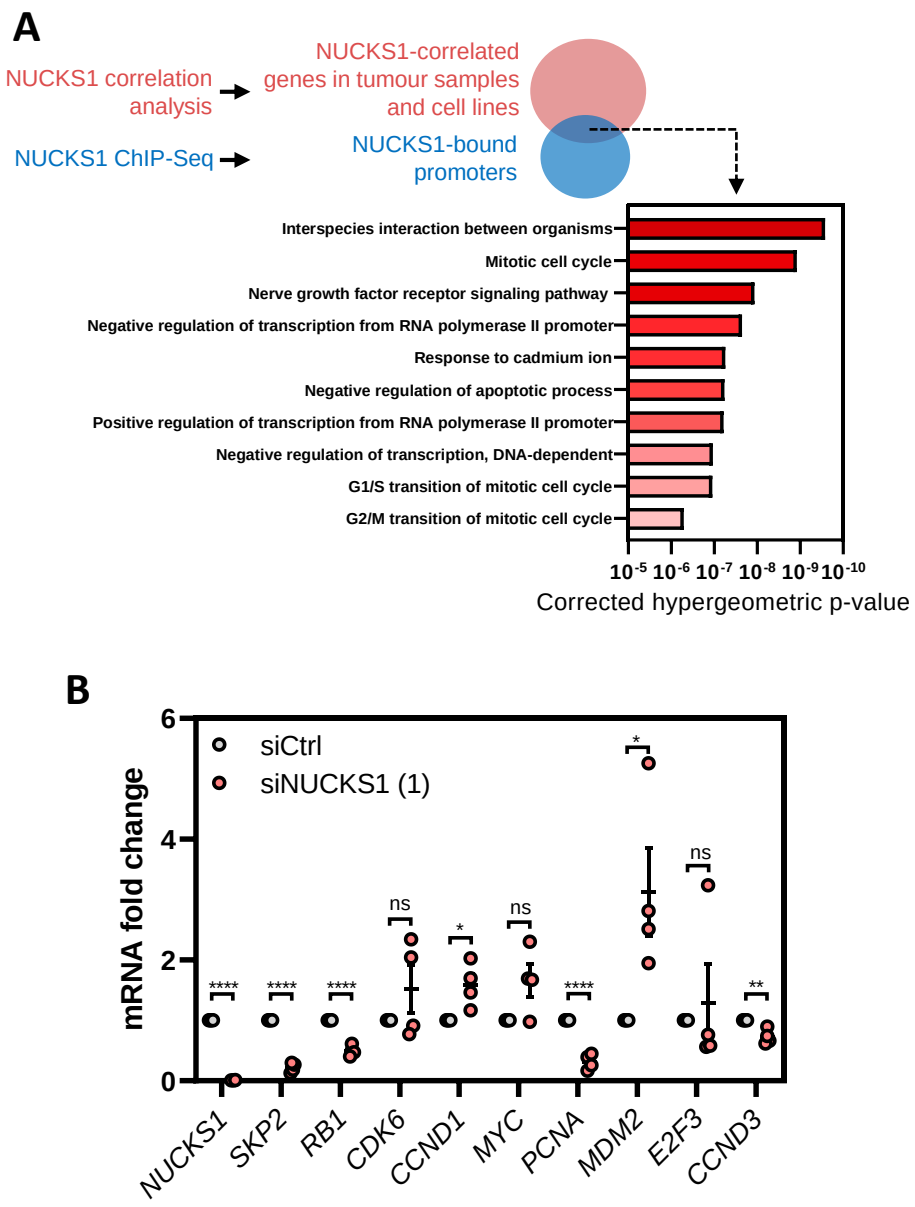


Figure 8: Identification of putative NUCKS1 targets. A) Schematic demonstrating the protocol to identify potential transcriptional targets for NUCKS1. A list of the 1,000 genes correlating most with *NUCKS1* from the SEEK Princeton database (Zhu et al., 2015b) was crossed with a list of 586 genes whose promoters NUCKS1 binds, identified by ChIP-Seq (Qiu et al., 2014). Shared between these two lists are putative transcriptional targets for NUCKS1. Biological pathways enrichment was analysed using Genecodis3 (Tabas-Madrid et al., 2012). **B)** RT-qPCR analysis of gene expression changes following NUCKS1 depletion in RPE1-hTERT cells. Student's T test. Error bars are SEMs.

(but not *B2M* or *GAPDH*) in glioblastoma (GBM), kidney renal papillary cell carcinoma (KIRP), skin cutaneous melanoma (SKCM), and uveal melanoma (UVM) (Figure 9C).

To confirm and expand on data demonstrating binding of NUCKS1 at the *SKP2* promoter in genome-wide studies (Qiu et al., 2014), we employed 10 distinct primer sets, corresponding to different regions of the *SKP2* promoter [from ~10,000 base pairs upstream of the first nucleotide to ~10,000 base pairs downstream (Figure 10A)] and used ChIP-qPCR to map the binding site of NUCKS1. Performing these assays, we found that position -25 - +148 of the *SKP2* locus is most enriched in NUCKS1 chromatin immunoprecipitates, but this enrichment falls off as primer sets move away from *SKP2*'s transcription start site (which is at position +122). That is, NUCKS1 displays a specificity for the chromatin that is directly upstream of the *SKP2* transcription start site (Figure 10B).

Next, we sought to confirm these findings *in vitro*, using the electrophoretic mobility shift assay (EMSA). To do this, we started by purifying the NUCKS1 protein from Sf9 insect cells, which preserves NUCKS1's post-translational modifications, including its phosphorylations (the purification and Coomassie gel shown in Figure 11 were performed by Dr. Claudia Grou). We found that increasing the titration of in-tact, phosphorylated NUCKS1 protein allows modest binding to the fluorescent *SKP2* promoter probe, with interaction only readily apparent at 1000 nM of NUCKS1. However, dephosphorylation of NUCKS1 with lambda phosphatase enables striking binding of NUCKS1 to the *SKP2* probe, with interaction easily visible at 160 nM of NUCKS1 (Figure 12).

Extending this, we considered whether NUCKS1 might exhibit a preference for a particular sequence of DNA within the *SKP2* promoter. Since a previous study identified a GC-box as a candidate target sequence for NUCKS1 (Qiu et al., 2014), and since the *SKP2* probe we used in EMSA analyses in Figure 12 contains a GC box, we mutated this GC box sequence and re-evaluated binding. We found that binding of both

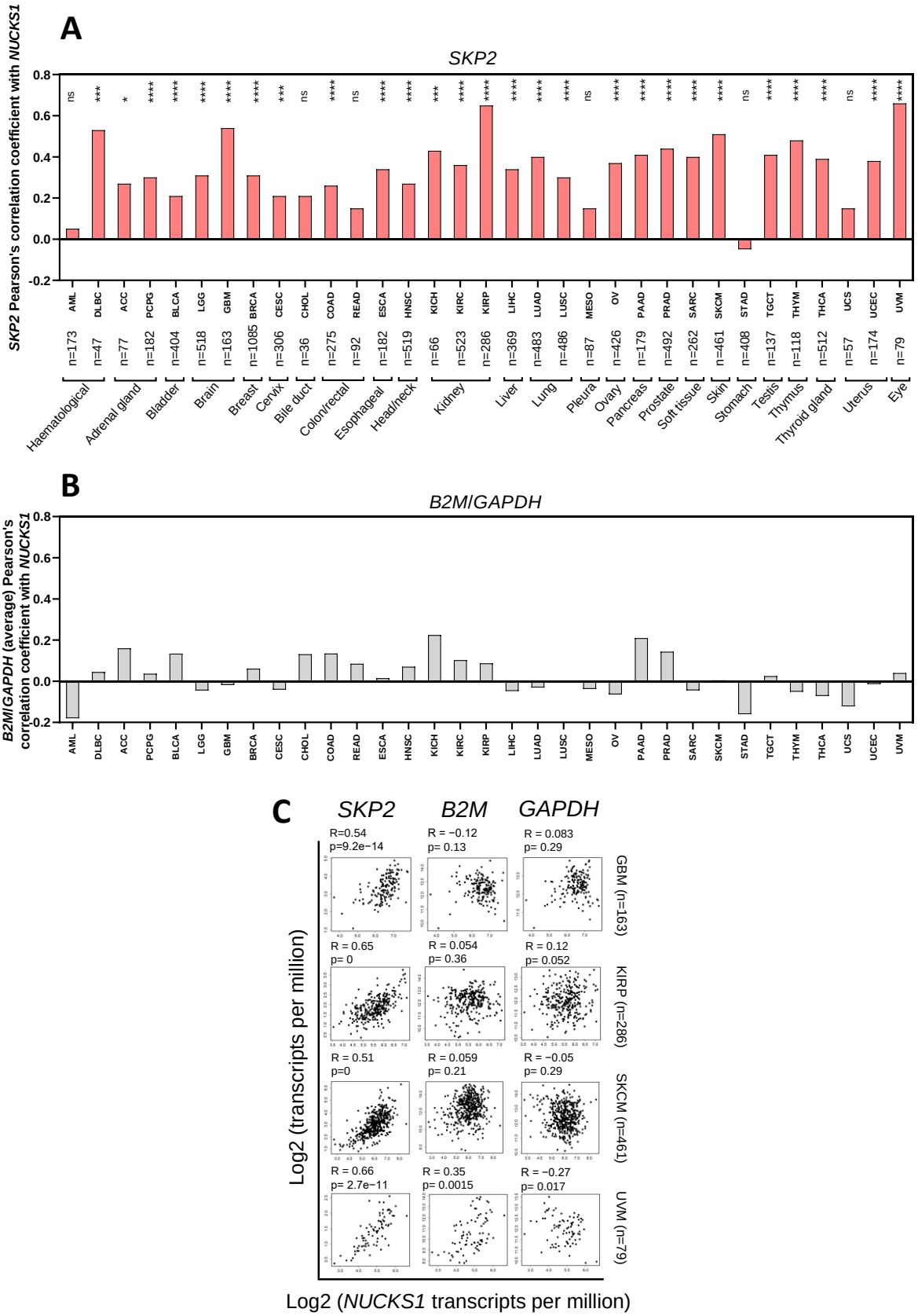


Figure 9: Correlation analysis of *NUCKS1* and *SKP2* mRNA levels. A) Pearson's coefficients demonstrating the correlation of *NUCKS1* with *SKP2*. **B)** Pearson's coefficients demonstrating the correlation of *NUCKS1* with *B2M* and *GAPDH* (used as control, housekeeping genes). **C)** Plots demonstrating the correlation of *NUCKS1* with *SKP2*, *B2M*, and *GAPDH* mRNAs in glioblastoma (GBM), kidney renal papillary cell carcinoma (KIRP), skin cutaneous melanoma (SKCM), and uveal melanoma (UVM). A-C) use data from GEPIA2 (Tang et al, 2019).

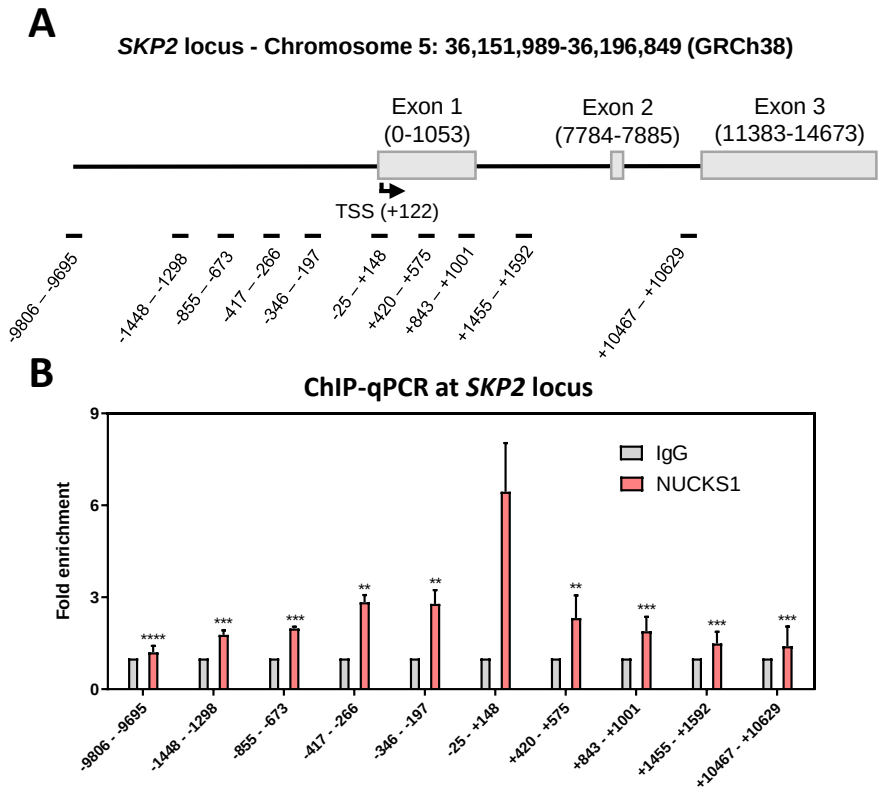


Figure 10: Binding of NUCKS1 at the *SKP2* promoter. A) Map of the *SKP2* locus, annotated with positions of primers used in ChIP-qPCR assay. **B)** ChIP-qPCR of NUCKS1 at the *SKP2* promoter. Ordinary one-way ANOVA with Dunnett's multiple comparisons test, using -25 - +148 as a reference. NUCKS1 occupancy is plotted as a fold change relative to IgG. Error bars are SEMs.

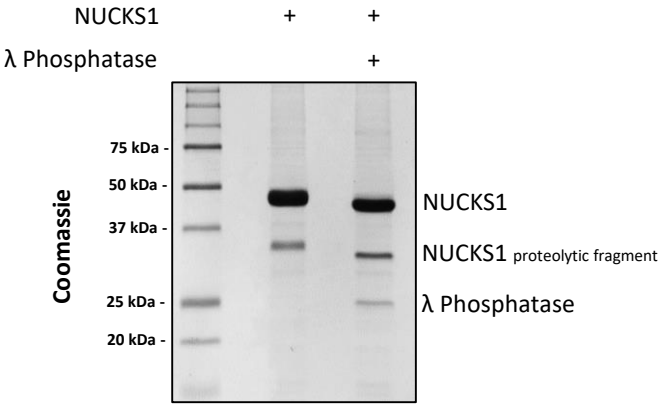


Figure 11: Purification of NUCKS1. NUCKS1 was purified from Sf9 insect cells and visualised by Coomassie staining after SDS-PAGE. NUCKS1 is a heavily phosphorylated protein, and its molecular weight shifts down upon dephosphorylation by λ phosphatase. NUCKS1's purification, and this Coomassie gel, were performed by Dr. Claudia Grou.

phosphorylated and dephosphorylated versions of NUCKS1 to the WT probe is readily outcompeted by addition of a 100 X molar excess of 'cold' (unlabelled) WT probe, but not by cold mutant probe. This demonstrates that NUCKS1's affinity for the GC box-containing sequence is substantially higher than NUCKS1's affinity for the same sequence without a GC box (Figure 13). Finally, using nuclear extract, we found that extract from WT cells exhibits significantly stronger binding to the *SKP2* probe than extract from *NUCKS1*-KO cells, and the binding of both *NUCKS1*-WT and -KO extract to labelled probe is outcompeted by cold WT competition, demonstrating specificity (Figure 14). Overall, these results suggest that NUCKS1 binds the *SKP2* locus via a GC-box in the *SKP2* promoter, and are consistent with other reports that the NUCKS1-DNA interaction is negatively regulated by phosphorylation (Grundt et al., 2002).

Next, we used a panel of 8 cell lines from varying genetic and tissue backgrounds, including cell lines with differential status in the pathways of p53, Rb, MAPK, and varying microsatellite instability (MSI) status. In these cell lines, we measured *SKP2* mRNA levels after NUCKS1 depletion or deletion by RT-qPCR (Figure 15A). We found that loss of NUCKS1 substantially reduces *SKP2* levels, suggesting that NUCKS1 is required for maintaining *SKP2* expression under basal conditions, in a manner that is independent of genetic background.

SKP2's expression is under the control of the cell cycle, with its expression lowest in G1 and highest in S phase (Imaki et al., 2003). However, ruling out cell cycle changes in NUCKS1-depleted cells providing an indirect mechanism for reduced *SKP2* levels, we found that NUCKS1 depletion in G0/G1-synchronised cells (Figure 15B) also reduces *SKP2* expression (Figure 15C). Moreover, we found that NUCKS1 depletion, in RPE1-hTERT cells, causes downregulation of SKP2 protein levels, with concomitant upregulation of SKP2's degradation targets, p21 and p27, demonstrating that both the levels and activity of the SKP2 protein are reduced upon NUCKS1 depletion (Figure 16).

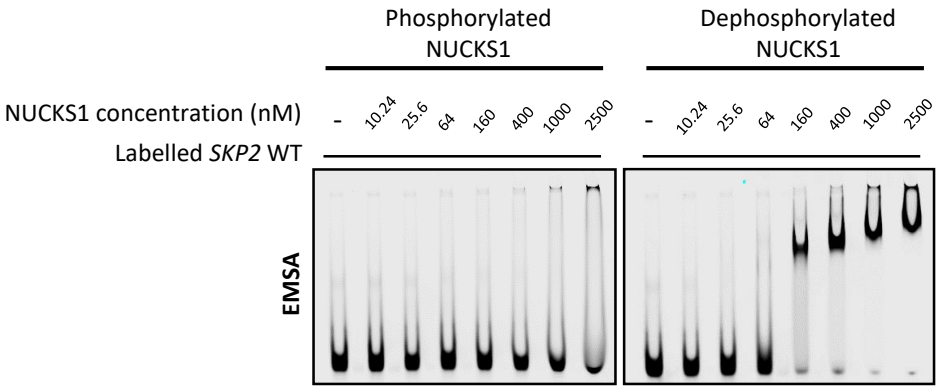


Figure 12: Characterisation of NUCKS1's binding at the *SKP2* promoter by EMSA: phosphorylated vs. dephosphorylated NUCKS1. EMSA demonstrating binding of increasing concentrations of purified phosphorylated or dephosphorylated NUCKS1 to the *SKP2* promoter. The lower band represents unbound DNA, while shifted bands represent NUCKS1-DNA complexes.

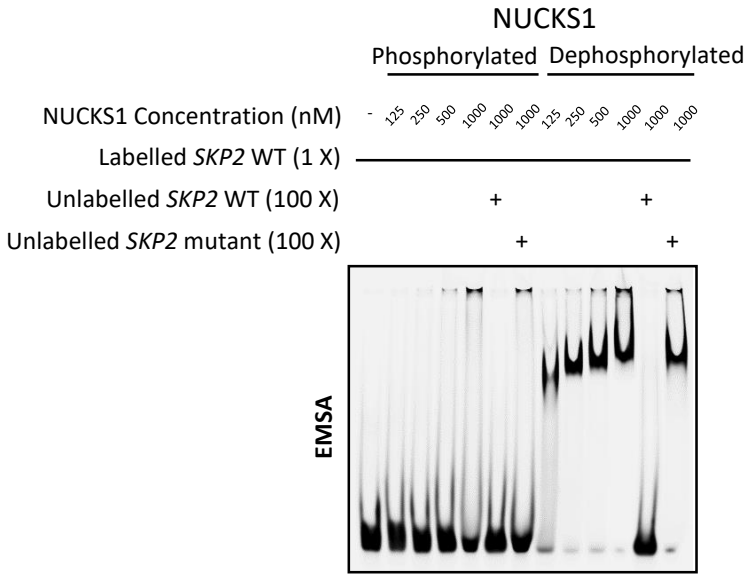


Figure 13: Characterisation of NUCKS1's binding at the *SKP2* promoter by EMSA: competition with WT and mutant probes. Competition EMSAs using phosphorylated and dephosphorylated NUCKS1 with WT or mutant versions of the *SKP2* promoter. The WT *SKP2* probe contains a GC box, ggcggg, that was mutated to aaaaaa in the mutant probe. The lower band represents unbound DNA, while shifted bands represent NUCKS1-DNA complexes.

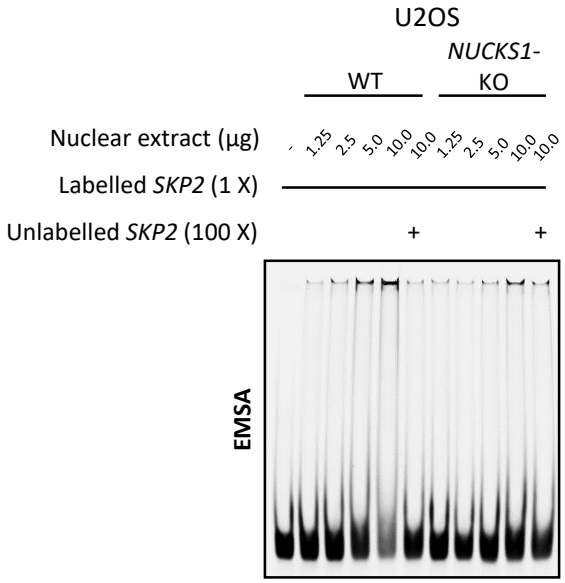


Figure 14: Characterisation of NUCKS1's binding at the *SKP2* promoter by EMSA: WT vs. *NUCKS1*-KO nuclear extract. EMSA demonstrating binding of increasing quantities of wildtype or *NUCKS1*-KO nuclear extract to the *SKP2* promoter. The lower band represents free DNA, while shifted bands represent protein-DNA complexes.

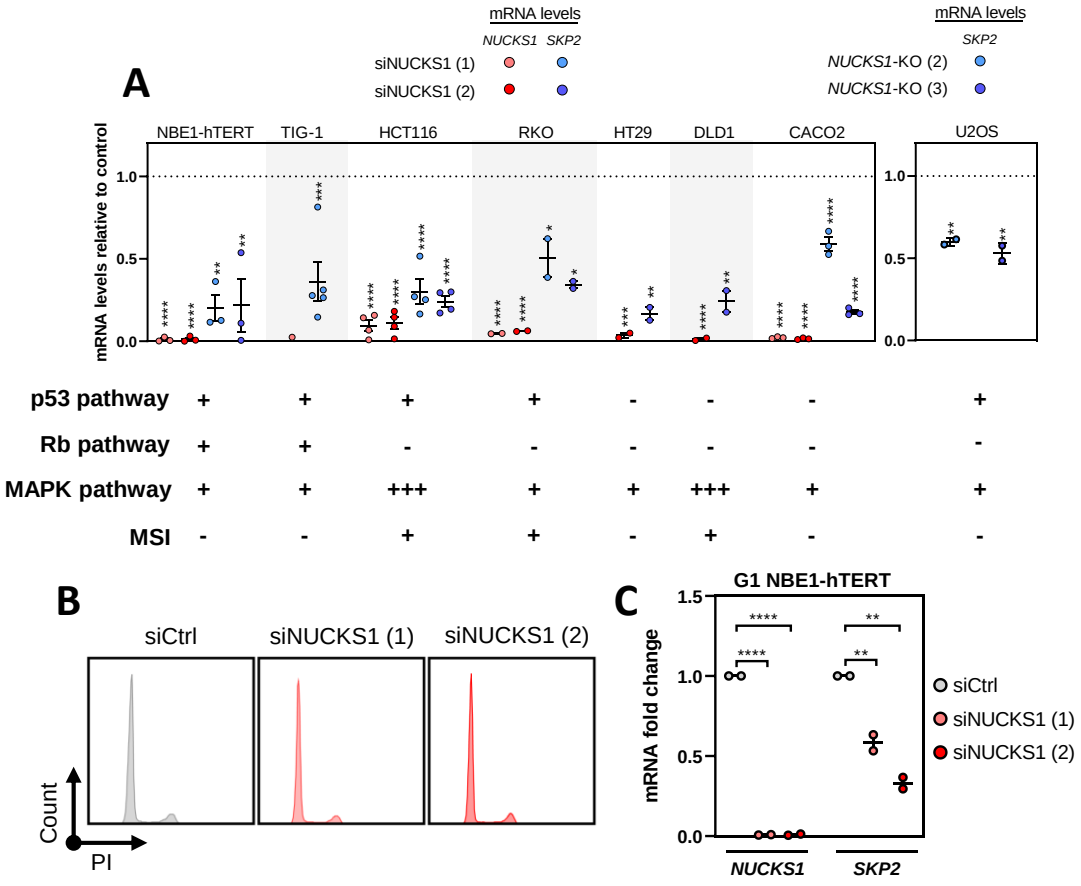


Figure 15: NUCKS1 is required for *SKP2* expression. A) mRNA levels of *NUCKS1* and *SKP2* following NUCKS1 depletion in a range of cell lines (left), or *NUCKS1* deletion from U2OS cells (right), measured by RT-qPCR. mRNA levels in control-treated cells are represented by the dotted line. Genetic background of the cell lines shown is indicated below the figure. **B)** NBE1-hTERT cells were synchronised in G0/G1 phase by contact inhibition, treated with siRNAs as indicated, and analysed by propidium iodide flow cytometry to confirm synchronisation. **C)** Cells treated as in B were analysed by RT-qPCR. Ordinary one-way ANOVA with Dunnett's multiple comparisons test. Error bars are SEMs.

Seeking to explore the relationship between NUCKS1 and SKP2 further, we depleted both proteins independently, and measured cells' ability to enter S phase following release from G0/G1 synchronisation. We found that loss of NUCKS1, which causes a substantial S phase entry defect, markedly phenocopies loss of SKP2 (Figure 17A and B). This is consistent with SKP2's established role in S phase entry (Carrano et al., 1999; Bornstein et al., 2003; Frescas and Pagano, 2008). While the entry of control cells into S phase is visible at 20 h after release, NUCKS1- or SKP2-depleted cells' S phase entry is only visible (using these timepoints) at 42 h after release. Furthermore, comparison at 24 h following release demonstrates the strength of the S phase entry defect in NUCKS1- or SKP2-depleted cells (Figure 17A).

Next, we asked whether loss of SKP2 contributes to the phenotypes of NUCKS1-depleted cells. Firstly, we found that overexpression of SKP2, both in HCT116 (Figure 18A) and A549 cells (Figure 18B) reduces the accumulation of p21 and p27 in these cells. That is, while NUCKS1 depletion induces the characteristic upregulation of p21 and p27, this is largely suppressed when SKP2 is overexpressed, demonstrating that SKP2 downregulation is the cause of p21/p27 upregulation in NUCKS1-depleted cells (Figure 18).

Furthermore, we found that SKP2 overexpression in HCT116 (Figure 19A: EdU/PI profiles and Figure 19D: quantification) and A549 cells (Figure 19B: EdU/PI profiles and Figure 19E: quantification) is mostly sufficient to rescue cell cycle progression in NUCKS1-depleted cells, measured using the EdU/PI assay. Similarly, co-depletion of SKP2's degradation targets, p21 or p27, also largely rescues the cell cycle defects of NUCKS1-depleted cells (Figure 19C: EdU/PI profiles and Figure 19F: quantification). Strikingly, overexpression of SKP2 (Figure 20A) – or co-depletion of p21 or p27 (Figure 20B) – also partially rescues the proliferation defects of NUCKS1-depleted cells. Together, these data demonstrate that NUCKS1 controls G1/S progression and proliferation through its transcriptional stimulation of *SKP2*.

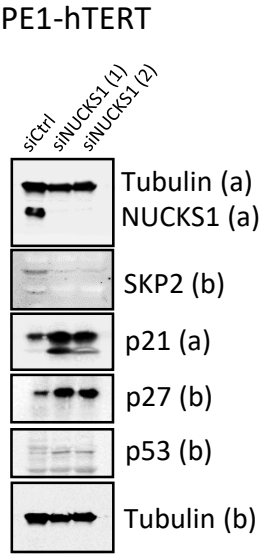


Figure 16: NUCKS1 depletion inhibits the SKP2 pathway. Western blot in RPE1-hTERT cells following NUCKS1 depletion. (a) and (b) indicate antibodies probed against the same samples, loaded on two different gels.

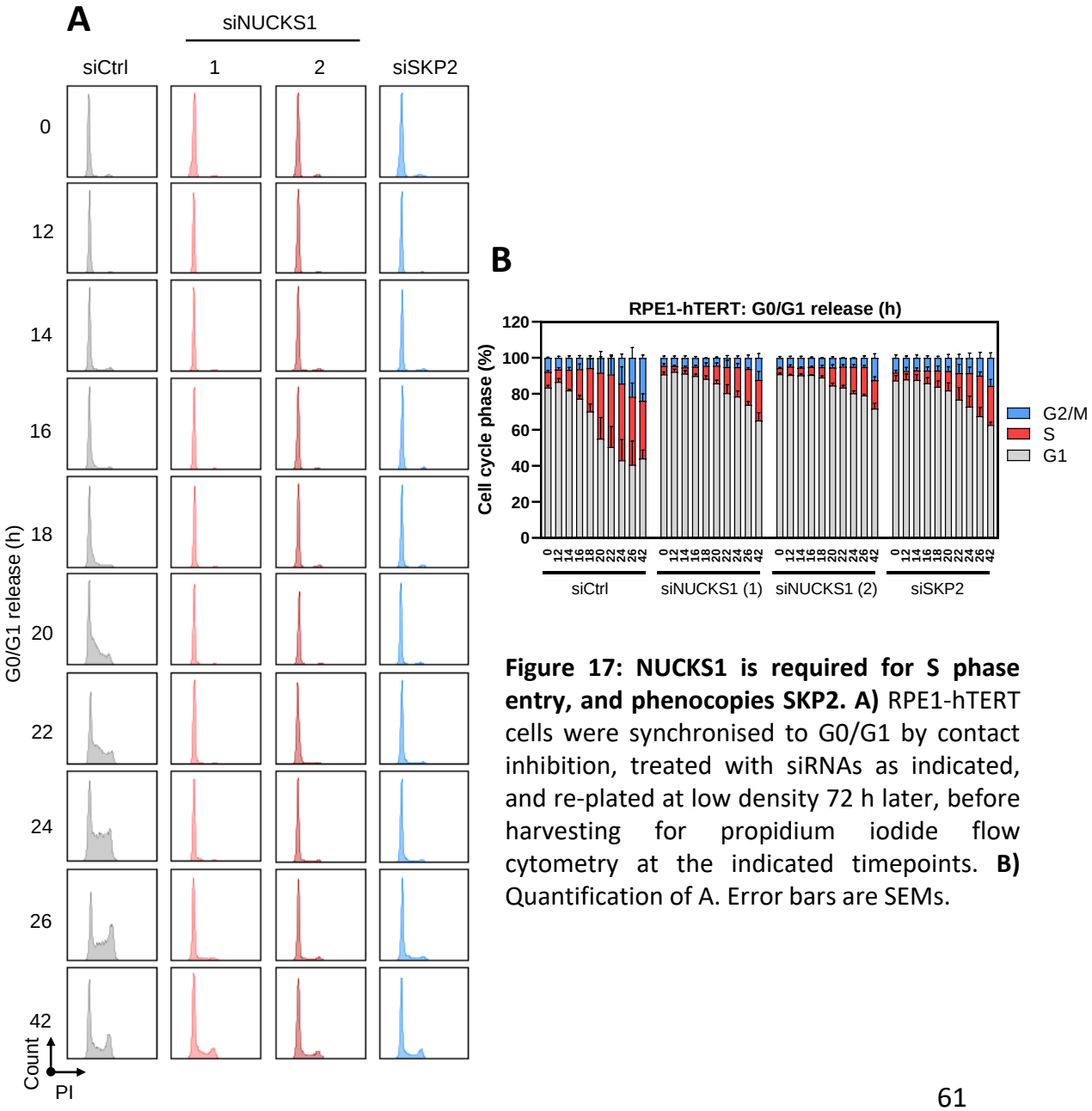


Figure 17: NUCKS1 is required for S phase entry, and phenocopies SKP2. A) RPE1-hTERT cells were synchronised to G0/G1 by contact inhibition, treated with siRNAs as indicated, and re-plated at low density 72 h later, before harvesting for propidium iodide flow cytometry at the indicated timepoints. **B)** Quantification of A. Error bars are SEMs.

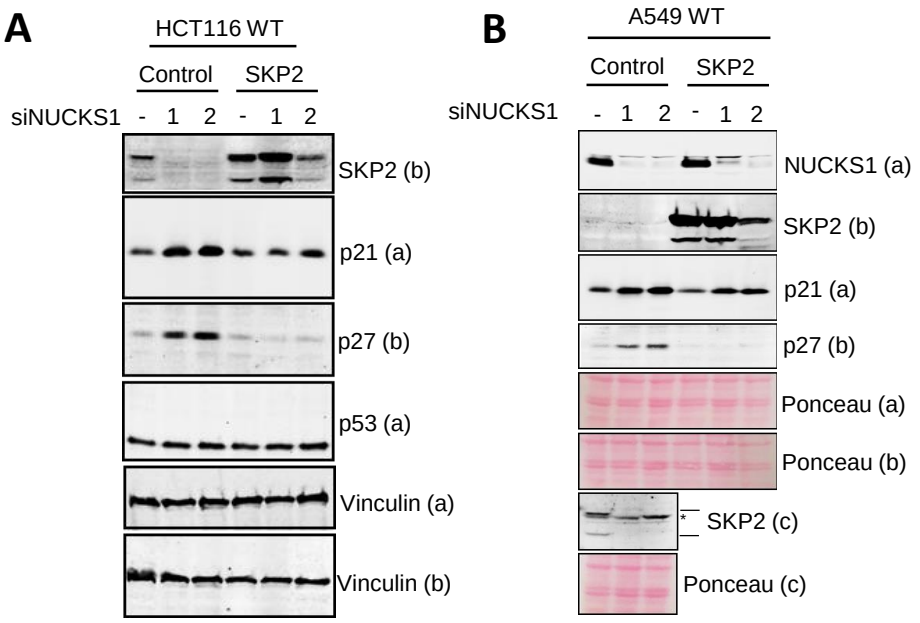


Figure 18: SKP2 overexpression reduces the accumulation of p21 and p27 in NUCKS1-depleted cells. A) Western blot following NUCKS1 depletion and SKP2 overexpression in HCT116 cells. **B)** Western blot following NUCKS1 depletion and SKP2 overexpression in A549 cells. The star denotes a non-specific band. (a), (b), (c) indicate the same samples loaded on different gels.

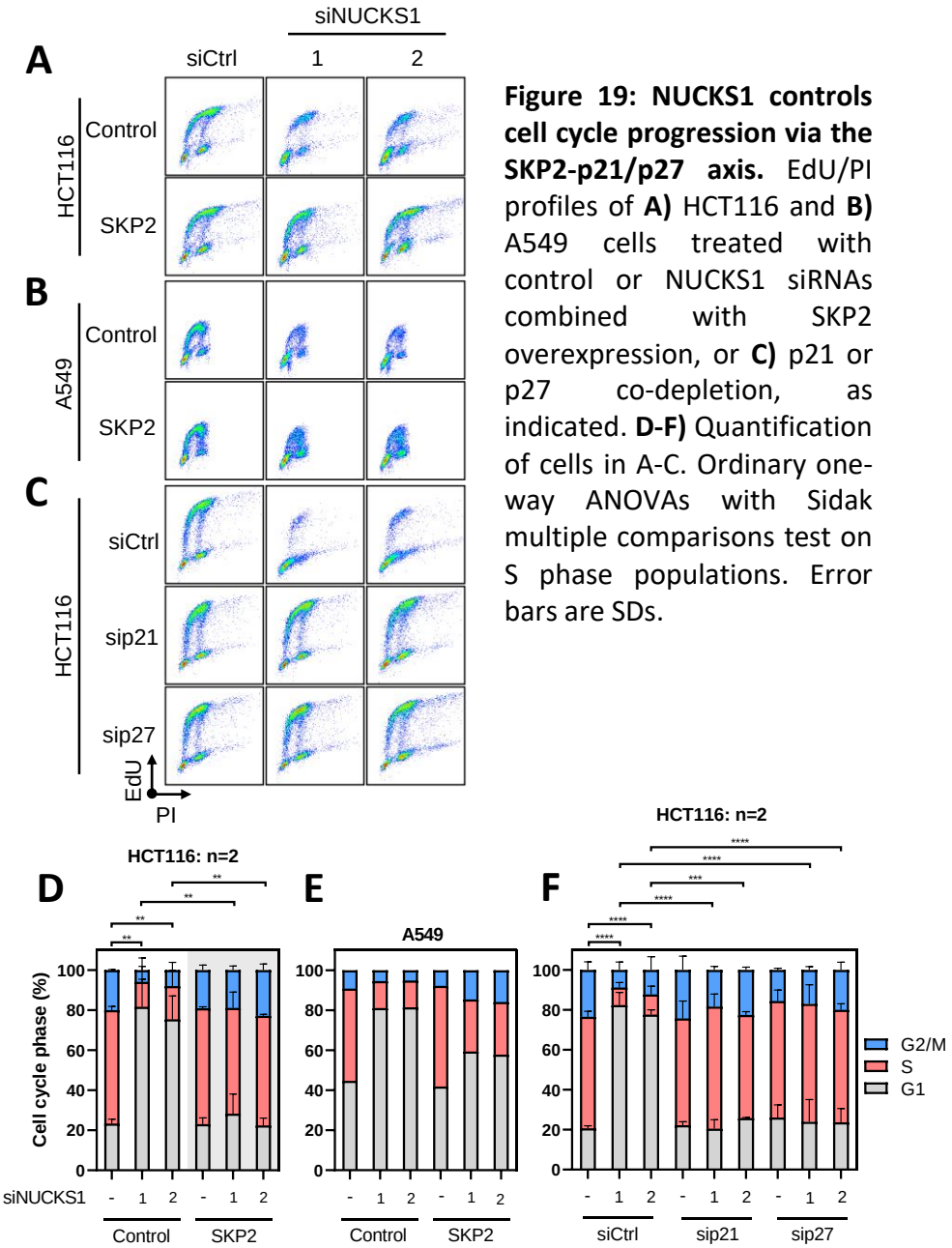


Figure 19: NUCKS1 controls cell cycle progression via the SKP2-p21/p27 axis. EdU/PI profiles of **A)** HCT116 and **B)** A549 cells treated with control or NUCKS1 siRNAs combined with SKP2 overexpression, or **C)** p21 or p27 co-depletion, as indicated. **D-F)** Quantification of cells in A-C. Ordinary one-way ANOVAs with Sidak multiple comparisons test on S phase populations. Error bars are SDs.

Concluding this chapter, we investigated whether NUCKS1 is subject to cell cycle-dependent regulation. We observed that protein levels of NUCKS1 and SKP2 are low in early G1, and increase as cells progress through G1 and into S phase (Figure 21A). SKP2's induction could be partially [but not completely (Bashir et al., 2004; Wei et al., 2004)] explained by its transcriptional upregulation, which does not occur in NUCKS1-depleted cells (Figure 21B). Since NUCKS1 is a chromatin-associated protein, we also measured levels of NUCKS1 at the chromatin during G1/S progression. Consistent with its upregulation as cells progress into S phase, we found that NUCKS1 is recruited to chromatin during G1 progression (Figure 21C). Finally, we found that NUCKS1 is also recruited to chromatin following mitogenic stimulation, demonstrating that NUCKS1 senses – and is activated by – mitogens (Figure 21D). Together, these results demonstrate that NUCKS1 becomes activated during G1 progression and in response to mitogenic stimulation, and contributes to the G1/S-specific transcriptional induction of *SKP2*.

Results Chapter 3: DNA damage inhibits the NUCKS1-SKP2 axis through p53

Given the potent inhibitory effect of DNA damage on G1/S progression, we asked how DNA damage affects the NUCKS1-SKP2 axis. We found that treatment with 5-fluorouracil (5-FU), a chemotherapeutic and DNA-damaging drug that induces potent G0/G1 arrest, dramatically reduces levels of NUCKS1 and SKP2, increases levels of p27, and, as expected, increases the levels of p53 and p21 (Figure 22A). Consistent with loss of the NUCKS1 protein, its occupancy at the *SKP2* promoter, measured by ChIP-qPCR, is abrogated by treatment with 5-FU (Figure 22B). Furthermore, investigating a potential role for p53, the major transcriptional regulator of the DDR, we found that *TP53*-KO cells are unable to downregulate NUCKS1 or SKP2 in response to 5-FU (Figure 22C).

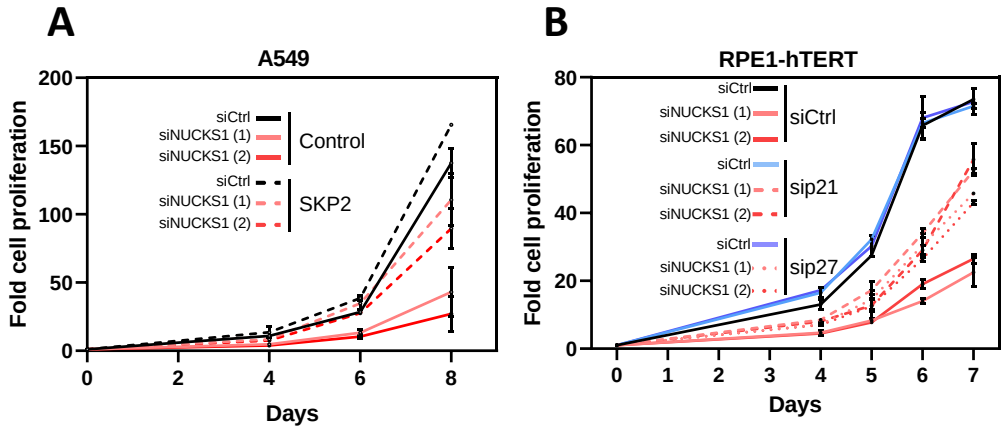


Figure 20: NUCKS1 controls cell proliferation via the SKP2 axis. A) Proliferation assay in A549 cells treated with NUCKS1 siRNAs followed by SKP2 overexpression. **B)** Proliferation assay in RPE1-hTERT cells treated with NUCKS1, p21, or p27 siRNAs, as indicated. Cell proliferation is plotted as fold change relative to the number of cells seeded at day 0. Error bars are SDs.

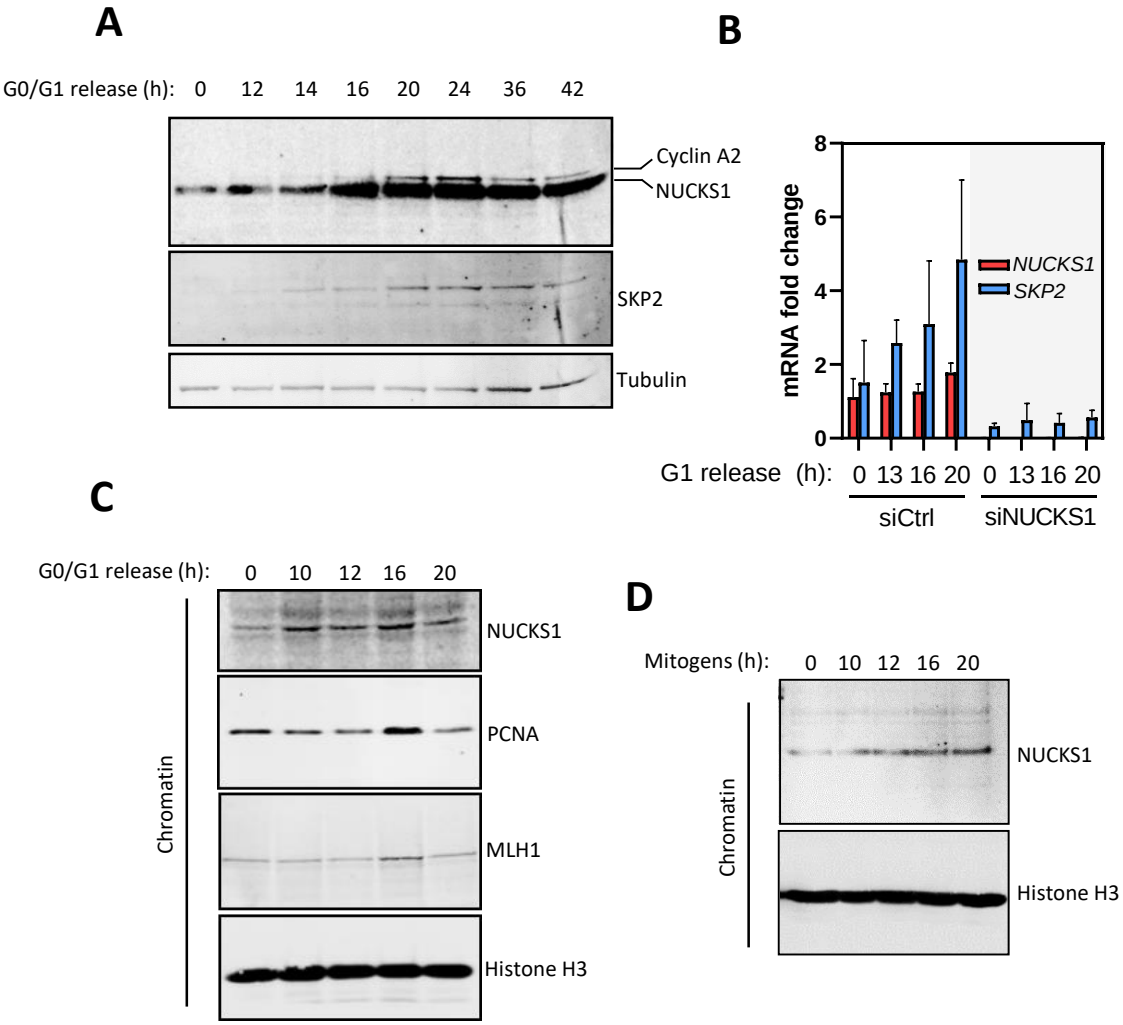


Figure 21: NUCKS1 is stimulated during G1/S progression and by mitogens. A) Western blot using whole cell extracts after cells were released from G0/G1 arrest induced by contact inhibition for 72 h and harvested at the indicated timepoints. **B)** RT-qPCR in cells released from contact inhibition-induced G0/G1 arrest and harvested at the indicated timepoints. **C)** Western blot in the chromatin fraction in cells released from contact inhibition-induced G0/G1 arrest and harvested at the indicated timepoints. **D)** Western blot in the chromatin fraction of cells released from 48 h mitogen starvation into mitogen-rich medium, and harvested at the indicated timepoints. Error bars are SEMs.

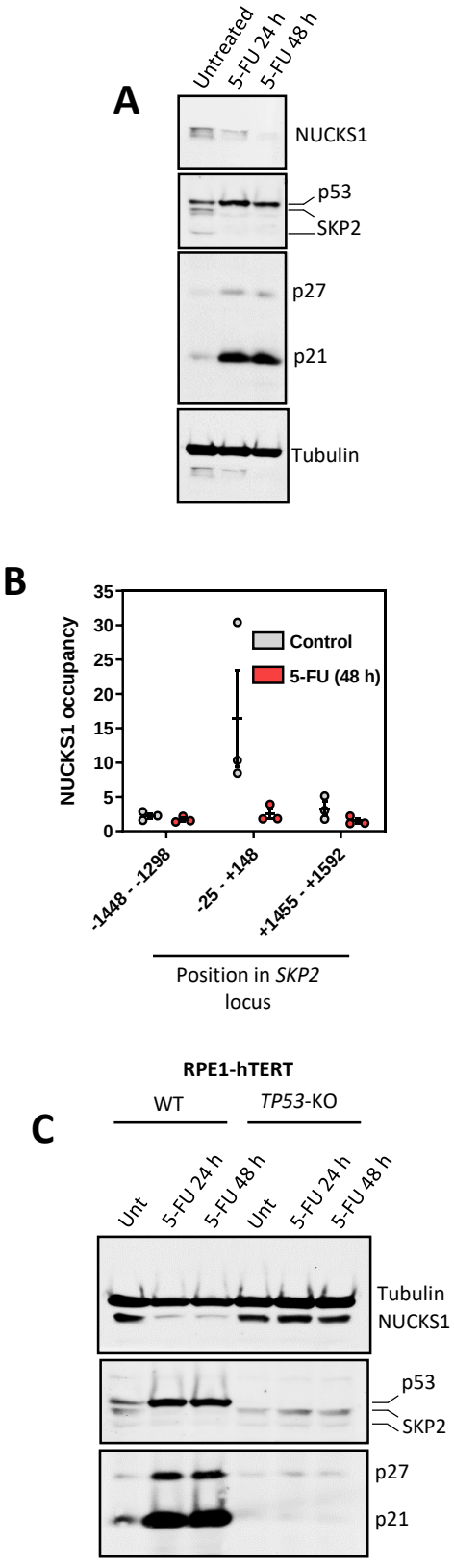


Figure 22: DNA damage inhibits the NUCKS1-SKP2 axis through p53. A) Western blot in U2OS cells treated with 50 µM 5-FU for 24 or 48 h. **B)** ChIP-qPCR in U2OS cells treated with 50 µM 5-FU for 48 h. Data represent fold change in anti-NUCKS1 ChIP vs. anti-IgG ChIP. **C)** Western blot in RPE1 WT or *TP53*-KO RPE1-hTERT cells treated with 10 µM 5-FU for 24 or 48 h. Error bars are SEMs.

Extending this, we explored the mechanism underpinning the downregulation of NUCKS1 and SKP2 upon DNA damage. Employing a panel of DNA-damaging drugs encompassing 5-FU, ionising radiation (IR), H_2O_2, and camptothecin (CPT), we detected downregulation of the transcripts of both *NUCKS1* and *SKP2*, as well as the upregulation of *CDKN1A*, used as a positive control for p53 activation, by RT-qPCR (Figure 23A). When we repeated the experiments in WT and *TP53*-KO cells, we found that the DNA damage-dependent downregulation of *NUCKS1* and *SKP2* is almost entirely dependent on p53, in response to all four drugs. As expected, transcripts of *CDKN1A* are only induced in p53-WT cells (Figures 23B-E). Together, these results demonstrate that p53 directs the DNA damage-dependent downregulation of both NUCKS1 and SKP2.

To explore the regulation by p53 further, we measured the effect of p53 in HCT116 cells. We found that p53-deficient HCT116 express increased *NUCKS1* and *SKP2* levels, an effect that is reversed through expression of WT p53. However, none of the p53 DNA-binding mutants that we tested, R175H, R248W, or R273H, could achieve a rescue (Figures 24A and B). Furthermore, depletion of p53 from TIG-1 cells substantively increases *NUCKS1* transcripts (Figure 24C), and transcripts of *NUCKS1* are moderately increased in *TP53*-KO RPE1-hTERT cells compared to their wildtype counterparts (Figure 24D). Altogether, these data demonstrate that p53 inhibits the expression of both *NUCKS1* and *SKP2*.

Results Chapter 4: NUCKS1 and SKP2 prevent genomic instability in the absence of p53

Given the pre-eminent role for p53 in cell cycle progression (Vousden and Prives, 2009), we then asked how p53 status affects depletion of NUCKS1 and SKP2. Employing WT and *TP53*-KO RPE1-hTERT cells, we firstly found that the downregulation of SKP2 upon NUCKS1 depletion is p53-independent, consistent with our earlier results and with a model depending on direct NUCKS1-driven *SKP2* expression. This is true both at protein (Figure 25A) and mRNA (Figure 25B) levels. Furthermore, while depletion of NUCKS1

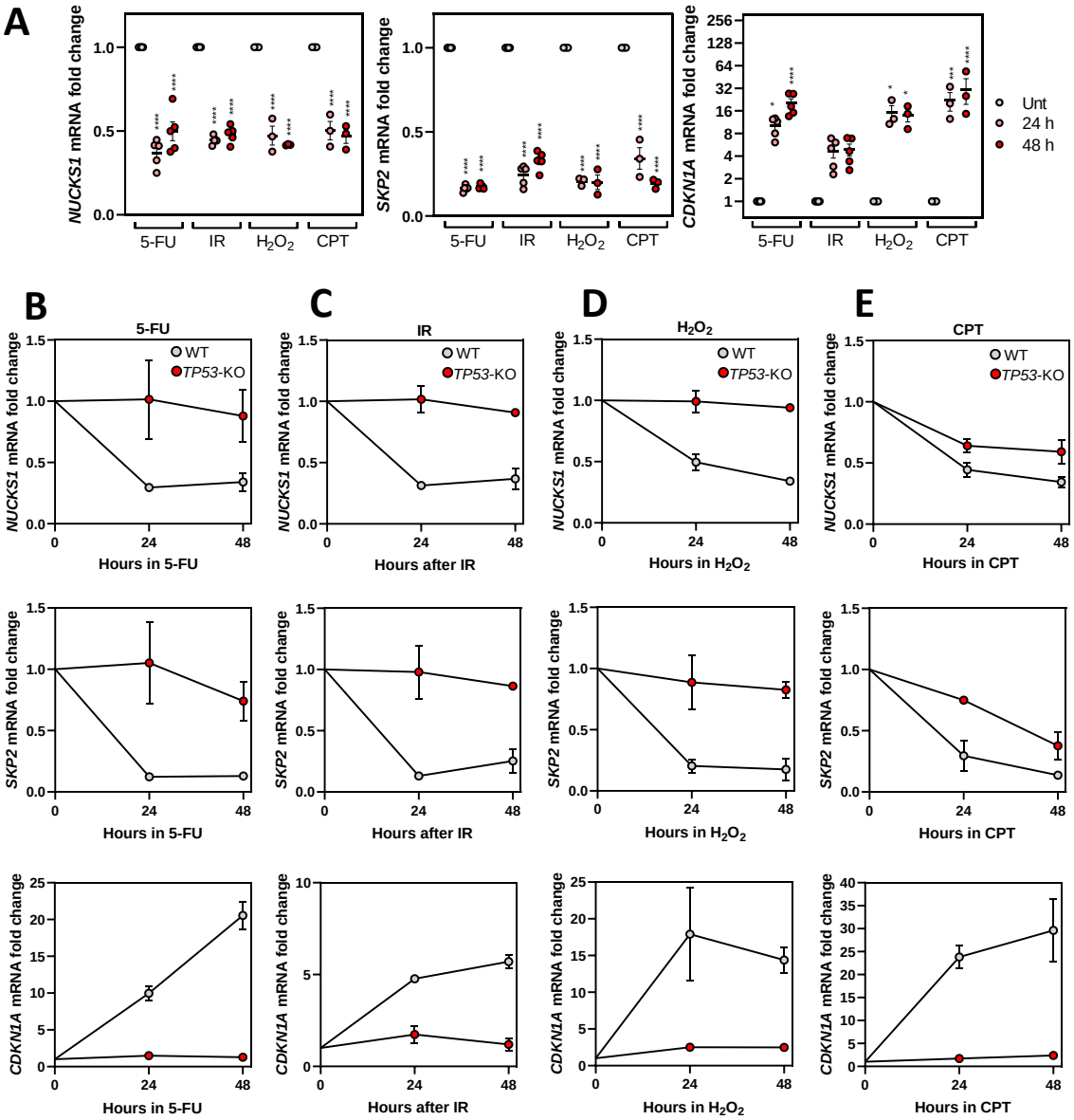


Figure 23: p53 mediates transcriptional repression of *NUCKS1* and *SKP2* following DNA damage. A) RT-qPCR assays in WT RPE1-hTERT cells treated with 5-FU (10 µM), IR (4 Gy), H2O2 (200 µM), or CPT (100 nM). Ordinary two-way ANOVA with Dunnett's multiple comparisons test. RT-qPCR assays in WT and *TP53*-KO RPE1-hTERT cells following treatment with **B)** 5-FU **C)** IR **D)** H2O2 and **E)** CPT. Error bars are SEMs.

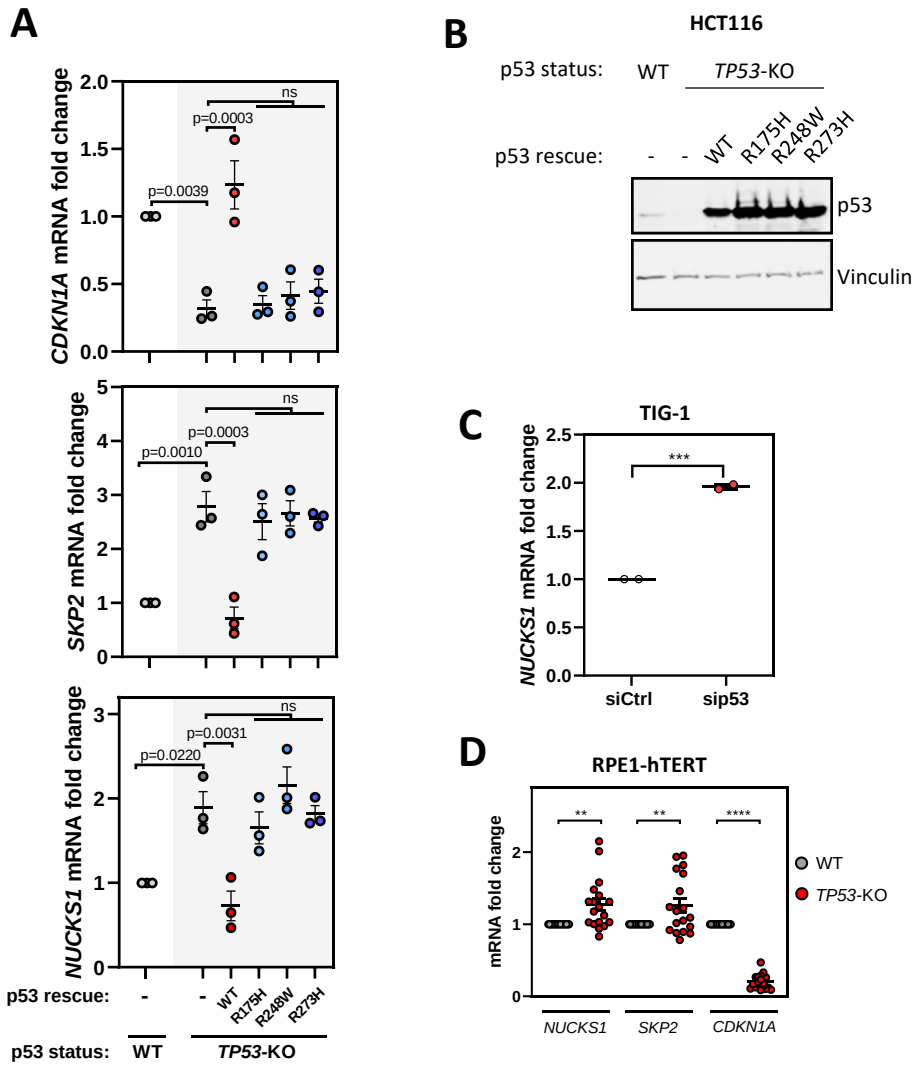


Figure 24: Wildtype p53 suppresses levels of *NUCKS1* and *SKP2*. A) RT-qPCR assays in WT and *TP53*-KO HCT116 cells expressing the indicated variants of p53. Ordinary one-way ANOVA with Tukey's multiple comparisons test. **B)** Western blot in cells treated as in A. **C)** RT-qPCR following p53 depletion in TIG-1 cells. Student's T test. **D)** RT-qPCR in WT and *TP53*-KO RPE1-hTERT cells. Student's T test. Error bars are SEMs.

or SKP2 triggers G0/G1 arrest and reduces S phase populations in WT cells, p53 deletion permits S phase entry after NUCKS1/SKP2 depletion (Figure 26A). Because EdU/PI profiles of NUCKS1/SKP2-depleted cells in *TP53*-KO cells show signs of replication stress (Figure 26A), we measured DNA damage in these cells. Strikingly, we found that NUCKS1 or SKP2-depleted *TP53*-KO cells display increased levels of DNA damage (measured by alkaline comet assay (Figure 26B)), as well as higher levels of DSBs (measured by neutral comet assay (Figure 26C)). These results suggest that NUCKS1 and SKP2 prevent DNA damage in p53-deficient cells.

Results Chapter 5: *NUCKS1* and *SKP2* are overexpressed in cancer

Finally, to gain a deeper understanding of the NUCKS1-SKP2 axis in cancer, we started by analysing the mRNA expression levels of *NUCKS1* and *SKP2* across a range of cancers from the TCGA. Confirming and expanding on other reports (Drosos et al., 2009; Liu et al., 2015; Qiu et al., 2015; Shi et al., 2017; Frescas and Pagano, 2008), we found widespread transcriptional overexpression of both *NUCKS1* and *SKP2* in cancer. *NUCKS1* is significantly overexpressed in 20 tumour types, while *SKP2* is significantly overexpressed in 22 tumour types, from a range of tissue backgrounds (Figures 27A and B). To investigate the mechanism behind this transcriptional overexpression, we looked at potential copy number changes, since copy number changes were previously demonstrated to account for *NUCKS1* overexpression in some cancers (Kikuchi et al., 2013; Drosos et al., 2009; Qiu et al., 2015). Indeed, we found that both *NUCKS1* and *SKP2* are subject to copy number gain and amplification in most cancer types. In particular, copy number gain of *NUCKS1* is strongest in breast invasive carcinoma (BRCA), liver hepatocellular carcinoma (LIHC), lung adenocarcinoma (LUAD) and uterine carcinosarcoma (UCS), while deletion of the *NUCKS1* gene is rare (with the exception of KICH) (Figures 28A and B). Therefore, increased copy number partially explains the transcriptional overexpression of *NUCKS1* and *SKP2* in cancer.

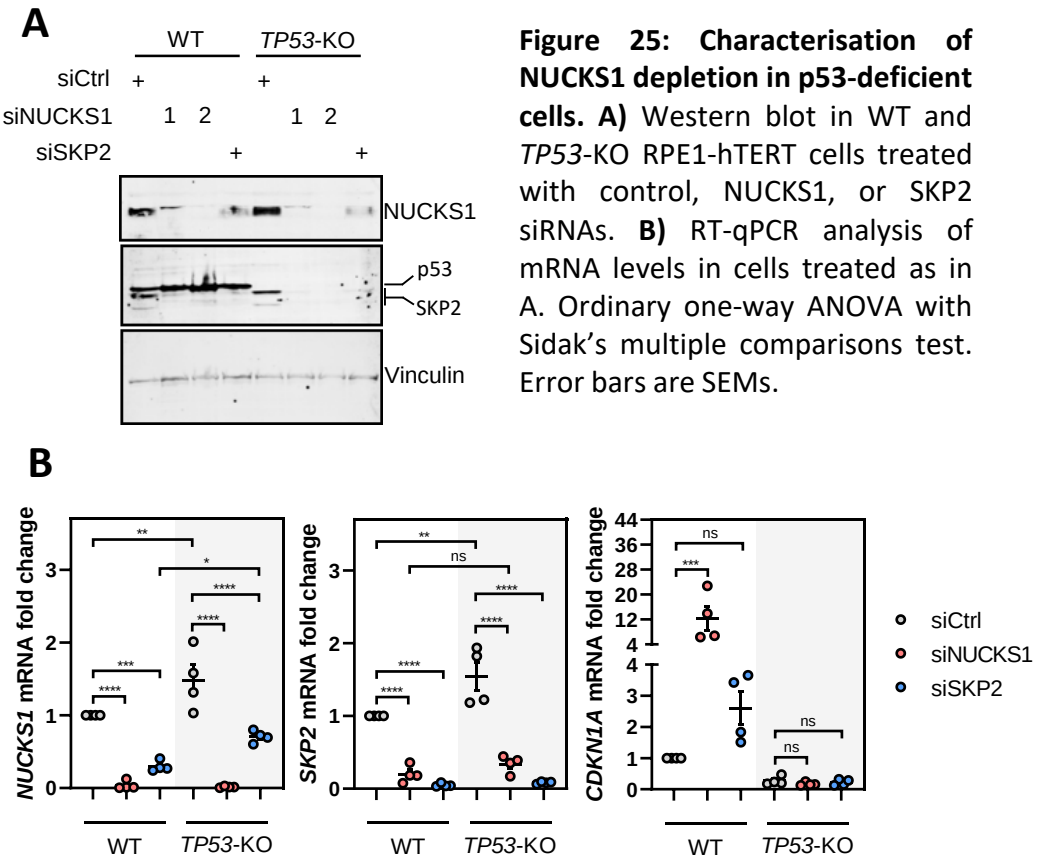


Figure 25: Characterisation of NUCKS1 depletion in p53-deficient cells. A) Western blot in WT and *TP53*-KO RPE1-hTERT cells treated with control, NUCKS1, or SKP2 siRNAs. **B)** RT-qPCR analysis of mRNA levels in cells treated as in A. Ordinary one-way ANOVA with Sidak's multiple comparisons test. Error bars are SEMs.

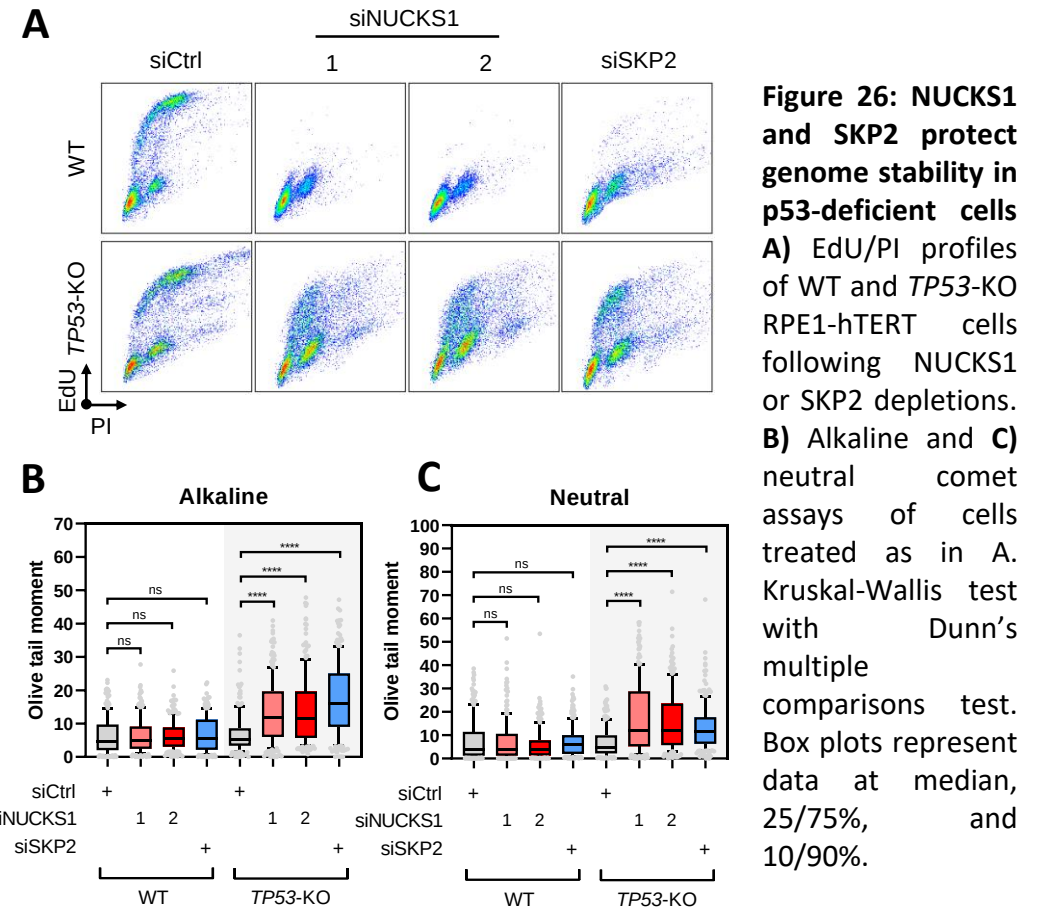


Figure 26: NUCKS1 and SKP2 protect genome stability in p53-deficient cells A) EdU/PI profiles of WT and *TP53*-KO RPE1-hTERT cells following NUCKS1 or SKP2 depletions. **B)** Alkaline and **C)** neutral comet assays of cells treated as in A. Kruskal-Wallis test with Dunn's multiple comparisons test. Box plots represent data at median, 25/75%, and 10/90%.

Since we identified repression of *NUCKS1* and *SKP2* by wildtype – but not mutant – p53, and since p53 is mutated more than any other gene in cancer (Muller and Vousden, 2013), we also investigated a potential role for p53. Markedly, we found that some *TP53*-mutant cancers, including esophageal carcinoma (ESCA), lung squamous cell carcinoma (LUSC), uterine corpus endometrial carcinoma (UCEC), breast invasive carcinoma (BRCA), and breast cancer (from the METABRIC dataset) indeed express higher levels of *NUCKS1* and *SKP2* than their wildtype counterparts (Figures 29A-E). Therefore, together, these results demonstrate the extensive overexpression of *NUCKS1* and *SKP2* in cancer, and suggest that both increased copy number and mutation of p53 may account for this.

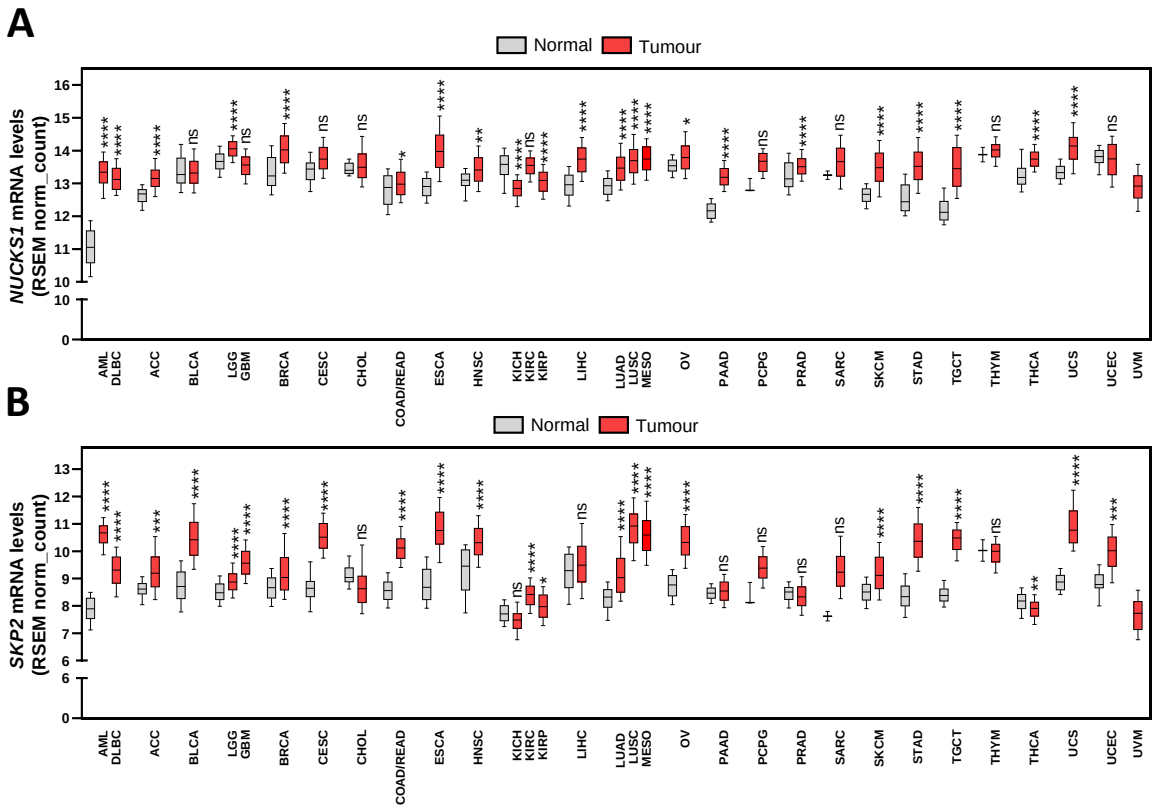


Figure 27: Analysis of *NUCKS1* and *SKP2* mRNA levels in cancer. A) RNA-Seq-measured mRNA levels of *NUCKS1*, in normal (grey) and tumour (red) tissues. **B)** RNA-Seq-measured mRNA levels of *SKP2*, in normal and tumour tissues. Kruskal Wallis with Dunn's. Data are from UCSC Xena (Goldman et al., 2019), using GTEX/TCGA normal datasets and TCGA tumour datasets. Box plots represent data at median, 25/75%, and 10/90%. Data represent mRNA expression as RSEM norm_count.

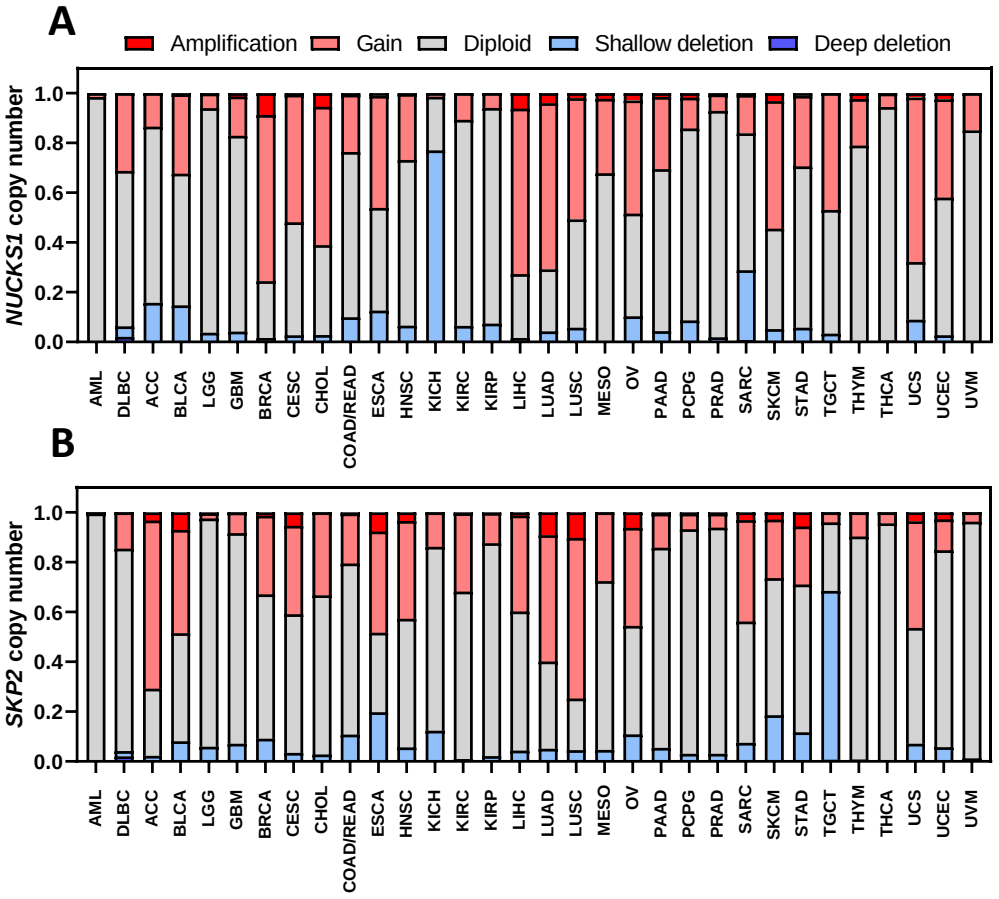


Figure 28: Analysis of *NUCKS1* and *SKP2* copy numbers in cancer. A) Copy number alterations of *NUCKS1* in TCGA cancer datasets. **B)** Copy number alterations of *SKP2* in TCGA cancer datasets. Data are from CBioPortal (Cerami et al., 2012; Gao et al., 2013).

Discussion

Here, we identify novel functions for NUCKS1 in cell cycle progression, DNA replication, and the DNA damage response. We show that NUCKS1 protein levels, as well as its recruitment to chromatin, are induced during G1 progression and upon mitogenic stimulation. NUCKS1 localises to the *SKP2* promoter, permitting *SKP2* expression and the consequent SCF-SKP2-dependent degradation of p21 and p27. As a result, NUCKS1-depleted or *NUCKS1*-knockout cells display defects in S phase entry, a phenotype that is largely rescued through SKP2 overexpression or co-depletion of p21 or p27. While NUCKS1 or SKP2 loss in wildtype cells prevents S phase entry, p53 deletion combined with NUCKS1/SKP2 loss permits S phase entry, but at the cost of genetic instability, suggesting that NUCKS1 and SKP2 protect genomic integrity upon loss of p53. Finally, we show that, consistent with the potent inhibition of DNA replication by DNA damage, numerous types of DNA damaging agents reduce *NUCKS1* and *SKP2* levels, in a manner depending almost entirely on p53. In cancer, p53 loss - in combination with increased copy number of the *NUCKS1* and *SKP2* genes - leads to *NUCKS1* and *SKP2* overexpression. Together, these data demonstrate that NUCKS1 is a crucial licencing protein for the G1/S transition, which integrates mitogenic and DNA damage stimuli to regulate progression into S phase (Figure 30).

Integration of mitogenic and DNA damage signalling

Mitogens and DNA damage are antagonistic signals, whose competition constitutes the most fundamental regulation of S phase entry (Yang et al., 2017). As a result, stringent regulation of the G1/S transition depends on proteins that are able to integrate mitogenic and DNA damage signals (Hume et al., 2020; Heldt et al., 2018). We previously proposed six conditions that candidate integrator molecules would fulfil: 1) Regulation of the G1/S transition; 2) Regulation of cyclins or CDK inhibitors; 3) Presence and activity in the mother G2 or mitosis, daughter G0, or daughter G1; 4) Regulation by mitogens; 5) Antagonistic regulation by DNA damage; and 6) Deregulation in cancer. We also

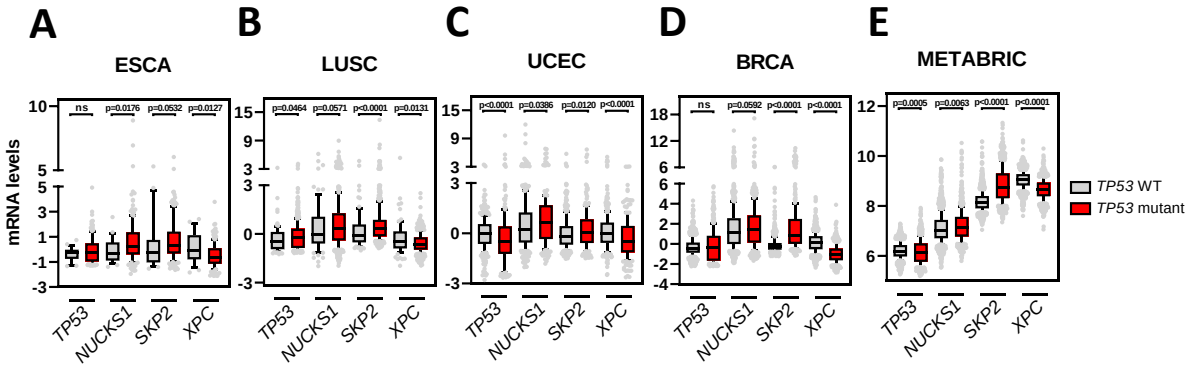


Figure 29: Analysis of *NUCKS1* and *SKP2* mRNA levels in WT vs. *TP53*-mutant tumours. mRNA levels of *TP53*, *NUCKS1*, *SKP2*, and *XPC* (used as a control for p53 activity) in WT and *TP53*-mutant **A)** esophageal carcinoma **B)** lung squamous cell carcinoma **C)** uterine corpus endometrial carcinoma **D)** breast invasive carcinoma and **E)** in breast tumours, from the METABRIC dataset. Mann-Whitney test. Data are from CBioPortal (Cerami et al., 2012; Gao et al., 2013). Box plots represent data at median, 25/75%, and 10/90%.

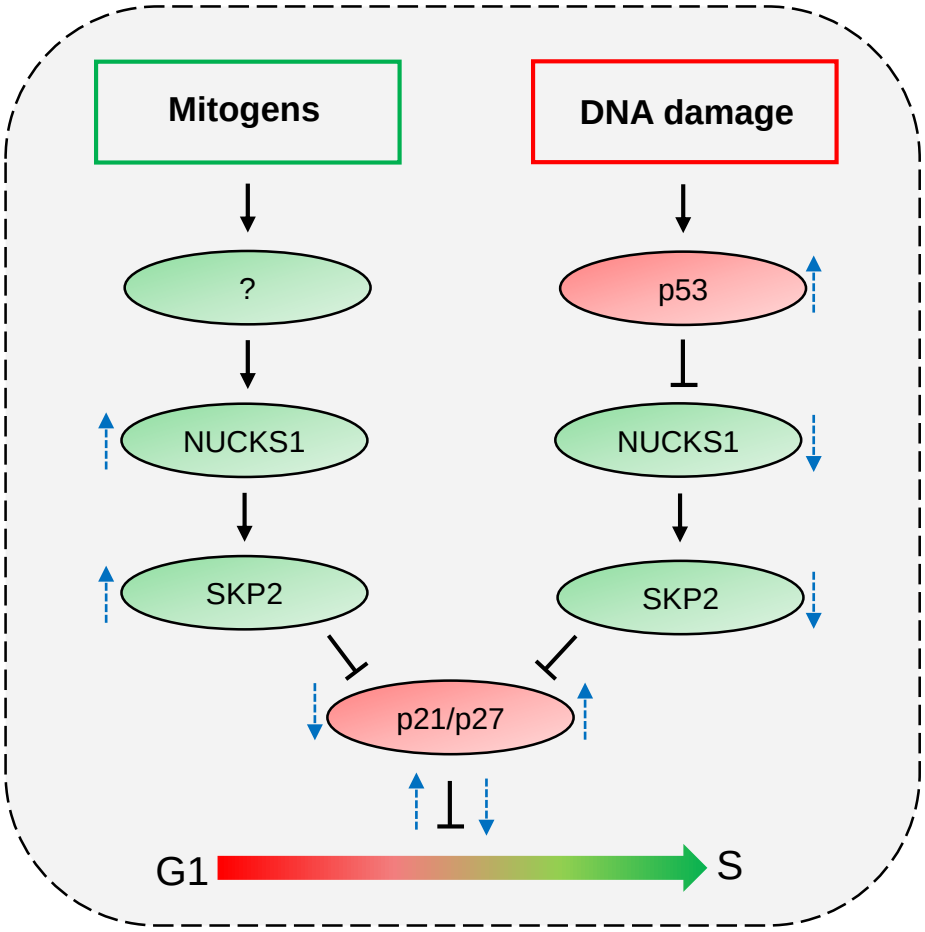


Figure 30: Model. Mitogens and DNA damage antagonistically regulate NUCKS1, feeding through to SKP2 levels and levels of the CDK inhibitors, p21 and p27, which ultimately control the S phase entry decision.

proposed c-Myc and cyclin D1 as putative candidate integrators (Hume et al., 2020). Since NUCKS1 fulfils condition 1 (Figures 5 and 17), condition 2 (Figures 16 and 18), condition 3 (Figure 21), condition 4 (Figure 21), condition 5 (Figures 22 and 23), and condition 6 (Figures 27-29), we now propose NUCKS1 as another candidate.

Regulation of *SKP2* by NUCKS1

We show that NUCKS1, a chromatin-remodelling transcription factor, localises to the *SKP2* promoter to promote *SKP2* expression (Figures 10-15). However, we do not identify how NUCKS1 does this, and precisely how NUCKS1 promotes chromatin accessibility remains an unanswered question. Given the lack of (known) enzymatic domains in the NUCKS1 structure, it is likely that NUCKS1 relies on binding partners to regulate chromatin structure. Therefore, identifying the full spectrum of NUCKS1 interactors will be a crucial step in elucidating the precise mechanism by which NUCKS1 regulates chromatin structure, and, consequently, transcription. Furthermore, measuring the effect of NUCKS1 on chromatin accessibility markers, such as histone acetylation or methylation, would be a useful line of future inquiry to address this. More widely, performing experiments such as ATAC-Seq, a genome-wide approach to measure chromatin accessibility (Buenrostro et al., 2015), would illuminate the full extent of chromatin regulation by NUCKS1.

Multiple proteins localise to the *SKP2* promoter *in vivo*, including E2F1 (Zhang and Wang, 2006) and c-Myc (Bretones et al., 2011). Given that NUCKS1 is also a core component of protein complexes at the *SKP2* promoter (Figure 14), it would be interesting to address the interplay of these factors at the promoter. Unlike the other reported *SKP2* transcription factors, NUCKS1 does not have a (reported) transactivation domain, instead performing chromatin remodelling (Qiu et al., 2014). Therefore, NUCKS1 may be the first protein to arrive at the *SKP2* promoter, opening the chromatin for recruitment of other factors and consequent RNAPII-dependent transcription of the *SKP2* gene. Alternatively, since NUCKS1 plays a putative role in NFκB activation (Poon

et al., 2017), and since NFκB promotes the expression of *SKP2* (Schneider et al., 2006), it is also possible that NUCKS1 plays a role as a cofactor of NFκB for regulation of *SKP2*. These possibilities should be explored in future studies.

Our data show that NUCKS1 directly binds the *SKP2* promoter via a GC box upstream of *SKP2*'s transcription start site (Figure 13). Intriguingly, the GC-box sequence that we identify (GGCGGG) is present twice in the 600 nucleotide region directly upstream of *SKP2*'s first exon, but completely absent from the remaining ~45,000 nucleotides of the *SKP2* gene, demonstrating a striking specificity that could explain the interaction of NUCKS1 to defined range of promoters (Qiu et al., 2014). In the future, structural studies would provide fascinating insight to elucidate exactly how the NUCKS1 protein interacts with the GC-box.

Regulation of NUCKS1 by the cell cycle

We show that NUCKS1 protein levels increase during G1 progression (Figure 21), although we did not identify the mechanism behind this. We do know that increased *NUCKS1* transcription during G1 progression does not explain the increase in its protein levels (Fig. 21B), suggesting that a change in stability of the NUCKS1 protein is possibly responsible. Many ubiquitin ligases could be responsible for modulating the stability of the NUCKS1 protein throughout the cell cycle, including, for example, cyclin F and APC/C-CDH1. Cyclin F is mainly active in G2 phase, and much less in G1 phase (D'Angiolella et al., 2013), while APC/C-CDH1 is mainly active in early – but not late – G1 cells (Zhou et al., 2016). Accordingly, specific degradation of NUCKS1 in G2 or early G1 cells, respectively, could explain its upregulation during G1 progression, and should be tested.

We show that NUCKS1's retention on chromatin is also induced during G1 progression (Figure 21C), but we do not expose the mechanism. Although this could be due to upregulation of NUCKS1 protein levels, it is known that CDK1 activity during G2/M phase

of the cell cycle reduces binding of NUCKS1 to DNA, by phosphorylating NUCKS1 at S181, a residue neighbouring the NUCKS1 DNA-binding domain (Grundt et al., 2002). This activity of CDK1 is lost during G1/S progression (Malumbres, 2014), which could explain the recruitment of NUCKS1 to chromatin at this time. Loss of S181 phosphorylation may also explain the striking increase in DNA-binding that we observe by EMSA upon NUCKS1 dephosphorylation (Figure 12).

Regulation of NUCKS1 by mitogens

NUCKS1 is recruited to chromatin by mitogenic stimulation (Figure 21). Although we do not characterise this fully, it would be intriguing to determine the precise growth factor and signalling pathway responsible for inducing this recruitment. To do this, we could treat cells with specific growth factors, such as IGF, FGF, or EGF, to determine whether individual growth factors can spontaneously induce binding of NUCKS1 to chromatin. It would also be fascinating to identify a precise post-translational modification [or, in light of our EMSA data (Figure 12), removal or a precise post-translational modification] that induces NUCKS1's chromatin recruitment. For this purpose, mass spectrometry-lead analysis of NUCKS1's post-translational modifications, in the presence and absence of specific growth factors, would give substantial insight.

Regulation of NUCKS1 by DNA damage

We show that the transcription of *NUCKS1* is repressed downstream of p53 (Figures 22 and 23). Genome-wide studies focusing on p53's chromatin binding strongly suggest that this repression involves direct binding of p53 to the *NUCKS1* promoter (Nikulenkov et al., 2012). However, it is generally understood that p53 cannot elicit direct transcriptional repression on its own, instead relying on other factors (Fischer et al., 2014). Our preliminary data demonstrate a role for the transcription factor, Sp1, in the positive regulation of *NUCKS1* transcription (data not shown). Therefore, one possible explanation is that p53 interferes with Sp1's binding to the *NUCKS1* promoter, as has been previously reported for other targets of p53-mediated repression (Jun et al., 2017).

Alternatively, it is possible that p53 recruits histone deacetylases to the *NUCKS1* promoter to direct *NUCKS1*'s transcriptional repression, also reported for other genes (Ho et al., 2005). Moving forward, it would also be important to test the p21-dependence of p53-mediated transcriptional repression of NUCKS1, to investigate a putative involvement for the DREAM complex (Engeland, 2018).

We have shown that loss of p53 triggers upregulation of *NUCKS1* (Figure 24). Furthermore, and notably, expression of WT p53 in *TP53*-KO cells, but not some of p53's most common cancer mutants, R175H, R248W, and R273H, reduces *NUCKS1* levels (Figure 24). Similarly, *NUCKS1* levels are increased in most cancer types (Figure 27), and p53 mutation correlates with increased *NUCKS1* levels in some cancers (Figure 29). Given that NUCKS1 drives cell cycle progression, proliferation (Figures 5 and 6), and tumourigenesis (Cheong et al., 2016; Zhao et al., 2020b), does this mean that binding of p53 at the *NUCKS1* promoter, and consequent transcriptional repression, contributes to p53-mediated tumour suppression? To answer this question, we could engineer a CRISPR-Cas9-mediated mutation to p53's putative binding site in the *NUCKS1* promoter, as previously performed in a similar manner for the *MYC* gene in an elegant study (Olivero et al., 2020). We could first test whether this mutation abrogates p53 binding and increases NUCKS1 levels *in vitro*. We could then progress to measure the effect of this mutation on cell cycle progression, proliferation, and, ultimately, xenograft growth in mice. These experiments would aid our understanding of p53's functional interactions with NUCKS1, and more deeply explore p53's tumour suppressor functions.

p53-dependent transcriptional repression of *NUCKS1* provides a durable - but relatively slow - method to inactivate NUCKS1 upon DNA damage. However, intriguingly, phosphorylation of NUCKS1 at S181 is an (indirect) ATM-dependent modification following DNA damage (Bensimon et al., 2010). Given that phosphorylation of this residue prevents binding of NUCKS1 to DNA (Grundt et al., 2002), DNA damage-

induced S181 phosphorylation may provide a more rapid, parallel mechanism to prevent NUCKS1 activity upon DNA damage, and should be explored.

Regulation of cancer by NUCKS1

Multiple studies have now shown that overexpression of NUCKS1 increases xenograft tumour growth in mice (Zhao et al., 2020b; Cheong et al., 2016). Further lines of enquiry to explore NUCKS1's role in tumourigenesis *in vivo* would include, for example, investigation into whether *NUCKS1*-knockout mice are resistant to tumourigenesis, and whether these mice display signs of senescence. Given the putative oncogenic nature of NUCKS1, its potential targeting in cancer should also be considered.

Genomic instability triggered by loss of the NUCKS1-SKP2 axis in p53-deficient cells

We show that loss of NUCKS1 triggers DSB formation in p53-deficient cells, but not in WT cells (Figure 26). These results are consistent with data showing that loss of NUCKS1 in a p53-deficient background causes tumourigenesis when provoked by IR (Yue et al., 2016), and could have numerous interpretations and consequences.

Firstly, many examples have now been published of inappropriate or premature S phase entry triggering DNA damage. For example, cyclin E or c-Myc overexpression induces replication stress and DNA damage by shortening G1 phase and expediting S phase entry (Macheret and Halazonetis, 2018; Hills and Diffley, 2014). Mechanistically, this is due to premature licencing of replication origins usually supressed by transcription in G1, leading to transcription-replication collisions, replication fork collapse, and DSBs (Macheret and Halazonetis, 2018). It is possible that an analogous mechanism operates in NUCKS1-depleted *TP53*-KO cells, especially given NUCKS1's combined roles in transcription and in S phase entry.

An alternative explanation depends on NUCKS1's role in HR-mediated DSB repair (Parplys et al., 2015; Maranon et al., 2020). In this explanation, DSBs are not formed

upon NUCKS1 depletion in WT cells because these cells do not undertake DNA replication, where the majority of endogenous DSBs are formed (Tubbs and Nussenzweig, 2017). However, NUCKS1-depleted *TP53*-KO cells do undergo DNA replication – and accordingly replicate DNA in the absence of a functional HR pathway, consequently accumulating DSBs. Given that NUCKS1 promotes entry into S phase (Figure 17), and that NUCKS1's levels remain high throughout S phase (Figure 21), an appealing overarching model is that NUCKS1 acts to promote entry into S phase while remaining at high levels during the ensuing S phase, to directly promote replication fidelity through stimulation of HR.

Conclusion and future perspectives

Together, this thesis identifies a core regulatory mechanism for the G1/S transition, revolving around integration of mitogenic and DNA damage signals by a transcription factor, NUCKS1. Despite this, further characterisation of the NUCKS1 protein is essential.

Specifically, identifying NUCKS1's interaction partners would be an essential future direction. To do this, mass spectrometry-based identification of proteins in NUCKS1 immunoprecipitates would be required. This analysis could also easily be expanded, for example, to measure how NUCKS1's interactome is altered following alterations in mitogen, cell cycle, or DNA damage signalling. This analysis would also be likely to illuminate potential mechanisms used by NUCKS1 to regulate transcription.

Moreover, given the roles for NUCKS1 in cancer, searching for small molecule inhibitors or PROTACs (Sun et al., 2019) for NUCKS1 is a particularly promising future direction. Given that NUCKS1 has no (known) enzymatic activity, putative NUCKS1-directed PROTACs are the most hopeful approach to target NUCKS1, by selectively inducing its proteolytic degradation. This would have a dual benefit, simultaneously providing a more intricate method to probe the academic function of NUCKS1 *in vitro*, but also potentially

enabling the targeting of NUCKS1 in cancer. To this end, measuring how NUCKS1 PROTACs affect proliferation *in vitro* and tumourigenesis *in vivo* would be the first exploratory step. Given that we and others have identified overexpression of NUCKS1 in cancer (Drosos et al., 2009; Liu et al., 2015; Qiu et al., 2015; Shi et al., 2017), high levels of NUCKS1 in tumour biopsies, measured by immunohistochemistry, would be an insightful biomarker for response prior to the administration of putative NUCKS1 PROTACs in patients.

Appendix

In this section is a description of the collaborative work I performed during my DPhil. Specifically, I worked on projects focused on A) cyclin F-dependent E2F1 degradation, with members of the D'Angiolella laboratory (Burdova et al., 2019), B) TEX264-dependent repair of topoisomerase 1-cleavage complexes (Top1-CCs), with members of the Ramadan laboratory (Fielden et al., 2020), and C) the relationship between XRCC1 and ALDH2, with members of the Dianov laboratory (Chen et al., 2018).

Collaborative project 1: E2F1 proteolysis via SCF-cyclin F underlies synthetic lethality between cyclin F loss and Chk1 inhibition

Cyclin F is an F-box protein whose protein levels and activity peak in G2 phase of the cell cycle, and which is responsible for the proteolytic degradation of many cell cycle and DNA repair factors as part of the SCF-cyclin F complex. These targets include RRM2, which synthesises deoxynucleotides for DNA replication and repair (D'Angiolella et al., 2012), CDC6, a member of the pre-replicative complex required for licensing replication origins (Walter et al., 2016), and SLBP, which regulates *H2AFX* mRNA (and consequently γH2AX and DSB signalling) (Dankert et al., 2016). In this way, cyclin F plays a central role in regulation of cell cycle progression and genome stability (D'Angiolella et al., 2013).

To more deeply explore the functions of cyclin F, and to investigate potential vulnerabilities of cells deficient in cyclin F, which is often lost in cancer (Cerami et al., 2012; Gao et al., 2013), the D'Angiolella laboratory performed viability screens in WT and *CCNF*-KO cells, with over 180 inhibitors of protein kinases (Burdova et al., 2019). This analysis found that inhibitors of Chk1, an effector kinase in the replication stress response, profoundly sensitise *CCNF*-KO cells. Further investigation revealed that inhibition of Chk1 in *CCNF*-KO cells causes DNA replication catastrophe, as well as activating ATM and ATR signalling. This led to the hypothesis that *CCNF*-KO cells

accumulate DSBs upon treatment with Chk1i, and, to directly test this, I performed alkaline and neutral comet assays (Figure 31). As expected, Chk1i induces DNA damage (measured by alkaline comet assay) in WT cells, as well as modest DSB formation (measured by neutral comet assay). However, treatment of *CCNF*-KO cells with Chk1i induces massive amounts of DNA damage (measured by both alkaline and neutral comet assays) (Figure 31). Therefore, Chk1 inhibition in *CCNF*-KO cells causes replication catastrophe, leading to DSB formation and ATM/ATR activation (Burdova et al., 2019).

Mechanistically, the synthetic lethality underlying cyclin F loss and Chk1 inhibition is driven by cyclin F-dependent degradation of E2F1. This study found that, in G2 phase, cyclin F binds to and polyubiquitinates E2F1, and, as a result, *CCNF*-KO cells accumulate E2F1 (Burdova et al., 2019). Furthermore, cyclin F degrades E2F1 upon treatment with Chk1i. However, *CCNF*-KO cells are unable to achieve this, sustaining high E2F1 levels that cause inappropriate DNA replication, replication catastrophe, DSB formation, and cell death (Burdova et al., 2019; Clijsters et al., 2019).

Therefore, this study identified E2F1 as a crucial degradation substrate for cyclin F in G2 phase. This activity of cyclin F resets cell cycle transcription at the end of the mother cell cycle, ready for an accumulation of E2F1 activity at the beginning of the daughter cell cycle (Burdova et al., 2019; Clijsters et al., 2019). This study also identified Chk1 inhibition as a potential vulnerability of cyclin F-deficient cells. Given that some tumours – most notably glioblastomas – lose expression of cyclin F (Cerami et al., 2012; Gao et al., 2013), this suggests that glioblastoma patients with low cyclin F levels may benefit from stratification for Chk1 inhibitors, and this may be tested in clinical trials (Burdova et al., 2019).

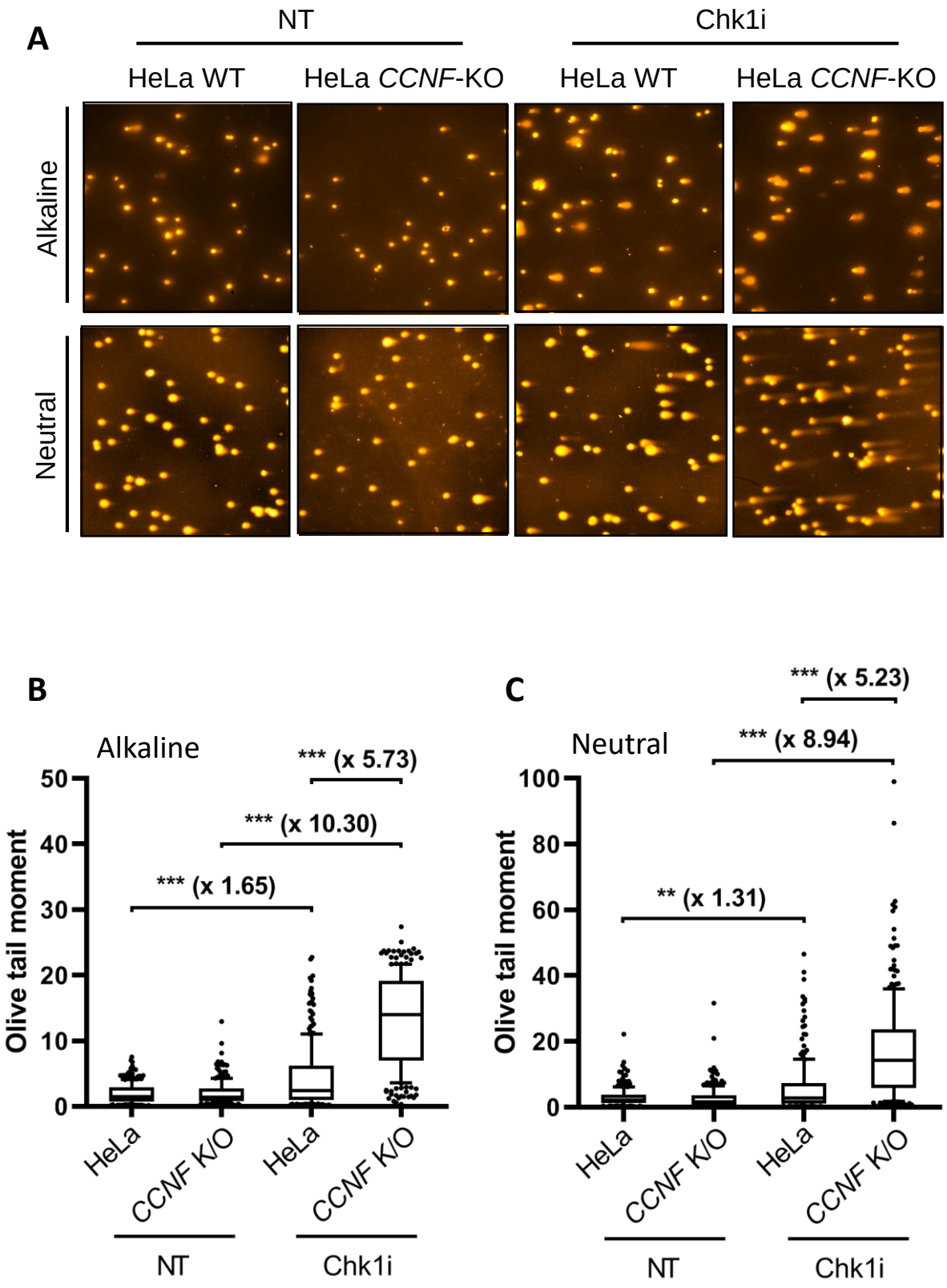


Figure 31: Chk1 inhibition induces massive DSB formation in *CCNF*-KO cells. A) Representative images of alkaline and neutral comet assays performed in WT and *CCNF*-KO HeLa cells, either non-treated (NT) or treated with Chk1 inhibitor. **B)** and **C)** Quantification of alkaline and neutral comet asssays, respectively. Mann-Whitney test. These data are published in Burdova et al., EMBO Journal 2019.

Collaborative project 2: TEX264 coordinates p97- and SPRTN-mediated resolution of topoisomerase 1-DNA adducts

Topoisomerase 1 (Top1) relaxes DNA supercoils that are generated during DNA replication (Chen et al., 2013b). During its catalytic cycle, topoisomerase 1 becomes covalently trapped to DNA, forming a Top1-CC, which is a prototype DNA-protein crosslink (Fielden et al., 2018; Vaz et al., 2016). Top1-CCs form organically during physiological DNA replication, but can also be stabilised (and therefore induced) by the chemotherapeutic, camptothecin (Chen et al., 2013b; Fielden et al., 2018). For this reason, understanding Top1-CC repair is important both from academic and clinical perspectives. Tyrosyl-DNA phosphodiesterase 1 (TDP1) is responsible for repair of Top1-CCs, which cleaves Top1's covalent bond with DNA to resolve the damage (Interthal et al., 2005). However, TDP1 can only access small peptides - that are much smaller than the intact 100 kDa Top1 protein (Debéthune et al., 2002) - highlighting a fundamental problem the cell must solve. How is Top1-CC repair initiated upstream of TDP1?

Solving this question is a newly-discovered TEX264/p97/SPRTN-dependent pathway (Fielden et al., 2020). TEX264 is a nuclear envelope-tethered protein and cofactor for the hexameric ATPase, p97. TEX264 moves with the replication fork, interacts directly with Top1-CCs, and is enriched at Top1-CCs following their induction. TEX264 directly binds to p97, recruiting SPRTN, a metalloprotease for DNA-protein crosslinks (Vaz et al., 2016; Stingele et al., 2016), to Top1-CCs. Here, SPRTN degrades the Top1 component of the Top1-CC, generating small fragments that act as the substrate for repair by TDP1 (Fielden et al., 2020).

Consistent with this model, loss of TEX264 causes the accumulation of Top1-CCs, disrupts DNA replication, and sensitises cells to camptothecin (Fielden et al., 2020). Colony formation assays also reveal that TEX264 and TDP1 are epistatic with respect to camptothecin sensitivity. That is, the combined loss of TEX264 *and* TDP1 does not

increase sensitivity when compared to loss of either protein alone, demonstrating that TEX264 and TDP1 act within the same pathway (Fielden et al., 2020). To complement this analysis, I performed alkaline comet assays in cells treated with control, TEX264, and TDP1 siRNAs, as well as the combination of TEX264 and TDP1 siRNAs. We found that, consistent with colony formation data and with a model comprising TEX264-dependent repair of Top1-CCs by TDP1, TEX264 depletion delays repair of CPT-induced lesions, and TEX264 is epistatic with TDP1 in this capacity (Figure 32).

Altogether, these results identify a TEX264-p97-SPRTN complex that degrades Top1-CCs upstream of repair by TDP1. This pathway is essential for progression of replication forks, and provides resistance to CPT in cells. As a result, this pathway may act as a biomarker for CPT response in cancer patients, and may be targeted to sensitise tumours to CPT (Fielden et al., 2020).

Collaborative project 3: Interplay between base excision repair protein XRCC1 and ALDH2 predicts overall survival in lung and liver cancer patients

X-ray repair cross-complementing protein 1 (XRCC1) coordinates multiple stages of base excision repair (BER), the pathway dedicated to the repair of small base lesions and SSBs (Dianov and Hubscher, 2013). This pathway is essential for maintaining genome integrity, and is often altered in cancer (Legrand et al., 2018; The ICGC/TCGA Pan-Cancer Analysis of Whole Genomes Consortium, 2020). Similarly, alcohol dehydrogenase 2 (ALDH2), which detoxifies alcohol, is essential for the maintenance of genome stability, and is also altered in many cancers. ALDH2 has particular physiological relevance in the liver, where the majority of alcohol detoxification occurs in the body (Chen et al., 2014).

In this descriptive paper (Chen et al., 2018), building on previous work demonstrating upregulation of *ALDH2* upon loss of XRCC1 (Legrand et al., 2018), we set out to

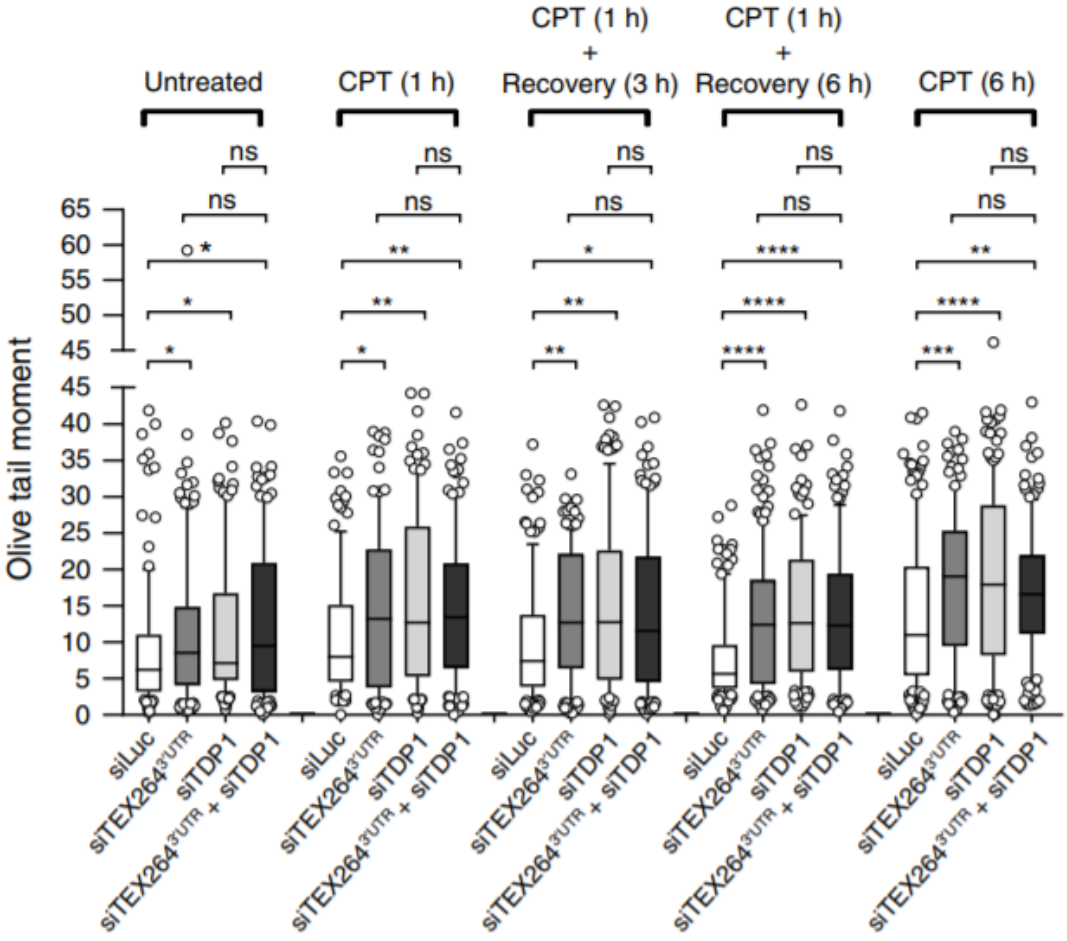


Figure 32: Loss of TEX264 delays repair of CPT-induced lesions via the TDP1 pathway. Alkaline comet assay in RPE1-hTERT cells treated with siLuc, siTEX264, siTDP1, or both. Cells were treated with 100 nM CPT and allowed to recover (or not) for the indicated amounts of time. Kruskal–Wallis ANOVA with multiple comparisons, with Benjamini–Hochberg post-test. These data are published in Fielden et al., Nature Communications 2020.

investigate the functional interactions between XRCC1 and ALDH2 in liver cancer. We first reproduced the upregulation of *ALDH2* upon siRNA-mediated depletion of XRCC1 in multiple cell lines, and could also show that depletion of TDP1 (which also plays an essential role in BER) similarly upregulates *ALDH2*, suggesting that it is loss of BER – and not of XRCC1 itself – that upregulates *ALDH2* (Chen et al., 2018). Next, and consistent with this, we found that the expression of *ALDH2* tends to be reduced in cancer (including in liver cancer), while the expression of *XRCC1* in cancer tends to be increased, mirroring the expression of *ALDH2*. Furthermore, survival of patients with liver cancer is substantially reduced in patients that have a combination of low *ALDH2* and high *XRCC1* levels, strengthening the relationship between XRCC1 and ALDH2, and suggesting that this combination may be a promising target in cancer. To exploit this, we propose that Sp1 inhibitors, which inhibit the transcription of BER genes (Fletcher et al., 2018), may be used to target cancer cells with high and low levels of XRCC1 and ALDH2, respectively (Chen et al., 2018).

In my contribution to this project, I performed the experiments showing that loss of XRCC1 triggers upregulation of *ALDH2* transcripts in TIG1 and Wi38 cells, two fibroblast cell lines (Figure 33 A and B), and could also show that loss of TDP1 similarly triggers the transcriptional upregulation of *ALDH2* (Figure 33C). Finally, I showed, in both liver (JHH4) and lung (H1299) cell lines, that treatment with the Sp1 inhibitor, Mithramycin A, reduces the expression of both *XRCC1* and *ALDH2* (Figure 33D and E).

Altogether, this project demonstrates an interesting inverse relationship between XRCC1 and ALDH2, that could be therapeutically actionable in liver cancer through the inhibition of BER.

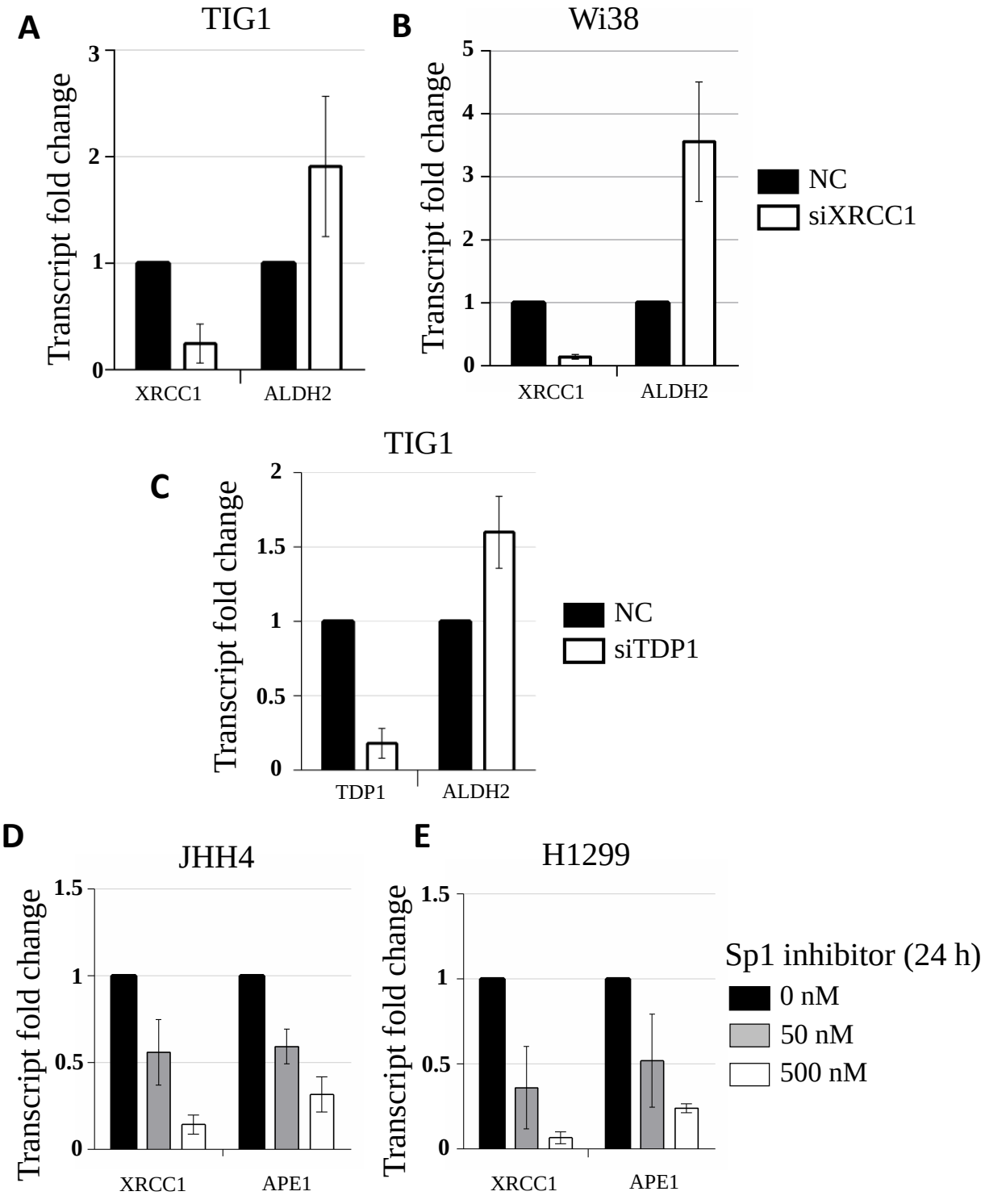


Figure 33. Analysis of the inverse relationship between *XRCC1* and *ALDH2*. A) TIG1 cells were treated with control or XRCC1 siRNA, and *XRCC1* and *ALDH2* mRNA levels were measured by RT-qPCR. **B)** Wi38 cells were treated with control or XRCC1 siRNA, and *XRCC1* and *ALDH2* mRNA levels were measured by RT-qPCR. **C)** TIG1 cells were treated with TDP1 siRNA, and *TDP1* and *ALDH2* mRNA levels were measured by RT-qPCR. **D)** JHH4 cells were treated with the indicated doses of Sp1 inhibitor for 24 h, and *XRCC1* and *APE1* mRNA levels were measured by RT-qPCR. **E)** H1299 cells were treated with the indicated doses of Sp1 inhibitor for 24 h, and *XRCC1* and *APE1* mRNA levels were measured by RT-qPCR. These data are published in Xin et al., Cellular Oncology 2018.

Publications

Work during my DPhil has contributed to the following publications:

1. Xin Chen, Arnaud J Legrand, Siobhan Cunniffe, **Samuel Hume**, Mattia Poletto, Bruno Vaz, Kristijan Ramadan, Dengfu Yao, Grigory L Dianov. Interplay between base excision repair protein XRCC1 and ALDH2 predicts overall survival in lung and liver cancer patients. *Cellular Oncology*, 2018.
2. Kamila Burdova, Hongbin Yang, Roberta Faedda, **Samuel Hume**, Jagat Chauhan, Daniel Ebner, Benedikt M Kessler, Iolanda Vendrell, David H Drewry, Carrow I Wells, Stephanie B Hatch, Grigory L Dianov, Francesca M Buffa, Vincenzo D'Angiolella. E2F1 proteolysis via SCF-cyclin F underlies synthetic lethality between cyclin F loss and Chk1 inhibition. *The EMBO Journal*, 2019.
3. John Fielden, Katherine Wiseman, Ignacio Torrecilla, Shudong Li, **Samuel Hume**, Shih-Chieh Chiang, Annamaria Ruggiano, Abhay Narayan Singh, Raimundo Freire, Sylvana Hassanieh, Enric Domingo, Iolanda Vendrell, Roman Fischer, Benedikt M. Kessler, Timothy S. Maughan, Sherif F. El-Khamisy & Kristijan Ramadan. TEX264 coordinates p97- and SPRTN-mediated resolution of topoisomerase 1-DNA adducts. *Nature Communications*, 2020.
4. **Samuel Hume**, Grigory L Dianov, Kristijan Ramadan. A unified model for the G1/S cell cycle transition. *Nucleic Acids Research*, 2020.
5. **Samuel Hume**, Claudia Grou, Pauline Lascaux, Arnaud J Legrand, Kristijan Ramadan, Grigory L Dianov. The NUCKS1-SKP2-p21/p27 axis controls S phase entry. *In review at Nature Communications.*

References

Abbas, T., and A. Dutta. 2009. p21 in cancer: intricate networks and multiple activities. *Nat. Rev. Cancer*. 9:400–414. doi:10.1038/nrc2657.

Alvarez-Fernandez, M., and M. Malumbres. 2020. Mechanisms of Sensitivity and Resistance to CDK4/6 Inhibition. *Cancer Cell*. 37:514–529. doi:10.1016/j.ccell.2020.03.010.

De Angelis, P.M., A.R. Schjolberg, J.B. Hughes, H.S. Huitfeldt, S. Norheim Andersen, and A.C. Ostvold. 2018. Nondysplastic Ulcerative Colitis Has High Levels of the Homologous Recombination Repair Protein NUCKS1 and Low Levels of the DNA Damage Marker Gamma-H2AX. *Inflamm. Bowel Dis.* 24:593–600. doi:10.1093/ibd/izx071.

Arias, E.E., and J.C. Walter. 2006. PCNA functions as a molecular platform to trigger Cdt1 destruction and prevent re-replication. *Nat. Cell Biol.* 8:84–90. doi:10.1038/ncb1346.

Arora, M., J. Moser, H. Phadke, A.A. Basha, and S.L. Spencer. 2017. Endogenous Replication Stress in Mother Cells Leads to Quiescence of Daughter Cells. *Cell Rep.* 19:1351–1364. doi:10.1016/j.celrep.2017.04.055.

Balbin, M., G.J. Hannon, A.M. Pendas, A.A. Ferrando, F. Vizoso, A. Fueyo, and C. Lopez-Otin. 1996. Functional analysis of a p21WAF1,CIP1,SDI1 mutant (Arg94 --> Trp) identified in a human breast carcinoma. Evidence that the mutation impairs the ability of p21 to inhibit cyclin-dependent kinases. *J. Biol. Chem.* 271:15782–15786.

Barbash, O., P. Zamfirova, D.I. Lin, X. Chen, K. Yang, H. Nakagawa, F. Lu, A.K. Rustgi, and J.A. Diehl. 2008. Mutations in Fbx4 inhibit dimerization of the SCF(Fbx4) ligase and contribute to cyclin D1 overexpression in human cancer. *Cancer Cell*. 14:68–78. doi:10.1016/j.ccr.2008.05.017.

Barr, A.R., S. Cooper, F.S. Heldt, F. Butera, H. Stoy, J. Mansfeld, B. Novák, and C. Bakal. 2017. DNA damage during S-phase mediates the proliferation-quiescence decision in the subsequent G1 via p21 expression. *Nat. Commun.* doi:10.1038/ncomms14728.

Bashir, T., N.V. Dorrello, V. Amador, D. Guardavaccaro, and M. Pagano. 2004. Control of the SCF(Skp2-Cks1) ubiquitin ligase by the APC/C(Cdh1) ubiquitin ligase. *Nature*. 428:190–193. doi:10.1038/nature02330.

Bass, T.E., J.W. Luzwick, G. Kavanaugh, C. Carroll, H. Dungrawala, G.G. Glick, M.D. Feldkamp, R. Putney, W.J. Chazin, and D. Cortez. 2016. ETAA1 acts at stalled replication forks to maintain genome integrity. *Nat. Cell Biol.* doi:10.1038/ncb3415.

Bates, S., K.M. Ryan, A.C. Phillips, and K.H. Vousden. 1998. Cell cycle arrest and DNA endoreduplication following p21Waf1/Cip1 expression. *Oncogene*. 17:1691–1703. doi:10.1038/sj.onc.1202104.

Bensimon, A., A. Schmidt, Y. Ziv, R. Elkon, S.-Y. Wang, D.J. Chen, R. Aebersold, and Y. Shiloh. 2010. ATM-dependent and -independent dynamics of the nuclear phosphoproteome after DNA damage. *Sci. Signal.* 3:rs3. doi:10.1126/scisignal.2001034.

van den Berg, J., A. G Manjón, K. Kielbassa, F.M. Feringa, R. Freire, and R.H. Medema. 2018. A limited number of double-strand DNA breaks is sufficient to delay cell cycle progression. *Nucleic Acids Res.* 46:10132–10144. doi:10.1093/nar/gky786.

Beroukhim, R., C.H. Mermel, D. Porter, G. Wei, S. Raychaudhuri, J. Donovan, J. Barretina, J.S. Boehm, J. Dobson, M. Urashima, K.T. Mc Henry, R.M. Pinchback, A.H. Ligon, Y.-J. Cho, L. Haery, H. Greulich, M. Reich, W. Winckler, M.S. Lawrence, B.A. Weir, K.E. Tanaka, D.Y. Chiang, A.J. Bass, A. Loo, C. Hoffman, J. Prensner, T. Liefeld, Q. Gao, D. Yecies, S. Signoretti, E. Maher, F.J. Kaye, H. Sasaki, J.E. Tepper, J.A. Fletcher, J. Tabernero, J. Baselga, M.-S. Tsao, F. Demichelis, M.A. Rubin, P.A. Janne, M.J. Daly, C. Nucera, R.L. Levine, B.L. Ebert, S. Gabriel, A.K. Rustgi, C.R. Antonescu, M. Ladanyi, A. Letai, L.A. Garraway, M. Loda, D.G. Beer, L.D. True, A. Okamoto, S.L. Pomeroy, S. Singer, T.R. Golub, E.S. Lander, G. Getz, W.R. Sellers, and M. Meyerson. 2010. The landscape of somatic copy-number alteration across human cancers. *Nature*. 463:899–905. doi:10.1038/nature08822.

Bertoli, C., J.M. Skotheim, and R.A.M. de Bruin. 2013. Control of cell cycle transcription during G1 and S phases. *Nat. Rev. Mol. Cell Biol.* 14:518–528. doi:10.1038/nrm3629.

Bieging, K.T., S.S. Mello, and L.D. Attardi. 2014. Unravelling mechanisms of p53-mediated tumour suppression. *Nat. Rev. Cancer*. 14:359–370. doi:10.1038/nrc3711.

Blackford, A.N., and S.P. Jackson. 2017. ATM, ATR, and DNA-PK: The Trinity at the Heart of the DNA Damage Response. *Mol. Cell*. 66:801–817. doi:10.1016/j.molcel.2017.05.015.

Blain, S.W. 2008. Switching cyclin D-Cdk4 kinase activity on and off. *Cell Cycle*. 7:892–898. doi:10.4161/cc.7.7.5637.

Boettcher, S., P.G. Miller, R. Sharma, M. McConkey, M. Leventhal, A. V Krivtsov, A.O. Giacomelli, W. Wong, J. Kim, S. Chao, K.J. Kurppa, X. Yang, K. Milenkowic, F. Piccioni, D.E. Root, F.G. Rücker, Y. Flamand, D. Neuberg, R.C. Lindsley, P.A. Jänne, W.C. Hahn, T. Jacks, H. Döhner, S.A. Armstrong, and B.L. Ebert. 2019. A dominant-negative effect drives selection of TP53 missense mutations in myeloid malignancies. *Science*. 365:599–604. doi:10.1126/science.aax3649.

Bornstein, G., J. Bloom, D. Sitry-Shevah, K. Nakayama, M. Pagano, and A. Hershko. 2003. Role of the SCFSkp2ubiquitin ligase in the degradation of p21Cip1in S phase. *J. Biol. Chem.* doi:10.1074/jbc.M301774200.

Boyd, S.D., K.Y. Tsai, and T. Jacks. 2000. An intact HDM2 RING-finger domain is required for nuclear exclusion of p53. *Nat. Cell Biol.* 2:563–568. doi:10.1038/35023500.

Bretones, G., J.C. Acosta, J.M. Caraballo, N. Ferrándiz, M.T. Gómez-Casares, M. Albajar, R. Blanco, P. Ruiz, W.-C. Hung, M.P. Albero, I. Perez-Roger, and J. León. 2011. SKP2 oncogene is a direct MYC target gene and MYC down-regulates p27(KIP1) through SKP2 in human leukemia cells. *J. Biol. Chem.* 286:9815–9825. doi:10.1074/jbc.M110.165977.

Brotherton, D.H., V. Dhanaraj, S. Wick, L. Brizuela, P.J. Domaille, E. Volyanik, X. Xu, E. Parisini, B.O. Smith, S.J. Archer, M. Serrano, S.L. Brenner, T.L. Blundell, and E.D. Laue. 1998. Crystal structure of the complex of the cyclin D-dependent kinase Cdk6 bound to the cell-cycle inhibitor p19INK4d. *Nature*. 395:244–250. doi:10.1038/26164.

Buenrostro, J.D., B. Wu, H.Y. Chang, and W.J. Greenleaf. 2015. ATAC-seq: A Method for Assaying Chromatin Accessibility Genome-Wide. *Curr. Protoc. Mol. Biol.* 109:21.29.1-21.29.9. doi:10.1002/0471142727.mb2129s109.

Bunz, F., A. Dutriaux, C. Lengauer, T. Waldman, S. Zhou, J.P. Brown, J.M. Sedivy, K.W. Kinzler, and B. Vogelstein. 1998. Requirement for p53 and p21 to sustain G2 arrest after DNA damage. *Science (80-.).* doi:10.1126/science.282.5393.1497.

Burdova, K., H. Yang, R. Faedda, S. Hume, J. Chauhan, D. Ebner, B.M. Kessler, I. Vendrell, D.H. Drewry, C.I. Wells, S.B. Hatch, G.L. Dianov, F.M. Buffa, and V. D'Angiolella. 2019. E2F1 proteolysis via SCF-cyclin F underlies synthetic lethality between cyclin F loss and Chk1 inhibition. *EMBO J.* e101443. doi:10.15252/embj.2018101443.

Busino, L., M. Donzelli, M. Chiesa, D. Guardavaccaro, D. Ganoth, N.V. Dorrello, A. Hershko, M. Pagano, and G.F. Draetta. 2003. Degradation of Cdc25A by β-TrCP during S phase and in response to DNA damage. *Nature*. doi:10.1038/nature02082.

Cappell, S.D., M. Chung, A. Jaimovich, S.L. Spencer, and T. Meyer. 2016. Irreversible APC(Cdh1) Inactivation Underlies the Point of No Return for Cell-Cycle Entry. *Cell*. 166:167–180. doi:10.1016/j.cell.2016.05.077.

Cappell, S.D., K.G. Mark, D. Garbett, L.R. Pack, M. Rape, and T. Meyer. 2018. EMI1 switches from being a substrate to an inhibitor of APC/C(CDH1) to start the cell cycle. *Nature*. 558:313–317. doi:10.1038/s41586-018-0199-7.

Carrano, A.C., E. Eytan, A. Hershko, and M. Pagano. 1999. SKP2 is required for ubiquitin-mediated degradation of the CDK inhibitor p27. *Nat. Cell Biol.* 1:193–199. doi:10.1038/12013.

Cerami, E., J. Gao, U. Dogrusoz, B.E. Gross, S.O. Sumer, B.A. Aksoy, A. Jacobsen, C.J. Byrne, M.L. Heuer, E. Larsson, Y. Antipin, B. Reva, A.P. Goldberg, C. Sander, and N. Schultz. 2012. The cBio cancer genomics portal: an open platform for exploring multidimensional cancer genomics data. *Cancer Discov.* 2:401–404. doi:10.1158/2159-8290.CD-12-0095.

Chan, C.-H., J.K. Morrow, C.-F. Li, Y. Gao, G. Jin, A. Moten, L.J. Stagg, J.E. Ladbury, Z. Cai, D. Xu, C.J. Logothetis, M.-C. Hung, S. Zhang, and H.-K. Lin. 2013. Pharmacological inactivation of Skp2 SCF ubiquitin ligase restricts cancer stem cell traits and cancer progression. *Cell*. 154:556–568. doi:10.1016/j.cell.2013.06.048.

Chan, T.A., H. Hermeking, C. Lengauer, K.W. Kinzler, and B. Vogelstein. 1999. 14-3-3σ is required to prevent mitotic catastrophe after DNA damage. *Nature*. doi:10.1038/44188.

Chao, H.X., C.E. Poovey, A.A. Privette, G.D. Grant, H.Y. Chao, J.G. Cook, and J.E. Purvis. 2017.

Orchestration of DNA Damage Checkpoint Dynamics across the Human Cell Cycle. *Cell Syst.* 5:445-459.e5. doi:10.1016/j.cels.2017.09.015.

Chavez-Reyes, A., J.M. Parant, L.L. Amelse, R.M. de Oca Luna, S.J. Korsmeyer, and G. Lozano. 2003. Switching mechanisms of cell death in mdm2- and mdm4-null mice by deletion of p53 downstream targets. *Cancer Res.* 63:8664–8669.

Chen, C.-H., J.C.B. Ferreira, E.R. Gross, and D. Mochly-Rosen. 2014. Targeting aldehyde dehydrogenase 2: new therapeutic opportunities. *Physiol. Rev.* 94:1–34. doi:10.1152/physrev.00017.2013.

Chen, J.-Y., J.-R. Lin, F.-C. Tsai, and T. Meyer. 2013a. Dosage of Dyrk1a shifts cells within a p21-cyclin D1 signaling map to control the decision to enter the cell cycle. *Mol. Cell*. 52:87–100. doi:10.1016/j.molcel.2013.09.009.

Chen, S.H., N.-L. Chan, and T. Hsieh. 2013b. New mechanistic and functional insights into DNA topoisomerases. *Annu. Rev. Biochem.* 82:139–170. doi:10.1146/annurev-biochem-061809-100002.

Chen, X., A.J. Legrand, S. Cunniffe, S. Hume, M. Poletto, B. Vaz, K. Ramadan, D. Yao, and G.L. Dianov. 2018. Interplay between base excision repair protein XRCC1 and ALDH2 predicts overall survival in lung and liver cancer patients. *Cell. Oncol. (Dordr).* 41:527–539. doi:10.1007/s13402-018-0390-8.

Cheng, M., P. Olivier, J.A. Diehl, M. Fero, M.F. Roussel, J.M. Roberts, and C.J. Sherr. 1999. The p21(Cip1) and p27(Kip1) CDK "inhibitors" are essential activators of cyclin D-dependent kinases in murine fibroblasts. *EMBO J.* 18:1571–1583. doi:10.1093/emboj/18.6.1571.

Cheng, Q., and J. Chen. 2010. Mechanism of p53 stabilization by ATM after DNA damage. *Cell Cycle*. 9:472–478. doi:10.4161/cc.9.3.10556.

Cheng, Q., L. Chen, Z. Li, W.S. Lane, and J. Chen. 2009. ATM activates p53 by regulating MDM2 oligomerization and E3 processivity. *EMBO J.* 28:3857–3867. doi:10.1038/emboj.2009.294.

Cheng, Q., B. Cross, B. Li, L. Chen, Z. Li, and J. Chen. 2011. Regulation of MDM2 E3 ligase activity by phosphorylation after DNA damage. *Mol. Cell. Biol.* 31:4951–4963. doi:10.1128/MCB.05553-11.

Cheong, J.Y., Y.B. Kim, J.H. Woo, D.K. Kim, M. Yeo, S.-J. Yang, K.-S. Yang, S.K. Soon, H.J. Wang, B.W. Kim, J.-H. Park, and S.W. Cho. 2016. Identification of NUCKS1 as a putative oncogene and immunodiagnostic marker of hepatocellular carcinoma. *Gene*. 584:47–53. doi:10.1016/j.gene.2016.03.006.

Choi, M., T. Kipps, and R. Kurzrock. 2016. ATM Mutations in Cancer: Therapeutic Implications. *Mol. Cancer Ther.* 15:1781–1791. doi:10.1158/1535-7163.MCT-15-0945.

Chu, I., J. Sun, A. Arnaout, H. Kahn, W. Hanna, S. Narod, P. Sun, C.-K. Tan, L. Hengst, and J. Slingerland. 2007. p27 phosphorylation by Src regulates inhibition of cyclin E-Cdk2. *Cell*. 128:281–294. doi:10.1016/j.cell.2006.11.049.

Clijsters, L., C. Hoencamp, J.J.A. Calis, A. Marzio, S.M. Handgraaf, M.C. Cuitino, B.R. Rosenberg, G. Leone, and M. Pagano. 2019. Cyclin F Controls Cell-Cycle Transcriptional Outputs by Directing the Degradation of the Three Activator E2Fs. *Mol. Cell*. 74:1264-1277.e7. doi:10.1016/j.molcel.2019.04.010.

Cotta-Ramusino, C., E.R. 3rd McDonald, K. Hurov, M.E. Sowa, J.W. Harper, and S.J. Elledge. 2011. A DNA damage response screen identifies RHINO, a 9-1-1 and TopBP1 interacting protein required for ATR signaling. *Science*. 332:1313–1317. doi:10.1126/science.1203430.

Cummins, J.M., C. Rago, M. Kohli, K.W. Kinzler, C. Lengauer, and B. Vogelstein. 2004. Tumour suppression: disruption of HAUSP gene stabilizes p53. *Nature*. 428:1 p following 486. doi:10.1038/nature02501.

D'Angiolella, V., V. Donato, F.M. Forrester, Y.-T. Jeong, C. Pellacani, Y. Kudo, A. Saraf, L. Florens, M.P. Washburn, and M. Pagano. 2012. Cyclin F-mediated degradation of ribonucleotide reductase M2 controls genome integrity and DNA repair. *Cell*. 149:1023–1034. doi:10.1016/j.cell.2012.03.043.

D'Angiolella, V., M. Esencay, and M. Pagano. 2013. A cyclin without cyclin-dependent kinases: cyclin F controls genome stability through ubiquitin-mediated proteolysis. *Trends Cell Biol.* 23:135–140. doi:10.1016/j.tcb.2012.10.011.

Dang, C. V. 2012. MYC on the path to cancer. *Cell*. 149:22–35. doi:10.1016/j.cell.2012.03.003.

Dang, C. V, K.A. O'Donnell, K.I. Zeller, T. Nguyen, R.C. Osthus, and F. Li. 2006. The c-Myc target gene network. *Semin. Cancer Biol.* 16:253–264. doi:10.1016/j.semcancer.2006.07.014.

Dankert, J.F., G. Rona, L. Clijsters, P. Geter, J.R. Skaar, K. Bermudez-Hernandez, E. Sassani, D. Fenyö, B. Ueberheide, R. Schneider, and M. Pagano. 2016. Cyclin F-Mediated Degradation of SLBP Limits H2A.X Accumulation and Apoptosis upon Genotoxic Stress in G2. *Mol. Cell*. 64:507–519. doi:10.1016/j.molcel.2016.09.010.

Debéthune, L., G. Kohlhagen, A. Grandas, and Y. Pommier. 2002. Processing of nucleopeptides mimicking the topoisomerase I-DNA covalent complex by tyrosyl-DNA phosphodiesterase. *Nucleic Acids Res.* 30:1198–1204. doi:10.1093/nar/30.5.1198.

Dianov, G.L., and U. Hubscher. 2013. Mammalian base excision repair: the forgotten archangel. *Nucleic Acids Res.* 41:3483–3490. doi:10.1093/nar/gkt076.

Dick, F.A., and S.M. Rubin. 2013. Molecular mechanisms underlying RB protein function. *Nat. Rev. Mol. Cell Biol.* 14:297–306. doi:10.1038/nrm3567.

Diehl, J.A. 2002. Cycling to cancer with cyclin D1. *Cancer Biol. Ther.* 1:226–231.

Drosos, Y., M. Kouloukoussa, A.C. Østvold, K. Grundt, N. Goutas, D. Vlachodimitropoulos, S. Havaki, P. Kollia, C. Kittas, E. Marinos, and V. Aleporou-Marinou. 2009. NUCKS overexpression in breast cancer. *Cancer Cell Int.* 9:19. doi:10.1186/1475-2867-9-19.

Dulić, V., W.K. Kaufmann, S.J. Wilson, T.D. Tlsty, E. Lees, J.W. Harper, S.J. Elledge, and S.I. Reed. 1994. p53-dependent inhibition of cyclin-dependent kinase activities in human fibroblasts during radiation-induced G1 arrest. *Cell*. 76:1013–1023. doi:10.1016/0092-8674(94)90379-4.

Engeland, K. 2018. Cell cycle arrest through indirect transcriptional repression by p53: I have a DREAM. *Cell Death Differ.* 25:114–132. doi:10.1038/cdd.2017.172.

Fanning, E., V. Klimovich, and A.R. Nager. 2006. A dynamic model for replication protein A (RPA) function in DNA processing pathways. *Nucleic Acids Res.* 34:4126–4137. doi:10.1093/nar/gkl550.

Fielden, J., A. Ruggiano, M. Popović, and K. Ramadan. 2018. DNA protein crosslink proteolysis repair: From yeast to premature ageing and cancer in humans. *DNA Repair (Amst).* 71:198–204. doi:10.1016/j.dnarep.2018.08.025.

Fielden, J., K. Wiseman, I. Torrecilla, S. Li, S. Hume, S.-C. Chiang, A. Ruggiano, A. Narayan Singh, R. Freire, S. Hassanieh, E. Domingo, I. Vendrell, R. Fischer, B.M. Kessler, T.S. Maughan, S.F. El-Khamisy, and K. Ramadan. 2020. TEX264 coordinates p97- and SPRTN-mediated resolution of topoisomerase 1-DNA adducts. *Nat. Commun.* 11:1274. doi:10.1038/s41467-020-15000-w.

Fischer, M. 2017. Census and evaluation of p53 target genes. *Oncogene*. 36:3943–3956. doi:10.1038/onc.2016.502.

Fischer, M., P. Grossmann, M. Padi, and J.A. DeCaprio. 2016. Integration of TP53, DREAM, MMB-FOXM1 and RB-E2F target gene analyses identifies cell cycle gene regulatory networks. *Nucleic Acids Res.* 44:6070–6086. doi:10.1093/nar/gkw523.

Fischer, M., L. Steiner, and K. Engeland. 2014. The transcription factor p53: not a repressor, solely an activator. *Cell Cycle*. 13:3037–3058. doi:10.4161/15384101.2014.949083.

Fletcher, S.C., C.P. Grou, A.J. Legrand, X. Chen, K. Soderstrom, M. Poletto, and G.L. Dianov. 2018. Sp1 phosphorylation by ATM downregulates BER and promotes cell elimination in response to persistent DNA damage. *Nucleic Acids Res.* 46:1834–1846. doi:10.1093/nar/gkx1291.

Frescas, D., and M. Pagano. 2008. Deregulated proteolysis by the F-box proteins SKP2 and beta-TrCP: tipping the scales of cancer. *Nat. Rev. Cancer*. 8:438–449. doi:10.1038/nrc2396.

Fridman, J.S., and S.W. Lowe. 2003. Control of apoptosis by p53. *Oncogene*. 22:9030–9040. doi:10.1038/sj.onc.1207116.

Galanos, P., K. Vougas, D. Walter, A. Polyzos, A. Maya-Mendoza, E.J. Haagensen, A. Kokkalis, F.-M. Roumelioti, S. Gagos, M. Tzetis, B. Canovas, A. Igea, A.K. Ahuja, R. Zellweger, S. Havaki, E. Kanavakis, D. Kletsas, I.B. Roninson, S.D. Garbis, M. Lopes, A. Nebreda, D. Thanos, J.J. Blow, P. Townsend, C.S. Sorensen, J. Bartek, and V.G. Gorgoulis. 2016. Chronic p53-independent p21 expression causes genomic instability by deregulating replication licensing. *Nat. Cell Biol.* 18:777–789. doi:10.1038/ncb3378.

Gao, J., B.A. Aksoy, U. Dogrusoz, G. Dresdner, B. Gross, S.O. Sumer, Y. Sun, A. Jacobsen, R. Sinha, E. Larsson, E. Cerami, C. Sander, and N. Schultz. 2013. Integrative analysis of complex cancer genomics and clinical profiles using the cBioPortal. *Sci. Signal.* 6:pl1. doi:10.1126/scisignal.2004088.

Gelot, C., I. Magdalou, and B.S. Lopez. 2015. Replication stress in Mammalian cells and its consequences for mitosis. *Genes (Basel).* 6:267–298. doi:10.3390/genes6020267.

Geng, Y., E.N. Eaton, M. Picón, J.M. Roberts, A.S. Lundberg, A. Gifford, C. Sardet, and R.A. Weinberg. 1996. Regulation of cyclin E transcription by E2Fs and retinoblastoma protein. *Oncogene*. 12:1173–1180.

Geva-Zatorsky, N., N. Rosenfeld, S. Itzkovitz, R. Milo, A. Sigal, E. Dekel, T. Yarnitzky, Y. Liron, P. Polak, G. Lahav, and U. Alon. 2006. Oscillations and variability in the p53 system. *Mol. Syst. Biol.* 2:2006.0033. doi:10.1038/msb4100068.

Geyer, R.K., Z.K. Yu, and C.G. Maki. 2000. The MDM2 RING-finger domain is required to promote p53 nuclear export. *Nat. Cell Biol.* 2:569–573. doi:10.1038/35023507.

Goldman, M., B. Craft, M. Hastie, K. Repečka, F. McDade, A. Kamath, A. Banerjee, Y. Luo, D. Rogers, A.N. Brooks, J. Zhu, and D. Haussler. 2019. The UCSC Xena platform for public and private cancer genomics data visualization and interpretation. *bioRxiv*. 326470. doi:10.1101/326470.

Grimmler, M., Y. Wang, T. Mund, Z. Cilensek, E.-M. Keidel, M.B. Waddell, H. Jäkel, M. Kullmann, R.W. Kriwacki, and L. Hengst. 2007. Cdk-inhibitory activity and stability of p27Kip1 are directly regulated by oncogenic tyrosine kinases. *Cell*. 128:269–280. doi:10.1016/j.cell.2006.11.047.

Grundt, K., I. V Haga, H.S. Huitfeldt, and A.C. Ostvold. 2007. Identification and characterization of two putative nuclear localization signals (NLS) in the DNA-binding protein NUCKS. *Biochim. Biophys. Acta*. 1773:1398–1406. doi:10.1016/j.bbamcr.2007.05.013.

Grundt, K., L. Skjeldal, H.W. Anthonsen, T. Skauge, H.S. Huitfeldt, and A.C. Ostvold. 2002. A putative DNA-binding domain in the NUCKS protein. *Arch. Biochem. Biophys.* 407:168–175.

Gstaiger, M., R. Jordan, M. Lim, C. Catzavelos, J. Mestan, J. Slingerland, and W. Krek. 2001. Skp2 is oncogenic and overexpressed in human cancers. *Proc. Natl. Acad. Sci. U. S. A.* 98:5043–5048. doi:10.1073/pnas.081474898.

Gu, L., B. Xia, L. Zhong, Y. Ma, L. Liu, L. Yang, and G. Lou. 2014. NUCKS1 overexpression is a novel biomarker for recurrence-free survival in cervical squamous cell carcinoma. *Tumour Biol.* 35:7831–7836. doi:10.1007/s13277-014-2035-5.

Guiley, K.Z., J.W. Stevenson, K. Lou, K.J. Barkovich, V. Kumarasamy, T.U. Wijeratne, K.L. Bunch, S. Tripathi, E.S. Knudsen, A.K. Witkiewicz, K.M. Shokat, and S.M. Rubin. 2019. p27 allosterically activates cyclin-dependent kinase 4 and antagonizes palbociclib inhibition. *Science*. 366. doi:10.1126/science.aaw2106.

Gulbis, J.M., Z. Kelman, J. Hurwitz, M. O'Donnell, and J. Kuriyan. 1996. Structure of the C-terminal region of p21(WAF1/CIP1) complexed with human PCNA. *Cell*. 87:297–306.

Guo, Z., S. Kozlov, M.F. Lavin, M.D. Person, and T.T. Paull. 2010. ATM activation by oxidative stress. *Science*. 330:517–521. doi:10.1126/science.1192912.

Haahr, P., S. Hoffmann, M.A.X. Tollenaere, T. Ho, L.I. Toledo, M. Mann, S. Bekker-Jensen, M. Räschle, and N. Mailand. 2016. Activation of the ATR kinase by the RPA-binding protein ETAA1. *Nat. Cell Biol.* doi:10.1038/ncb3422.

Halazonetis, T.D., V.G. Gorgoulis, and J. Bartek. 2008. An oncogene-induced DNA damage model for cancer development. *Science*. 319:1352–1355. doi:10.1126/science.1140735.

Halder, S., I. Torrecilla, M.D. Burkhalter, M. Popovic, J. Fielden, B. Vaz, J. Oehler, D. Pilger, D. Lessel, K. Wiseman, A.N. Singh, I. Vendrell, R. Fischer, M. Philipp, and K. Ramadan. 2019. SPRTN protease and checkpoint kinase 1 cross-activation loop safeguards DNA replication. *Nat. Commun.* 10:3142. doi:10.1038/s41467-019-11095-y.

Hallett, S.T., M.W. Pastok, R.M.L. Morgan, A. Wittner, K.L.I.M. Blundell, I. Felletar, S.R. Wedge, C. Prodromou, M.E.M. Noble, L.H. Pearl, and J.A. Endicott. 2017. Differential Regulation of G1 CDK Complexes by the Hsp90-Cdc37 Chaperone System. *Cell Rep.* 21:1386–1398. doi:10.1016/j.celrep.2017.10.042.

Hanahan, D., and R.A. Weinberg. 2011. Hallmarks of cancer: The next generation. *Cell*. doi:10.1016/j.cell.2011.02.013.

Hao, B., N. Zheng, B.A. Schulman, G. Wu, J.J. Miller, M. Pagano, and N.P. Pavletich. 2005. Structural basis of the Cks1-dependent recognition of p27(Kip1) by the SCF(Skp2) ubiquitin ligase. *Mol. Cell*. 20:9–19. doi:10.1016/j.molcel.2005.09.003.

Harbour, J.W., R.X. Luo, A. Dei Santi, A.A. Postigo, and D.C. Dean. 1999. Cdk phosphorylation triggers sequential intramolecular interactions that progressively block Rb functions as cells move through G1. *Cell*. 98:859–869. doi:10.1016/s0092-8674(00)81519-6.

Haupt, Y., R. Maya, A. Kazaz, and M. Oren. 1997. Mdm2 promotes the rapid degradation of p53. *Nature*. doi:10.1038/387296a0.

He, S., S. Yang, M. Niu, Y. Zhong, D. Gao, Y. Zhang, H. Ma, W. Xiong, M. Zhou, Y. Zhou, B. Xiang, G. Li, C. Shuai, and S. Peng. 2018. HMG-box transcription factor 1: a positive regulator of the G1/S transition through the Cyclin-CDK-CDKI molecular network in nasopharyngeal carcinoma. *Cell Death Dis.* 9:100. doi:10.1038/s41419-017-0175-4.

Heldt, F.S., A.R. Barr, S. Cooper, C. Bakal, and B. Novak. 2018. A comprehensive model for the proliferation-quiescence decision in response to endogenous DNA damage in human cells. *Proc. Natl. Acad. Sci. U. S. A.* 115:2532–2537. doi:10.1073/pnas.1715345115.

Hermeking, H., C. Lengauer, K. Polyak, T.C. He, L. Zhang, S. Thiagalingam, K.W. Kinzler, and B. Vogelstein. 1997. 14-3-3sigma is a p53-regulated inhibitor of G2/M progression. *Mol. Cell*. 1:3–11.

Hills, S.A., and J.F.X. Diffley. 2014. DNA replication and oncogene-induced replicative stress. *Curr. Biol.* 24:R435-44. doi:10.1016/j.cub.2014.04.012.

Ho, J.S.L., W. Ma, D.Y.L. Mao, and S. Benchimol. 2005. p53-Dependent transcriptional repression of c-myc is required for G1 cell cycle arrest. *Mol. Cell. Biol.* 25:7423–7431. doi:10.1128/MCB.25.17.7423-7431.2005.

Hoeijmakers, J.H.J. 2009. DNA damage, aging, and cancer. *N. Engl. J. Med.* 361:1475–1485. doi:10.1056/NEJMra0804615.

Huang, Y.-K., W.-M. Kang, Z.-Q. Ma, Y.-Q. Liu, L. Zhou, and J.-C. Yu. 2019. NUCKS1 promotes gastric cancer cell aggressiveness by upregulating IGF-1R and subsequently activating the PI3K/Akt/mTOR signaling pathway. *Carcinogenesis*. 40:370–379. doi:10.1093/carcin/bgy142.

Huang, Y., M.-K. Yoon, S. Otieno, M. Lelli, and R.W. Kriwacki. 2015. The activity and stability of the intrinsically disordered Cip/Kip protein family are regulated by non-receptor tyrosine kinases. *J. Mol. Biol.* 427:371–386. doi:10.1016/j.jmb.2014.11.011.

Hume, S., G.L. Dianov, and K. Ramadan. 2020. A unified model for the G1/S cell cycle transition. *Nucleic Acids Res.* 48:12483–12501. doi:10.1093/nar/gkaa1002.

Hustedt, N., and D. Durocher. 2016. The control of DNA repair by the cell cycle. *Nat. Cell Biol.* 19:1–9. doi:10.1038/ncb3452.

Imaki, H., K. Nakayama, S. Delehouzee, H. Handa, M. Kitagawa, T. Kamura, and K.I. Nakayama. 2003. Cell cycle-dependent regulation of the Skp2 promoter by GA-binding protein. *Cancer Res.* 63:4607–4613.

Innocente, S.A., J.L. Abrahamson, J.P. Cogswell, and J.M. Lee. 1999. p53 regulates a G2 checkpoint through cyclin B1. *Proc. Natl. Acad. Sci. U. S. A.* 96:2147–2152.

Inoue, K., and E.A. Fry. 2015. Aberrant expression of cyclin D1 in cancer. *Sign. Transduct. Insights*. 4:1–13. doi:10.4137/STI.S30306.

Interthal, H., H.J. Chen, and J.J. Champoux. 2005. Human Tdp1 cleaves a broad spectrum of substrates, including phosphoamide linkages. *J. Biol. Chem.* 280:36518–36528. doi:10.1074/jbc.M508898200.

Issaeva, N., P. Bozko, M. Enge, M. Protopopova, L.G.G.C. Verhoef, M. Masucci, A. Pramanik, and G. Selivanova. 2004. Small molecule RITA binds to p53, blocks p53-HDM-2 interaction and activates p53 function in tumors. *Nat. Med.* 10:1321–1328. doi:10.1038/nm1146.

Iyer, D.R., and N. Rhind. 2017. The Intra-S Checkpoint Responses to DNA Damage. *Genes (Basel).* 8. doi:10.3390/genes8020074.

Janic, A., L.J. Valente, M.J. Wakefield, L. Di Stefano, L. Milla, S. Wilcox, H. Yang, L. Tai, C.J. Vandenberg, A.J. Kueh, S. Mizutani, M.S. Brennan, R.L. Schenk, L.M. Lindqvist, A.T. Papenfuss, L. O'Connor, A. Strasser, and M.J. Herold. 2018. DNA repair processes are critical mediators of p53-dependent tumor suppression. *Nat. Med.* 24:947–953. doi:10.1038/s41591-018-0043-5.

Jeffrey, P.D., L. Tong, and N.P. Pavletich. 2000. Structural basis of inhibition of CDK-cyclin complexes by INK4 inhibitors. *Genes Dev.* 14:3115–3125. doi:10.1101/gad.851100.

Jun, D.Y., J.Y. Lee, H.S. Park, Y.H. Lee, and Y.H. Kim. 2017. Tumor suppressor protein p53-mediated repression of human mitotic centromere-associated kinesin gene expression is exerted via down-regulation of Sp1 level. *PLoS One*. 12:e0189698. doi:10.1371/journal.pone.0189698.

Kamura, T., T. Hara, S. Kotoshiba, M. Yada, N. Ishida, H. Imaki, S. Hatakeyama, K. Nakayama, and K.I. Nakayama. 2003. Degradation of p57Kip2 mediated by SCFSkp2-dependent ubiquitylation. *Proc. Natl. Acad. Sci. U. S. A.* 100:10231–10236. doi:10.1073/pnas.1831009100.

Kastan, M.B., and J. Bartek. 2004. Cell-cycle checkpoints and cancer. *Nature*. 432:316–323. doi:10.1038/nature03097.

Kastenhuber, E.R., and S.W. Lowe. 2017. Putting p53 in Context. *Cell*. 170:1062–1078. doi:10.1016/j.cell.2017.08.028.

Kategaya, L., P. Di Lello, L. Rouge, R. Pastor, K.R. Clark, J. Drummond, T. Kleinheinz, E. Lin, J.-P. Upton, S. Prakash, J. Heideker, M. McCleland, M.S. Ritorto, D.R. Alessi, M. Trost, T.W. Bainbridge, M.C.M. Kwok, T.P. Ma, Z. Stiffler, B. Brasher, Y. Tang, P. Jaishankar, B.R. Hearn, A.R. Renslo, M.R. Arkin, F. Cohen, K. Yu, F. Peale, F. Gnad, M.T. Chang, C. Klijn, E. Blackwood, S.E. Martin, W.F. Forrest, J.A. Ernst, C. Ndubaku, X. Wang, M.H. Beresini, V. Tsui, C. Schwerdtfeger, R.A. Blake, J. Murray, T. Maurer, and I.E. Wertz. 2017. USP7 small-molecule inhibitors interfere with ubiquitin binding. *Nature*. 550:534–538. doi:10.1038/nature24006.

Kent, L.N., and G. Leone. 2019. The broken cycle: E2F dysfunction in cancer. *Nat. Rev. Cancer*. 19:326–338. doi:10.1038/s41568-019-0143-7.

Khoronenkova, S. V, and G.L. Dianov. 2015. ATM prevents DSB formation by coordinating SSB repair and cell cycle progression. *Proc. Natl. Acad. Sci. U. S. A.* 112:3997–4002. doi:10.1073/pnas.1416031112.

Khoronenkova, S. V, I.I. Dianova, N. Ternette, B.M. Kessler, J.L. Parsons, and G.L. Dianov. 2012. ATM-dependent downregulation of USP7/HAUSP by PPM1G activates p53 response to DNA damage. *Mol. Cell*. 45:801–813. doi:10.1016/j.molcel.2012.01.021.

Kikuchi, A., T. Ishikawa, K. Mogushi, M. Ishiguro, S. Iida, H. Mizushima, H. Uetake, H. Tanaka, and K. Sugihara. 2013. Identification of NUCKS1 as a colorectal cancer prognostic marker through integrated expression and copy number analysis. *Int. J. cancer*. 132:2295–2302. doi:10.1002/ijc.27911.

Kim, J.K., and J.A. Diehl. 2009. Nuclear cyclin D1: an oncogenic driver in human cancer. *J. Cell. Physiol.* 220:292–296. doi:10.1002/jcp.21791.

Kim, S.Y., A. Herbst, K.A. Tworkowski, S.E. Salghetti, and W.P. Tansey. 2003. Skp2 regulates Myc protein stability and activity. *Mol. Cell*. 11:1177–1188. doi:10.1016/s1097-2765(03)00173-4.

Kitagawa, M., S.H. Lee, and F. McCormick. 2008. Skp2 suppresses p53-dependent apoptosis by inhibiting p300. *Mol. Cell*. 29:217–231. doi:10.1016/j.molcel.2007.11.036.

Krenning, L., F.M. Feringa, I.A. Shaltiel, J. van den Berg, and R.H. Medema. 2014. Transient activation of p53 in G2 phase is sufficient to induce senescence. *Mol. Cell*. 55:59–72. doi:10.1016/j.molcel.2014.05.007.

Kubbutat, M.H.G., S.N. Jones, and K.H. Vousden. 1997. Regulation of p53 stability by Mdm2. *Nature*. doi:10.1038/387299a0.

Kumagai, A., J. Lee, H.Y. Yoo, and W.G. Dunphy. 2006. TopBP1 activates the ATR-ATRIP complex. *Cell*. doi:10.1016/j.cell.2005.12.041.

Kumar, R., P.M. Neilsen, J. Crawford, R. McKirdy, J. Lee, J.A. Powell, Z. Saif, J.M. Martin, M. Lombaerts, C.J. Cornelisse, A.-M. Cleton-Jansen, and D.F. Callen. 2005. FBXO31 is the chromosome 16q24.3 senescence gene, a candidate breast tumor suppressor, and a component of an SCF complex. *Cancer Res.* 65:11304–11313. doi:10.1158/0008-5472.CAN-05-0936.

Kussie, P.H., S. Gorina, V. Marechal, B. Elenbaas, J. Moreau, A.J. Levine, and N.P. Pavletich. 1996. Structure of the MDM2 oncoprotein bound to the p53 tumor suppressor transactivation domain. *Science*. 274:948–953.

Lahav, G., N. Rosenfeld, A. Sigal, N. Geva-Zatorsky, A.J. Levine, M.B. Elowitz, and U. Alon. 2004. Dynamics of the p53-Mdm2 feedback loop in individual cells. *Nat. Genet.* doi:10.1038/ng1293.

Lane, D.P. 1992. p53, guardian of the genome. *Nature*. doi:10.1038/358015a0.

Lange, S.S., D.L. Mitchell, and K.M. Vasquez. 2008. High mobility group protein B1 enhances DNA repair and chromatin modification after DNA damage. *Proc. Natl. Acad. Sci. U. S. A.* 105:10320–10325. doi:10.1073/pnas.0803181105.

Larrea, M.D., J. Liang, T. Da Silva, F. Hong, S.H. Shao, K. Han, D. Dumont, and J.M. Slingerland. 2008. Phosphorylation of p27Kip1 regulates assembly and activation of cyclin D1-Cdk4. *Mol. Cell. Biol.* 28:6462–6472. doi:10.1128/MCB.02300-07.

Lee, J.-H., and T.T. Paull. 2005. ATM activation by DNA double-strand breaks through the Mre11-Rad50-Nbs1 complex. *Science*. 308:551–554. doi:10.1126/science.1108297.

Legrand, A.J., M. Poletto, D. Pankova, E. Clementi, J. Moore, F. Castro-Giner, A.J. Ryan, E. O'Neill, E. Markkanen, and G.L. Dianov. 2018. Persistent DNA strand breaks induce a CAF-like phenotype in normal fibroblasts. *Oncotarget*. 9:13666–13681. doi:10.18632/oncotarget.24446.

Leng, P., D.R. Brown, C. V Shivakumar, S. Deb, and S.P. Deb. 1995. N-terminal 130 amino acids of MDM2 are sufficient to inhibit p53-mediated transcriptional activation. *Oncogene*.

Li, M., C.L. Brooks, N. Kon, and W. Gu. 2004. A dynamic role of HAUSP in the p53-Mdm2 pathway. *Mol. Cell*. 13:879–886.

Li, M., C.L. Brooks, F. Wu-Baer, D. Chen, R. Baer, and W. Gu. 2003. Mono- versus polyubiquitination: differential control of p53 fate by Mdm2. *Science*. 302:1972–1975. doi:10.1126/science.1091362.

Li, M., D. Chen, A. Shiloh, J. Luo, A.Y. Nikolaev, J. Qin, and W. Gu. 2002. Deubiquitination of p53 by HAUSP is an important pathway for p53 stabilization. *Nature*. 416:648–653. doi:10.1038/nature737.

Lin, C.Y., J. Lovén, P.B. Rahl, R.M. Paranal, C.B. Burge, J.E. Bradner, T.I. Lee, and R.A. Young. 2012. Transcriptional amplification in tumor cells with elevated c-Myc. *Cell*. 151:56–67. doi:10.1016/j.cell.2012.08.026.

Litovchick, L., S. Sadasivam, L. Florens, X. Zhu, S.K. Swanson, S. Velmurugan, R. Chen, M.P. Washburn, X.S. Liu, and J.A. DeCaprio. 2007. Evolutionarily conserved multisubunit RBL2/p130 and E2F4 protein complex represses human cell cycle-dependent genes in quiescence. *Mol. Cell*. 26:539–551. doi:10.1016/j.molcel.2007.04.015.

Liu, G.Y., and D.M. Sabatini. 2020. mTOR at the nexus of nutrition, growth, ageing and disease. *Nat. Rev. Mol. Cell Biol.* 21:183–203. doi:10.1038/s41580-019-0199-y.

Liu, Q., S. Guntuku, X.S. Cui, S. Matsuoka, D. Cortez, K. Tamai, G. Luo, S. Carattini-Rivera, F. DeMayo, A. Bradley, L.A. Donehower, and S.J. Elledge. 2000. Chk1 is an essential kinase that is regulated by Atr and required for the G(2)/M DNA damage checkpoint. *Genes Dev.* 14:1448–1459.

Liu, T., S. Tan, Y. Xu, F. Meng, C. Yang, and G. Lou. 2015. Increased NUCKS expression is a risk factor for poor prognosis and recurrence in endometrial cancer. *Am. J. Cancer Res.* 5:3659–3667.

Loewer, A., E. Batchelor, G. Gaglia, and G. Lahav. 2010. Basal dynamics of p53 reveal transcriptionally attenuated pulses in cycling cells. *Cell*. 142:89–100. doi:10.1016/j.cell.2010.05.031.

Lord, C.J., and A. Ashworth. 2012. The DNA damage response and cancer therapy. *Nature*. 481:287–294. doi:10.1038/nature10760.

Macheret, M., and T.D. Halazonetis. 2018. Intragenic origins due to short G1 phases underlie oncogene-induced DNA replication stress. *Nature*. 555:112–116. doi:10.1038/nature25507.

Mailand, N., J. Falck, C. Lukas, R.G. Syljuåsen, M. Welcker, J. Bartek, and J. Lukas. 2000. Rapid destruction of human Cdc25A in response to DNA damage. *Science (80-.).* doi:10.1126/science.288.5470.1425.

Malkin, D. 2011. Li-fraumeni syndrome. *Genes Cancer*. 2:475–484. doi:10.1177/1947601911413466.

Malumbres, M. 2014. Cyclin-dependent kinases. *Genome Biol.* 15:122. doi:10.1186/gb4184.

Malumbres, M., and M. Barbacid. 2009. Cell cycle, CDKs and cancer: a changing paradigm. *Nat. Rev. Cancer*. 9:153–166. doi:10.1038/nrc2602.

Mannefeld, M., E. Klassen, and S. Gaubatz. 2009. B-MYB is required for recovery from the DNA damage-induced G2 checkpoint in p53 mutant cells. *Cancer Res.* 69:4073–4080. doi:10.1158/0008-5472.CAN-08-4156.

Manning, B.D., and A. Toker. 2017. AKT/PKB Signaling: Navigating the Network. *Cell*. 169:381–405. doi:10.1016/j.cell.2017.04.001.

Maranon, D.G., N. Sharma, Y. Huang, P. Selemenakis, M. Wang, N. Altina, W. Zhao, and C. Wiese. 2020. NUCKS1 promotes RAD54 activity in homologous recombination DNA repair. *J. Cell Biol.* 219. doi:10.1083/jcb.201911049.

Matsuoka, S., B.A. Ballif, A. Smogorzewska, E.R. 3rd McDonald, K.E. Hurov, J. Luo, C.E. Bakalarski, Z. Zhao, N. Solimini, Y. Lerenthal, Y. Shiloh, S.P. Gygi, and S.J. Elledge. 2007. ATM and ATR substrate analysis reveals extensive protein networks responsive to DNA damage. *Science*. 316:1160–1166. doi:10.1126/science.1140321.

Mejia-Guerrero, S., M. Quejada, N. Gokgoz, M. Gill, R.K. Parkes, J.S. Wunder, and I.L. Andrulis. 2010. Characterization of the 12q15 MDM2 and 12q13-14 CDK4 amplicons and clinical correlations in osteosarcoma. *Genes. Chromosomes Cancer*. 49:518–525. doi:10.1002/gcc.20761.

Meloche, S., and J. Pouysségur. 2007. The ERK1/2 mitogen-activated protein kinase pathway as a master regulator of the G1- to S-phase transition. *Oncogene*. 26:3227–3239. doi:10.1038/sj.onc.1210414.

Min, M., Y. Rong, C. Tian, and S. Spencer. 2020. Temporal integration of mitogen history in mother cells controls proliferation of daughter cells. *Science*. doi:10.1126/science.aay8241.

Moldovan, G.-L., B. Pfander, and S. Jentsch. 2007. PCNA, the maestro of the replication fork. *Cell*. 129:665–679. doi:10.1016/j.cell.2007.05.003.

Momand, J., G.P. Zambetti, D.C. Olson, D. George, and A.J. Levine. 1992. The mdm-2 oncogene product forms a complex with the p53 protein and inhibits p53-mediated transactivation. *Cell*. 69:1237–1245.

Montes de Oca Luna, R., D.S. Wagner, and G. Lozano. 1995. Rescue of early embryonic lethality in mdm2-deficient mice by deletion of p53. *Nature*. 378:203–206. doi:10.1038/378203a0.

Moser, J., I. Miller, D. Carter, and S.L. Spencer. 2018. Control of the Restriction Point by Rb and p21. *Proc. Natl. Acad. Sci. U. S. A.* 115:E8219–E8227. doi:10.1073/pnas.1722446115.

Muller, P.A.J., and K.H. Vousden. 2013. p53 mutations in cancer. *Nat. Cell Biol.* 15:2–8. doi:10.1038/ncb2641.

Narasimha, A.M., M. Kaulich, G.S. Shapiro, Y.J. Choi, P. Sicinski, and S.F. Dowdy. 2014. Cyclin D activates the Rb tumor suppressor by mono-phosphorylation. *Elife*. 3. doi:10.7554/eLife.02872.

Naylor, T.L., J. Greshock, Y. Wang, T. Colligon, Q.C. Yu, V. Clemmer, T.Z. Zaks, and B.L. Weber. 2005. High resolution genomic analysis of sporadic breast cancer using array-based comparative genomic hybridization. *Breast Cancer Res.* 7:R1186-98. doi:10.1186/bcr1356.

Niculescu, A.B. 3rd, X. Chen, M. Smeets, L. Hengst, C. Prives, and S.I. Reed. 1998. Effects of p21(Cip1/Waf1) at both the G1/S and the G2/M cell cycle transitions: pRb is a critical determinant in blocking DNA replication and in preventing endoreduplication. *Mol. Cell. Biol.* 18:629–643.

Nikulenkov, F., C. Spinnler, H. Li, C. Tonelli, Y. Shi, M. Turunen, T. Kivioja, I. Ignatiev, A. Kel, J. Taipale, and G. Selivanova. 2012. Insights into p53 transcriptional function via genome-wide chromatin occupancy and gene expression analysis. *Cell Death Differ.* 19:1992–2002. doi:10.1038/cdd.2012.89.

O'Connell, M.J., J.M. Raleigh, H.M. Verkade, and P. Nurse. 1997. Chk1 is a wee1 kinase in the G2 DNA damage checkpoint inhibiting cdc2 by Y15 phosphorylation. *EMBO J.* 16:545–554. doi:10.1093/emboj/16.3.545.

Oliner, J.D., J.A. Pietenpol, S. Thiagalingam, J. Gyuris, K.W. Kinzler, and B. Vogelstein. 1993. Oncoprotein MDM2 conceals the activation domain of tumour suppressor p53. *Nature*. 362:857–860. doi:10.1038/362857a0.

Olivero, C.E., E. Martinez-Terroba, J. Zimmer, C. Liao, E. Tesfaye, N. Hooshdaran, J.A. Schofield, J. Bendor, D. Fang, M.D. Simon, J.R. Zamudio, and N. Dimitrova. 2020. p53 Activates the Long Noncoding RNA Pvt1b to Inhibit Myc and Suppress Tumorigenesis. *Mol. Cell*. 77:761-774.e8. doi:10.1016/j.molcel.2019.12.014.

Orlando, G., S. V Khoronenkova, I.I. Dianova, J.L. Parsons, and G.L. Dianov. 2014. ARF induction in response to DNA strand breaks is regulated by PARP1. *Nucleic Acids Res.* 42:2320–2329. doi:10.1093/nar/gkt1185.

Ostvold, A.C., J. Holtlund, and S.G. Laland. 1985. A novel, highly phosphorylated protein, of the high-mobility group type, present in a variety of proliferating and non-proliferating mammalian cells. *Eur. J. Biochem.* 153:469–475.

Ostvold, A.C., J.H. Norum, S. Mathiesen, B. Wanvik, I. Sefland, and K. Grundt. 2001. Molecular cloning of a mammalian nuclear phosphoprotein NUCKS, which serves as a substrate for Cdk1 in vivo. *Eur. J. Biochem.* 268:2430–2440. doi:10.1046/j.1432-1327.2001.02120.x.

Ozenne, P., B. Eymin, E. Brambilla, and S. Gazzeri. 2010. The ARF tumor suppressor: structure, functions and status in cancer. *Int. J. cancer*. 127:2239–2247. doi:10.1002/ijc.25511.

Ozturk, N., I. Singh, A. Mehta, T. Braun, and G. Barreto. 2014. HMGA proteins as modulators of chromatin structure during transcriptional activation. *Front. cell Dev. Biol.* 2:5. doi:10.3389/fcell.2014.00005.

Panagopoulos, A., and M. Altmeyer. 2020. The Hammer and the Dance of Cell Cycle Control. *Trends Biochem. Sci.* doi:10.1016/j.tibs.2020.11.002.

Pardee, A.B. 1974. A restriction point for control of normal animal cell proliferation. *Proc. Natl. Acad. Sci. U. S. A.* 71:1286–1290. doi:10.1073/pnas.71.4.1286.

Parker, L.L., and H. Piwnica-Worms. 1992. Inactivation of the p34cdc2-cyclin B complex by the human WEE1 tyrosine kinase. *Science*. 257:1955–1957.

Parplys, A.C., W. Zhao, N. Sharma, T. Groesser, F. Liang, D.G. Maranon, S.G. Leung, K. Grundt, E. Dray, R. Idate, A.C. Ostvold, D. Schild, P. Sung, and C. Wiese. 2015. NUCKS1 is a novel RAD51AP1 paralog important for homologous recombination and genome stability. *Nucleic Acids Res.* 43:9817–9834. doi:10.1093/nar/gkv859.

Patel, P., B. Asbach, E. Shteyn, C. Gomez, A. Coltoff, S. Bhuyan, A.L. Tyner, R. Wagner, and S.W. Blain. 2015. Brk/Protein tyrosine kinase 6 phosphorylates p27KIP1, regulating the activity of cyclin D-cyclin-dependent kinase 4. *Mol. Cell. Biol.* 35:1506–1522. doi:10.1128/MCB.01206-14.

Pelengaris, S., M. Khan, and G. Evan. 2002. c-MYC: more than just a matter of life and death. *Nat. Rev. Cancer*. 2:764–776. doi:10.1038/nrc904.

Pines, J. 2011. Cubism and the cell cycle: the many faces of the APC/C. *Nat. Rev. Mol. Cell Biol.* 12:427–438. doi:10.1038/nrm3132.

Poletto, M., A.J. Legrand, S.C. Fletcher, and G.L. Dianov. 2016. p53 coordinates base excision repair to prevent genomic instability. *Nucleic Acids Res.* 44:3165–3175. doi:10.1093/nar/gkw015.

Poon, M.-W., D. Jiang, P. Qin, Y. Zhang, B. Qiu, S. Chanda, V. Tergaonkar, Q. Li, I.Y. Wong, Z. Yu, H.-F. Tse, D.S.H. Wong, and Q. Lian. 2017. Inhibition of NUCKS Facilitates Corneal Recovery Following Alkali Burn. *Sci. Rep.* 7:41224. doi:10.1038/srep41224.

Porter, J.R., B.E. Fisher, L. Baranello, J.C. Liu, D.M. Kambach, Z. Nie, W.S. Koh, J. Luo, J.M. Stommel, D. Levens, and E. Batchelor. 2017. Global Inhibition with Specific Activation: How p53 and MYC Redistribute the Transcriptome in the DNA Double-Strand Break Response. *Mol. Cell*. 67:1013-1025.e9. doi:10.1016/j.molcel.2017.07.028.

Purvis, J.E., K.W. Karhohs, C. Mock, E. Batchelor, A. Loewer, and G. Lahav. 2012. p53 dynamics control cell fate. *Science*. 336:1440–1444. doi:10.1126/science.1218351.

Qiu, B., W. Han, and V. Tergaonkar. 2015. NUCKS: a potential biomarker in cancer and metabolic disease. *Clin. Sci. (Lond).* 128:715–721. doi:10.1042/CS20140656.

Qiu, B., X. Shi, E.T. Wong, J. Lim, M. Bezzi, D. Low, Q. Zhou, S.C. Akincilar, M. Lakshmanan, H.L.F. Swa, J.M.L. Tham, J. Gunaratne, K.K.Y. Cheng, W. Hong, K.S.L. Lam, M. Ikawa, E. Guccione, A. Xu, W. Han, and V. Tergaonkar. 2014. NUCKS is a positive transcriptional regulator of insulin signaling. *Cell Rep.* 7:1876–1886. doi:10.1016/j.celrep.2014.05.030.

Ren, B., H. Cam, Y. Takahashi, T. Volkert, J. Terragni, R.A. Young, and B.D. Dynlacht. 2002. E2F integrates cell cycle progression with DNA repair, replication, and G(2)/M checkpoints. *Genes Dev.* 16:245–256. doi:10.1101/gad.949802.

Roe, J.-S., H.-R. Kim, I.-Y. Hwang, E.-J. Cho, and H.-D. Youn. 2011. von Hippel-Lindau protein promotes Skp2 destabilization on DNA damage. *Oncogene*. 30:3127–3138. doi:10.1038/onc.2011.40.

Roninson, I.B. 2002. Oncogenic functions of tumour suppressor p21(Waf1/Cip1/Sdi1): association with cell senescence and tumour-promoting activities of stromal fibroblasts. *Cancer Lett.* 179:1–14.

Rothblum-Oviatt, C., J. Wright, M.A. Lefton-Greif, S.A. McGrath-Morrow, T.O. Crawford, and H.M. Lederman. 2016. Ataxia telangiectasia: a review. *Orphanet J. Rare Dis.* 11:159. doi:10.1186/s13023-016-0543-7.

Roy, P.G., and A.M. Thompson. 2006. Cyclin D1 and breast cancer. *Breast*. 15:718–727. doi:10.1016/j.breast.2006.02.005.

Russo, A.A., L. Tong, J.O. Lee, P.D. Jeffrey, and N.P. Pavletich. 1998. Structural basis for inhibition of the cyclin-dependent kinase Cdk6 by the tumour suppressor p16INK4a. *Nature*. 395:237–243. doi:10.1038/26155.

Sadasivam, S., and J.A. DeCaprio. 2013. The DREAM complex: master coordinator of cell cycle-dependent gene expression. *Nat. Rev. Cancer*. 13:585–595. doi:10.1038/nrc3556.

Saldivar, J.C., S. Hamperl, M.J. Bocek, M. Chung, T.E. Bass, F. Cisneros-Soberanis, K. Samejima, L. Xie, J.R. Paulson, W.C. Earnshaw, D. Cortez, T. Meyer, and K.A. Cimprich. 2018. An intrinsic S/G2 checkpoint enforced by ATR. *Science*. 361:806–810. doi:10.1126/science.aap9346.

Salvador-Barbero, B., M. Alvarez-Fernandez, E. Zapatero-Solana, A. El Bakkali, M.D.C. Menendez, P.P. Lopez-Casas, T. Di Domenico, T. Xie, T. VanArsdale, D.J. Shields, M. Hidalgo, and M. Malumbres. 2020. CDK4/6 Inhibitors Impair Recovery from Cytotoxic Chemotherapy in Pancreatic Adenocarcinoma. *Cancer Cell*. 37:340-353.e6. doi:10.1016/j.ccell.2020.01.007.

Santoro, A., T. Vlachou, L. Luzi, G. Melloni, L. Mazzarella, E. D'Elia, X. Aobuli, C.E. Pasi, L. Reavie, P. Bonetti, S. Punzi, L. Casoli, A. Sabo, M.C. Moroni, G.I. Dellino, B. Amati, F. Nicassio, L. Lanfrancone, and P.G. Pelicci. 2019. p53 Loss in Breast Cancer Leads to Myc Activation, Increased Cell Plasticity, and Expression of a Mitotic Signature with Prognostic Value. *Cell Rep.* 26:624-638.e8. doi:10.1016/j.celrep.2018.12.071.

Santra, M.K., N. Wajapeyee, and M.R. Green. 2009. F-box protein FBXO31 mediates cyclin D1 degradation to induce G1 arrest after DNA damage. *Nature*. 459:722–725. doi:10.1038/nature08011.

Schmit, F., M. Korenjak, M. Mannefeld, K. Schmitt, C. Franke, B. von Eyss, S. Gagrica, F. Hanel, A. Brehm, and S. Gaubatz. 2007. LINC, a human complex that is related to pRB-containing complexes in invertebrates regulates the expression of G2/M genes. *Cell Cycle*. 6:1903–1913. doi:10.4161/cc.6.15.4512.

Schneider, G., D. Saur, J.T. Siveke, R. Fritsch, F.R. Greten, and R.M. Schmid. 2006. IKKalpha controls p52/RelB at the skp2 gene promoter to regulate G1- to S-phase progression. *EMBO J.* 25:3801–3812. doi:10.1038/sj.emboj.7601259.

Schulze, A., K. Zerfass, D. Spitkovsky, S. Middendorp, J. Bergès, K. Helin, P. Jansen-Dürr, and B. Henglein. 1995. Cell cycle regulation of the cyclin A gene promoter is mediated by a variant E2F site. *Proc. Natl. Acad. Sci. U. S. A.* 92:11264–11268.

Shen, H., L. Wang, X. Ge, C.-F. Jiang, Z.-M. Shi, D.-M. Li, W.-T. Liu, X. Yu, and Y.-Q. Shu. 2016. MicroRNA-137 inhibits tumor growth and sensitizes chemosensitivity to paclitaxel and cisplatin in lung cancer. *Oncotarget*. 7:20728–20742. doi:10.18632/oncotarget.8011.

Shen, T., and S. Huang. 2012. The role of Cdc25A in the regulation of cell proliferation and apoptosis. *Anticancer. Agents Med. Chem.* 12:631–639.

Shi, C., L. Qin, H. Gao, L. Gu, C. Yang, H. Liu, and T. Liu. 2017. NUCKS nuclear elevated expression indicates progression and prognosis of ovarian cancer. *Tumour Biol.* 39:1010428317714631. doi:10.1177/1010428317714631.

Simoneschi, D., G. Rona, N. Zhou, Y.-T. Jeong, S. Jiang, G. Milletti, A.A. Arbini, A. O'Sullivan, A.A. Wang, S. Nithikasem, S. Keegan, Y. Siu, V. Cianfanelli, E. Maiani, F. Nazio, F. Cecconi, F. Boccalatte, D. Fenyö, D.R. Jones, L. Busino, and M. Pagano. 2021. CRL4(AMBRA1) is a master regulator of D-type cyclins. *Nature*. 592:789–793. doi:10.1038/s41586-021-03445-y.

Slebos, R.J., M.H. Lee, B.S. Plunkett, T.D. Kessis, B.O. Williams, T. Jacks, L. Hedrick, M.B. Kastan, and K.R. Cho. 1994. p53-dependent G1 arrest involves pRB-related proteins and is disrupted by the human papillomavirus 16 E7 oncoprotein. *Proc. Natl. Acad. Sci. U. S. A.* 91:5320–5324. doi:10.1073/pnas.91.12.5320.

Sørensen, C.S., R.G. Syljuåsen, J. Falck, T. Schroeder, L. Rönnstrand, K.K. Khanna, B.B. Zhou, J. Bartek, and J. Lukas. 2003. Chk1 regulates the S phase checkpoint by coupling the physiological turnover and ionizing radiation-induced accelerated proteolysis of Cdc25A. *Cancer Cell*. doi:10.1016/S1535-6108(03)00048-5.

Spencer, S.L., S.D. Cappell, F.-C. Tsai, K.W. Overton, C.L. Wang, and T. Meyer. 2013. The proliferation-quiescence decision is controlled by a bifurcation in CDK2 activity at mitotic exit. *Cell*. 155:369–383. doi:10.1016/j.cell.2013.08.062.

Stead, L.F., S. Berri, H.M. Wood, P. Egan, C. Conway, C. Daly, K. Papagiannopoulos, and P. Rabbitts. 2012. The transcriptional consequences of somatic amplifications, deletions, and rearrangements in a human lung squamous cell carcinoma. *Neoplasia*. 14:1075–1086. doi:10.1593/neo.121380.

Stingele, J., R. Bellelli, F. Alte, G. Hewitt, G. Sarek, S.L. Maslen, S.E. Tsutakawa, A. Borg, S. Kjaer, J.A. Tainer, J.M. Skehel, M. Groll, and S.J. Boulton. 2016. Mechanism and Regulation of DNA-Protein Crosslink Repair by the DNA-Dependent Metalloprotease SPRTN. *Mol. Cell*. 64:688–703. doi:10.1016/j.molcel.2016.09.031.

Sun, X., H. Gao, Y. Yang, M. He, Y. Wu, Y. Song, Y. Tong, and Y. Rao. 2019. PROTACs: great opportunities for academia and industry. *Signal Transduct. Target. Ther.* 4:64. doi:10.1038/s41392-019-0101-6.

Tabas-Madrid, D., R. Nogales-Cadenas, and A. Pascual-Montano. 2012. GeneCodis3: a non-redundant and modular enrichment analysis tool for functional genomics. *Nucleic Acids Res.* 40:W478-83. doi:10.1093/nar/gks402.

Tadesse, S., E.C. Caldon, W. Tilley, and S. Wang. 2019. Cyclin-Dependent Kinase 2 Inhibitors in Cancer Therapy: An Update. *J. Med. Chem.* 62:4233–4251. doi:10.1021/acs.jmedchem.8b01469.

Tajima, K., S. Matsuda, T. Yae, B.J. Drapkin, R. Morris, M. Boukhali, K. Niederhoffer, V. Comaills, T. Dubash, L. Nieman, H. Guo, N.K.C. Magnus, N. Dyson, T. Shioda, W. Haas, D.A. Haber, and S. Maheswaran. 2019. SETD1A protects from senescence through regulation of the mitotic gene expression program. *Nat. Commun.* 10:2854. doi:10.1038/s41467-019-10786-w.

Tang, Y., W. Zhao, Y. Chen, Y. Zhao, and W. Gu. 2008. Acetylation is indispensable for p53 activation. *Cell*. 133:612–626. doi:10.1016/j.cell.2008.03.025.

Tang, Z., B. Kang, C. Li, T. Chen, and Z. Zhang. 2019. GEPIA2: an enhanced web server for large-scale expression profiling and interactive analysis. *Nucleic Acids Res.* doi:10.1093/nar/gkz430.

Tarsounas, M., and P. Sung. 2020. The antitumorigenic roles of BRCA1-BARD1 in DNA repair and replication. *Nat. Rev. Mol. Cell Biol.* 21:284–299. doi:10.1038/s41580-020-0218-z.

Tateishi, Y., A. Matsumoto, T. Kanie, E. Hara, K. Nakayama, and K.I. Nakayama. 2012. Development of mice without Cip/Kip CDK inhibitors. *Biochem. Biophys. Res. Commun.* 427:285–292. doi:10.1016/j.bbrc.2012.09.041.

Taylor, W.R., and G.R. Stark. 2001. Regulation of the G2/M transition by p53. *Oncogene*. 20:1803–1815. doi:10.1038/sj.onc.1204252.

The ICGC/TCGA Pan-Cancer Analysis of Whole Genomes Consortium. 2020. Pan-cancer analysis of whole genomes. *Nature*. 578:82–93. doi:10.1038/s41586-020-1969-6.

Thut, C.J., J.A. Goodrich, and R. Tjian. 1997. Repression of p53-mediated transcription by MDM2: a dual mechanism. *Genes Dev.* 11:1974–1986.

Tsytlonok, M., H. Sanabria, Y. Wang, S. Felekyan, K. Hemmen, A.H. Phillips, M.-K. Yun, M.B. Waddell, C.-G. Park, S. Vaithiyalingam, L. Iconaru, S.W. White, P. Tompa, C.A.M. Seidel, and R. Kriwacki. 2019. Dynamic anticipation by Cdk2/Cyclin A-bound p27 mediates signal integration in cell cycle regulation. *Nat. Commun.* 10:1676. doi:10.1038/s41467-019-09446-w.

Tubbs, A., and A. Nussenzweig. 2017. Endogenous DNA Damage as a Source of Genomic Instability in Cancer. *Cell*. 168:644–656. doi:10.1016/j.cell.2017.01.002.

Turnbull, A.P., S. Ioannidis, W.W. Krajewski, A. Pinto-Fernandez, C. Heride, A.C.L. Martin, L.M. Tonkin, E.C. Townsend, S.M. Buker, D.R. Lancia, J.A. Caravella, A. V Toms, T.M. Charlton, J. Lahdenranta, E. Wilker, B.C. Follows, N.J. Evans, L. Stead, C. Alli, V. V Zarayskiy, A.C. Talbot, A.J. Buckmelter, M. Wang, C.L. McKinnon, F. Saab, J.F. McGouran, H. Century, M. Gersch, M.S. Pittman, C.G. Marshall, T.M. Raynham, M. Simcox, L.M.D. Stewart, S.B. McLoughlin, J.A. Escobedo, K.W. Bair, C.J. Dinsmore, T.R. Hammonds, S. Kim, S. Urbe, M.J. Clague, B.M. Kessler, and D. Komander. 2017. Molecular basis of USP7 inhibition by selective small-molecule inhibitors. *Nature*. 550:481–486. doi:10.1038/nature24451.

Ute M. Moll, O.P. 2002. The MDM2-p53 Interaction. *Cancer Res.* doi:10.1016/s0092-8674(00)81871-1.

Vassilev, L.T., B.T. Vu, B. Graves, D. Carvajal, F. Podlaski, Z. Filipovic, N. Kong, U. Kammlott, C. Lukacs, C. Klein, N. Fotouhi, and E.A. Liu. 2004. In Vivo Activation of the p53 Pathway by Small-Molecule Antagonists of MDM2. *Science (80-.).* doi:10.1126/science.1092472.

Vaz, B., M. Popovic, J.A. Newman, J. Fielden, H. Aitkenhead, S. Halder, A.N. Singh, I. Vendrell, R.

Fischer, I. Torrecilla, N. Drobnitzky, R. Freire, D.J. Amor, P.J. Lockhart, B.M. Kessler, G.W. McKenna, O. Gileadi, and K. Ramadan. 2016. Metalloprotease SPRTN/DVC1 Orchestrates Replication-Coupled DNA-Protein Crosslink Repair. *Mol. Cell*. 64:704–719. doi:10.1016/j.molcel.2016.09.032.

Vlach, J., S. Hennecke, and B. Amati. 1997. Phosphorylation-dependent degradation of the cyclin-dependent kinase inhibitor p27. *EMBO J.* 16:5334–5344. doi:10.1093/emboj/16.17.5334.

Vogelstein, B., D. Lane, and A.J. Levine. 2000. Surfing the p53 network. *Nature*. 408:307–310. doi:10.1038/35042675.

Vousden, K.H., and C. Prives. 2009. Blinded by the Light: The Growing Complexity of p53. *Cell*. 137:413–431. doi:10.1016/j.cell.2009.04.037.

Vousden, K.H., and K.M. Ryan. 2009. p53 and metabolism. *Nat. Rev. Cancer*. 9:691–700. doi:10.1038/nrc2715.

Wade, M., Y.-C. Li, and G.M. Wahl. 2013. MDM2, MDMX and p53 in oncogenesis and cancer therapy. *Nat. Rev. Cancer*. 13:83–96. doi:10.1038/nrc3430.

Waga, S., G.J. Hannon, D. Beach, and B. Stillman. 1994. The p21 inhibitor of cyclin-dependent kinases controls DNA replication by interaction with PCNA. *Nature*. 369:574–578. doi:10.1038/369574a0.

Walter, D., S. Hoffmann, E.-S. Komseli, J. Rappsilber, V. Gorgoulis, and C.S. Sorensen. 2016. SCF(Cyclin F)-dependent degradation of CDC6 suppresses DNA re-replication. *Nat. Commun.* 7:10530. doi:10.1038/ncomms10530.

Wang, X.W., Q. Zhan, J.D. Coursen, M.A. Khan, H.U. Kontny, L. Yu, M.C. Hollander, P.M. O'Connor, A.J.J. Fornace, and C.C. Harris. 1999. GADD45 induction of a G2/M cell cycle checkpoint. *Proc. Natl. Acad. Sci. U. S. A.* 96:3706–3711.

Wei, W., N.G. Ayad, Y. Wan, G.-J. Zhang, M.W. Kirschner, and W.G.J. Kaelin. 2004. Degradation of the SCF component Skp2 in cell-cycle phase G1 by the anaphase-promoting complex. *Nature*. 428:194–198. doi:10.1038/nature02381.

Wiese, C., E. Dray, T. Groesser, J. San Filippo, I. Shi, D.W. Collins, M.-S. Tsai, G.J. Williams, B. Rydberg, P. Sung, and D. Schild. 2007. Promotion of homologous recombination and genomic stability by RAD51AP1 via RAD51 recombinase enhancement. *Mol. Cell*. 28:482–490. doi:10.1016/j.molcel.2007.08.027.

Wisniewski, J.R., A. Zougman, S. Kruger, P. Ziolkowski, M. Pudelko, M. Bebenek, and M. Mann. 2008. Constitutive and dynamic phosphorylation and acetylation sites on NUCKS, a hypermodified nuclear protein, studied by quantitative proteomics. *Proteins*. 73:710–718. doi:10.1002/prot.22104.

Witsch, E., M. Sela, and Y. Yarden. 2010. Roles for growth factors in cancer progression. *Physiology (Bethesda).* 25:85–101. doi:10.1152/physiol.00045.2009.

Wood, D.J., and J.A. Endicott. 2018. Structural insights into the functional diversity of the CDK-cyclin family. *Open Biol.* 8. doi:10.1098/rsob.180112.

Wood, L.J., J.F. Maher, T.E. Bunton, and L.M. Resar. 2000. The oncogenic properties of the HMG-I gene family. *Cancer Res.* 60:4256–4261.

Wu, J., X. Zhang, L. Zhang, C.-Y. Wu, A.H. Rezaeian, C.-H. Chan, J.-M. Li, J. Wang, Y. Gao, F. Han, Y.S. Jeong, X. Yuan, K.K. Khanna, J. Jin, Y.-X. Zeng, and H.-K. Lin. 2012. Skp2 E3 ligase integrates ATM activation and homologous recombination repair by ubiquitinating NBS1. *Mol. Cell*. 46:351–361. doi:10.1016/j.molcel.2012.02.018.

Wu, S., C. Cetinkaya, M.J. Munoz-Alonso, N. von der Lehr, F. Bahram, V. Beuger, M. Eilers, J. Leon, and L.-G. Larsson. 2003. Myc represses differentiation-induced p21CIP1 expression via Miz-1-dependent interaction with the p21 core promoter. *Oncogene*. 22:351–360. doi:10.1038/sj.onc.1206145.

Xiao, Z., Z. Chen, A.H. Gunasekera, T.J. Sowin, S.H. Rosenberg, S. Fesik, and H. Zhang. 2003. Chk1 mediates S and G2 arrests through Cdc25A degradation in response to DNA-damaging agents. *J. Biol. Chem.* doi:10.1074/jbc.M300229200.

Yamano, H. 2019. APC/C: current understanding and future perspectives. *F1000Research*. 8. doi:10.12688/f1000research.18582.1.

Yang, H.W., S.D. Cappell, A. Jaimovich, C. Liu, M. Chung, L.H. Daigh, L.R. Pack, Y. Fan, S. Regot, M.

Covert, and T. Meyer. 2020. Stress-mediated exit to quiescence restricted by increasing persistence in CDK4/6 activation. *Elife*. 9. doi:10.7554/eLife.44571.

Yang, H.W., M. Chung, T. Kudo, and T. Meyer. 2017. Competing memories of mitogen and p53 signalling control cell-cycle entry. *Nature*. doi:10.1038/nature23880.

Yao, G., T.J. Lee, S. Mori, J.R. Nevins, and L. You. 2008. A bistable Rb-E2F switch underlies the restriction point. *Nat. Cell Biol.* 10:476–482. doi:10.1038/ncb1711.

Yokoi, S., K. Yasui, M. Mori, T. Iizasa, T. Fujisawa, and J. Inazawa. 2004. Amplification and overexpression of SKP2 are associated with metastasis of non-small-cell lung cancers to lymph nodes. *Am. J. Pathol.* 165:175–180. doi:10.1016/S0002-9440(10)63286-5.

Yuan, X., M. Zhang, J. Ao, Z. Zhen, X. Gao, and M. Li. 2019. NUCKS1 is a novel regulator of milk synthesis in and proliferation of mammary epithelial cells via the mTOR signaling pathway. *J. Cell. Physiol.* doi:10.1002/jcp.28240.

Yue, Y., S.G. Leung, Y. Liu, Y. Huang, K. Grundt, A.-C. Ostvold, K.-Y. Jen, D. Schild, J.-H. Mao, and C. Wiese. 2016. Nucks1 synergizes with Trp53 to promote radiation lymphomagenesis in mice. *Oncotarget*. 7:61874–61889. doi:10.18632/oncotarget.11297.

Yung, Y., J.L. Walker, J.M. Roberts, and R.K. Assoian. 2007. A Skp2 autoinduction loop and restriction point control. *J. Cell Biol.* 178:741–747. doi:10.1083/jcb.200703034.

Zetterberg, A., O. Larsson, and K.G. Wiman. 1995. What is the restriction point? *Curr. Opin. Cell Biol.* 7:835–842. doi:10.1016/0955-0674(95)80067-0.

Zhan, Q., M.J. Antinore, X.W. Wang, F. Carrier, M.L. Smith, C.C. Harris, and A.J.J. Fornace. 1999. Association with Cdc2 and inhibition of Cdc2/Cyclin B1 kinase activity by the p53-regulated protein Gadd45. *Oncogene*. 18:2892–2900. doi:10.1038/sj.onc.1202667.

Zhang, L., and C. Wang. 2006. F-box protein Skp2: a novel transcriptional target of E2F. *Oncogene*. 25:2615–2627. doi:10.1038/sj.onc.1209286.

Zhao, E., L. Feng, L. Bai, and H. Cui. 2020a. NUCKS promotes cell proliferation and suppresses autophagy through the mTOR-Beclin1 pathway in gastric cancer. *J. Exp. Clin. Cancer Res.* 39:194. doi:10.1186/s13046-020-01696-7.

Zhao, S., B. Wang, Y. Ma, J. Kuang, J. Liang, and Y. Yuan. 2020b. NUCKS1 Promotes Proliferation, Invasion and Migration of Non-Small Cell Lung Cancer by Upregulating CDK1 Expression. *Cancer Manag. Res.* 12:13311–13323. doi:10.2147/CMAR.S282181.

Zhou, Z., M. He, A.A. Shah, and Y. Wan. 2016. Insights into APC/C: from cellular function to diseases and therapeutics. *Cell Div.* 11:9. doi:10.1186/s13008-016-0021-6.

Zhu, J., M.A. Sammons, G. Donahue, Z. Dou, M. Vedadi, M. Getlik, D. Barsyte-Lovejoy, R. Al-awar, B.W. Katona, A. Shilatifard, J. Huang, X. Hua, C.H. Arrowsmith, and S.L. Berger. 2015a. Gain-of-function p53 mutants co-opt chromatin pathways to drive cancer growth. *Nature*. 525:206–211. doi:10.1038/nature15251.

Zhu, Q., A.K. Wong, A. Krishnan, M.R. Aure, A. Tadych, R. Zhang, D.C. Corney, C.S. Greene, L.A. Bongo, V.N. Kristensen, M. Charikar, K. Li, and O.G. Troyanskaya. 2015b. Targeted exploration and analysis of large cross-platform human transcriptomic compendia. *Nat. Methods*. 12:211–4, 3 p following 214. doi:10.1038/nmeth.3249.